UDC 622

ISSN 2334-8836 (Štampano izdanje)
ISSN 2406-1395 (Online)

Mining and Metallurgy Engineering Bor

3-4/2021

Published by: Mining and Metallurgy Institute Bor

Mining and Metallurgy Engineering Bor

3 - 4/2021

MINING AND METALLURGY ENGINEERING BOR is a journal based on the rich tradition of expert and scientific work from the field of mining, underground and open-pit mining, mineral processing, geology, mineralogy, petrology, geomechanics, metallurgy, materials, technology, as well as related fields of science. Since 2001, published twice a year, and since 2011 four times a year.

Editor-in-chief

Academic Dr Milenko Ljubojev,
Principal Research Fellow
Mining and Metallurgy Institute Bor
Full member of EAS
E-mail: milenko.ljubojev@irmbor.co.rs
Phone: +38130/454-109, 435-164

Editor

Vesna Marjanović, B.Eng.

English Translation

Nevenka Vukašinović, prof.

Technical Editor

Suzana Cvetković

Preprinting

Vesna Simić

Printed in: Grafomedtrade Bor

Circulation: 200 copies

Web site

www.irmbor.co.rs

Journal is financially supported by

The Ministry of Education, Science and Technological Development of the Republic Serbia
Mining and Metallurgy Institute Bor

ISSN 2334-8836 (Printed edition)

ISSN 2406-1395 (Online)

Journal indexing in SCIndex and ISI.

Published by

Mining and Metallurgy Institute Bor
19210 Bor, Zeleni bulevar 35
E-mail: milenko.ljubojev@irmbor.co.rs
Phone: +38130/454-110

Scientific – Technical Cooperation with the Engineering Academy of Serbia

CONTENS

SADRŽAJ

MINING AND METALLURGY INSTITUTE BOR
UDK: 622

ISSN: 2334-8836 (Štampano izdanje)
ISSN: 2406-1395 (Online)

UDK: 550.8.05:622.79(045)=111
DOI: 10.5937/mmeb2104001I

Received: 04.10.2021.
Revised: 04.11.2021.
Accepted: 06.12.2021.

Original Scientific Paper
Geotechnics

Dragan Ignjatović[*], *Dušan Tašić*[*], *Vanja Đurđevac*[*],
Mlađen Supić[*], *Dejan Mitić*[**]

GEOMECHANICAL TESTING ON THE LANDSLIDE AT THE ČUKARU PEKI FLOTATION TAILING DUMP[***]

Abstract

During formation of the flotation tailing dump Čukaru Peki, a landslide was activated above the mentioned location, which led to a standstill and endangerment of works. In order to obtain the geotechnical bases for designing the measures for its rehabilitation, the landslide tests were performed. Geomechanical works included the field research and testing, laboratory geomechanical testing and cabinet work.

Keywords: *geotechnical research, landslide, landslide remediation*

1 INTRODUCTION

Serbia Zijin Mining Doo Bor, as an Investor, ordered from the Mining and Metallurgy Institutre Bor to perform the geomechanical tests on the landslide, which was activated at the location of flotation tailing dump Čukaru Peki, in order to obtain the geotechnical bases for designing the measures for its rehabilitation. Geomechanical works included the field research and testing, laboratory geomechanical testing and cabinet work.

Works on the terrain preparation for dam construction and formation the flotation tailing dump Čukaru Peki, are performed according to the Main Mining Project for preparation the mineral raw materials and landfills for mining waste and pyrite concentrate from the Čukaru Peki deposit - Upper Zone, Mining and Metallurgy Institute Bor, 2020. In a part of terrain where preparation for construction the flotation tailing dumpis planned, the landslide was activated (Figure 1.1).

[*] *Mining and Metallurgy Institute Bor, Zeleni bulevar 35, 19210 Bor, Serbia*
[**] *Serbia Zijin Mining DOO Bor*
[***] *This work was financially supported by the Ministry of Education, Science and Technological Development of the Republic of Serbia, Grant No. 451-03-9/2021-14/200052*

Figure 1.1 *View of the landslide from the above (December 2020)*

2 TYPES AND SCOPE OF PERFORMED RESEARCH AND TESTING

2.1 Field research

Within the field research of the subject location, in the period of second half of December 2020, the following was performed:

- Terrain mapping;
- Sampling for laboratory tests;
- Shear "In Situ".

The terrain mapping was performed in order to better understand the real - real situation in the subject area, i.e. the active exodynamic process and results of its action in the field (Figure 2.1).

Figure 2.1 *Crack in terrain in the immediate vicinity of landslide (December 2020)*

Selection of samples for the laboratory geomechanical tests was performed during the engineering geological mapping of terrain. The total of 14 samples were taken.

Direct shear in the field was performed in order to determine the shear parameters along the sliding plane, i.e. mechanism of disturbed stability. It was performed in two places, according to a contact of the clay Quaternary cover with the Miocene substrate, according to the discontinuity for which it is assumed that the material slipped, Figure 2.2.

Figure 2.2 *Appearance of a build-in shear equipment in the field*

2.2 Laboratory geomechanical tests

In order to define the physical – mechanical and deformation parameters, the laboratory geomechanical tests were performed on the rock and soil samples.

The results obtained by testing the samples were used as the input parameters for analysis the stress states of material as well as the total displacements during sliding. The analysis was done using SLIDE v6.0.

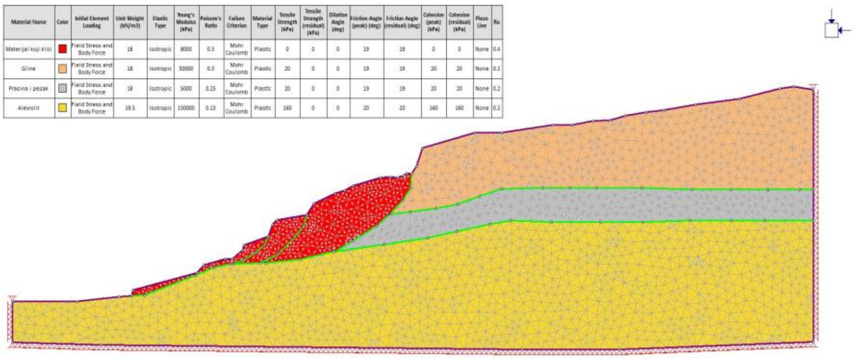

Material Name	Color	Initial Element Loading	Unit Weight (kN/m3)	Elastic Type	Young's Modulus (kPa)	Poisson's Ratio	Failure Criterion	Material Type	Tensile Strength (kPa)	Tensile Strength (residual) (kPa)	Dilation Angle (deg)	Friction Angle (peak) (deg)	Friction Angle (residual) (deg)	Cohesion (peak) (kPa)	Cohesion (residual) (kPa)	Piezo Line	Ru
Materijal koji klizi		Field Stress and Body Force	18	Isotropic	8000	0.3	Mohr Coulomb	Plastic	0	0	0	19	19	0	0	None	0.4
Gline		Field Stress and Body Force	18	Isotropic	50000	0.3	Mohr Coulomb	Plastic	20	0	0	19	19	20	20	None	0.2
Prasina i pesak		Field Stress and Body Force	18	Isotropic	5000	0.25	Mohr Coulomb	Plastic	20	0	0	19	19	20	20	None	0.2
Alevrolit		Field Stress and Body Force	19.5	Isotropic	150000	0.13	Mohr Coulomb	Plastic	160	0	0	20	20	160	160	None	0.2

Figure 2.3 *Analyzed materials with their characteristics*

Figure 2.4 shows the sliding tendency of material with total displacements, expressed in meters.

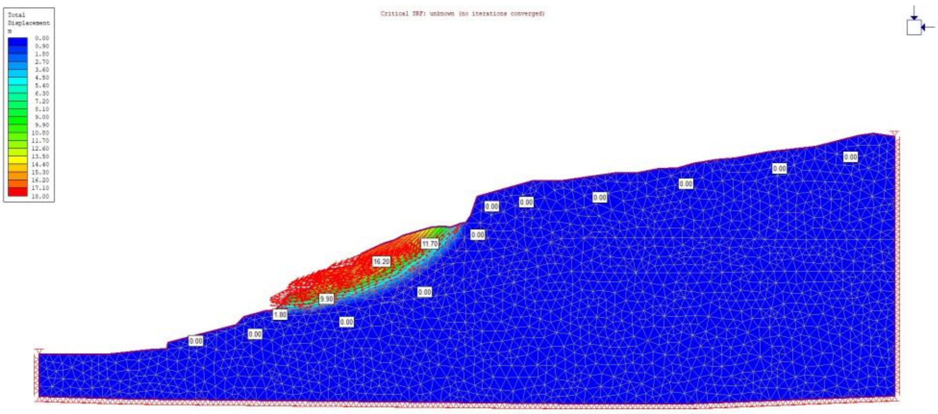

Figure 2.4 *Total displacements of sliding material, in meters*

Figure 2.5 shows the maximum shear deformations of sliding material.

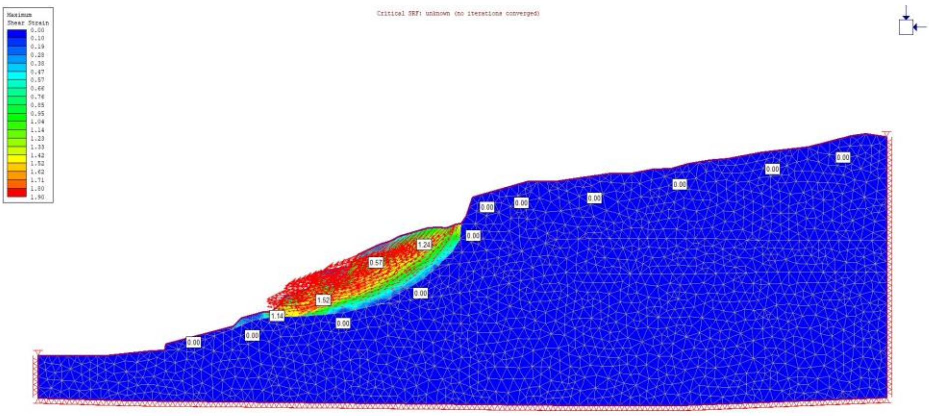

Figure 2.5 *Maximum shear deformations of sliding material*

3 RESEARCH RESULTS

Surface clayey cover is the subject to swelling, with a change in physical-mechanical and structural properties. The resulting masses, in the presence of water that accumulates above them, tend to move under the action of gravity, upon contact with a decomposed or fresh base rock. For that reason, the intensive, cyclic sliding processes take place on the right bank slopes, intended for the dam for mation, which are supported and accelerated by anthropogenic action, i.e. by removal of masses at the foot of slopes during excavation. Thus, by cutting the slope, the landslide in question was activated. The sliding affected an area of approximately 60 x 45 m. The frontal scar of landslide at the top of slope is noticeable, with an average jump of 3 m. It is assumed that the thickness of driven material in the upper part is up to 12 m and that it decreases towards the lower part of slope. In addition to landslides at the site in question, the landslides and cracks in terrain were observed in awider vicinity of t landslide.

In any case, the following factors contribute to the sliding process of microlocation and immediate environment:

- anthropogenic action, i.e. excavations in unstable or conditionally stable terrain;
- geological composition of the terrain - alternating batches of highly plastic clay with more sandy interbeds through which groundwater circulates, as well as a high level of groundwater (recorded in the exploration works in 2019);
- tendency of clays that build the terrain to swell and compress, as a result of which cracks of dm dimensions are formed, through which water from precipitation flows directly into the terrain.

CONCLUSION

Based on all the above, the following can be concluded:

- At the location of the right bank of dam of the flotation tailing dump Čukaru Peki, the occurrence of landslides was registered and geomechanical research was performed in order to understand the causes and mechanism of instability, engineering geological conditions in the field, and to implement the preventive and interventional remediation measures. For that purpose, a certain scope of geomechanical works was performed with accompanying field and laboratory tests.
- The investigated terrain was built in natural conditions from: clay Quaternary cover, within which the clay and sand-dust lots and siltstones in the floor alternate. Part of the clay deposits has undergone gravitational transport (sliding) and represents the colluvium (landslide body).
- The geomechanical parameters of the selected engineering geological environments have been determined, which will be used for the development of the Landslide Rehabilitation Project.
- It is recommended that the rehabilitation of landslide in question would be performed by removal the clay cover (layers 1 and 2) in the area covered by the landslide and its immediate surroundings, in order to fund the dam on the basic rock mass.
- During the execution of earthworks, it is obligatory to engage professional geological supervision by a geological engineer and a civil engineer - geotechnician. During the work realization, with the approval of geotechnical supervision, the project can be adjusted to the actual geotechnical conditions.

REFERENCES

[1] Ćorić S., 2008: Geostatic Calculations - Faculty of Mining and Geology, Belgrade (in Serbian)

[2] M. Ljubojev, R. Popović, Fundamentals of Geomechanics, Mining and Metallurgy Institute Bor, Bor 2006 (in Serbian)

[3] Obradović R., Najdanović N., 1999: Soil Mechanics in Engineering Practice - Mining Institute, Belgrade (in Serbian)

[4] Complex of Tailing Dumps "Čukaru Peki", Book - Study on Geotechnical Conditions - Volume 4 - Geotechnical Conditions for Designing the Flotation Tailing Dumps, Hidroenergo Petrović 2019 (in Serbian)

MINING AND METALLURGY INSTITUTE BOR
UDK: 622

ISSN: 2334-8836 (Štampano izdanje)
ISSN: 2406-1395 (Online)

UDK: 552.1:622(045)=111
DOI: 10.5937/mmeb2104007G

Received: 22.10.2021
Revised: 23.11.2021.
Accepted: 23.12.2021.

Original Scientific Paper
Mining

Aleksandar Grubić, Aleksej Milošević**, Ranko Cvijić*, Miodrag Čelebić**, Boško Vuković****

METALLOGENY OF THE LJUBIJA ORE REGION

Abstract

The Ljubija ore region is a part of the Triassic, regional, internal metallogenetic zone of the Middle Dinarides. It is located approximately in the middle of this larger metallogenetic unit and has many characteristics in common with its other parts. After many wanderings in the interpretation of the genesis of iron ore in Ljubija, it was definitely determined that the metallogeny of iron is of the Triassic age, then, that it is associated with the deep rift dislocations, which allowed the circulation of hydrothermal solutions originating from the Upper mantle, that the primary economic concentrations of iron are found only in the Olistostromic member of the Javorik flysch formation and the secondary ones, redeposited in the Neogene-Quaternary lake sediments of the Prijedor-Omarska basin. Based on the distribution of mineralization in the Ljubija ore region, two ore subregions, one polymetallic ore zone and a group of ore fields with barite, were identified. All the above knowledge, along with the analysis of control factors of mineralization and the main prospective indications, enabled the division of entire region into areas with various categories of perspectives according to the justification of further research. Based on the results of many years of research, this work presents the results of metallogenetic analysis of the Ljubija ore region. All results of the future research should continuously supplement, correct and improve the metallogenetic and prognostic map and our metallogenetic knowledge about the region.

***Keywords**: Ljubija ore region, Javorik flysch formation, Olistostrome member, metallogenetic analysis, metallogenetic map, metallogenetic regionalization, control factors*

1 INTRODUCTION

The Ljubija ore region covers the whole ore - bearing territory at the area of 1500 km^2, which represents part of the Dinaride metallogenetic province (as a major meta-llogenetic unit) and that is characterized by the same geological conditions and development of certain ore formations and types of economic deposits of iron and other minerals [1]. The Ljubija ore region is defined by the boundary of Sana-Una River nappe at the South, boundary of the Jurassic-Cretaceous formations on the east, the inner ophiolitic zone of Kozara Mountain on the north and tectonically defined riverbed of the Una River on the west, deeply carved into the terrain (Figure 1 and 3).

* *Institute of Mining Prijedor, Aleja kozarskog odreda br.1 Prijedor, e –mail: cvijic.ranko@gmail.com*
** *University in Banja Luka, Faculty of Mining Prijedor, Bulevar vojvode Petra Bojovića 1A ,78000, Banja Luka, Republic of Srpska, e –mail: aleksej.milosevic@rf.unibl.org*
*** *Mine and TPP Gacko, Industrijska zona bb, e –mail: bosko.vukovic@ritegacko.com*

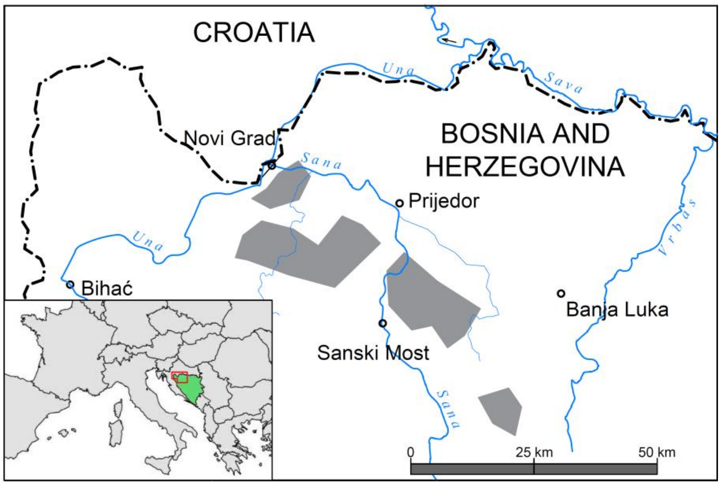

Figure 1. *Index maps with the location of the Ljubija ore mine. (a) Map od NW Bosnia and Herzegovina with marked areas od the Sana-Una Paleozoic complex (gray), (b) Geographic position of the area shown in Figure 1a; area of Bosnia and Herzegovna marked in green*

This work is the result of the Project of elaboration of Metallogenetic study of the Ljubija region. The Project was implemented in phases. In the first phase of the project implementation, the entire preparation for elaboration of the Metallogenetic Map of the Ljubija region was done. All existing data about exploration and mining works within the ore region were analyzed and based on that the Geological Background for Metallogenetic Map of the Ljubija Region M 1:50000 was developed. In the second phase, creation of the contracted maps started. Firstly, the mettalogenetic map was created, and then, based on that, the Perspective Projection Map of the Ljubija Region was developed in M 1: 50000.

2 LEVEL OF THE FIELD EXPLORATION

Generally, the level of exploration of the field is very good, according to the quantity of executed works and their diversity, but the density of exploration works is not equal. Their major concentration is usually in relation to the ore bodies and ore – bearing fields. Between them, the exploration works are reduced to minimum.

However, numerous explorations and analyzing the iron ore of the Ljubija region were carried out in different conditions and times, often uncompleted and nonsystematic, so the data about them are in most cases semi - usable. At the area of metallogenetic region, all in the total approximately 3500 drillholes were drilled. Most of them were "spent" in order to delineate the boundaries of known ore bodies and estimation of mineral resources/reserves because of the need for their distance to be less than 50 m and similar. There are about 600 regional drillholes. That implies that the information about high level of exploration of the field should be taken with reserve. The second problem is that the drill holes were limited upon exit from intersection with the ore body, because of unacquaintance with today's genetic model of ore forming.

The results of all exploration are registered in 300 different texts. Out of that, 130 are published papers, 170 are reports and elaborates of different volume. In 19 reports related to works executed 1987 to 1990, metallogenetic study has been given a special attention [2]. The three-volume study by M. Jurić on all phenomena of mineralization in the Sana Paleozoic is especially important [3].

3 STRATIGRAPHY

There are the following members of geologic column in the explored area: Carboniferous Javorik flysch formation, Formation of Perm - Triassic clastites, Terrigenous - Carbonate formation of Lower and Middle Triassic, Volcano - sedimentary formation, Triassic terrigenous and carbonate formation and Neogene – Quaternary formations [4] (Figure 3).

Javorik flysch formation

During earlier geological mapping, the Sana - Una Paleozoic was treated as a complex and unique whole in which no detailed dismembered is possible [3,5]. Recent geological works, however, have shown that such interpretation is not correct [6]. Carboniferous Javorik flysch formation is composed of three members, i.e., the Pre-flysch and Lower flysch, Olistostrome member and Upper flysch (Figure 2). All rocks of the Javorik Formation were epizonally metamorphosed maximum to the grade of greenschist facies.

The basal unit of the Javorik flysch formation is the Pre - flysch and Lower flysch member consisting of dark argillaceous schists with alternation of medium - grain sandstone [7]. It is well studied in the Adamuša opencast mine, in a core of large anticline structure. This member was probably formed in a deeper marine environment.

The Olistostrome member represents a middle part of the Javorik formation. Beneath it there is the Lower Flysch member which is exposed only in drill holes and, over it, there is the Upper Flysch member. It was formed under the deep marine conditions. This member is exposed in the middle parts of explored area and is built out of three types of rocks: flysch matrix, carbonate olistolithic blocks and mineralized bodies. The flysch matrix is made of two-member sequence of sandstones and black alevrolites with rare mechanoglyphs. Carbonate blocks are made of black micrites and grey organogenuous sparites and dolosparites. Within the Olistostrome member some authors distinguished more units, i.e. a Siderite – limonite member, and Wild – flysch and Middle flysch [6, 8]. Based on the fossils, it was concluded that the age of blocks is the Devon, Lower Devon or Middle Carboniferous age and whole member is of the Upper Carboniferous age [6]. This agrees with recent paleontological data according to which the carbonate blocks are of the Bashkirian age [7]. The mineralized bodies are siderite, ankerite, sideritic and ankeritic carbonates. Sometimes the entire olistolithic carbonate bodies were metasomatically replaced and some were only partially altered and then limonitized. Large stratiform mineralized bodies are specially notable, and their genesis was a subject of discussion for a long time. Thickness of this member is 100 to 300 m.

The Upper Flysch Member lies conformably over an Olistostrome member and unconformably below the Perm-Triassic Clastites Formation. It was formed under the deep marine conditions. Per superposition, it belongs to the Upper Carboniferous. It is built of the sandstone-siltstone two-member and three-member sequences with occurrences of gradation, parallel lamination and convolution [6]. There are the sporadic thinner siderite and limonite veins. Their thickness is up to 400 m.

Perm - Triassic Clastites Formation

This formation lies over the Javorik Formation unconformably and transgressively. It was developed and, because of erosion, kept only sporadically. It was formed in the continental, lagoon and sublittoral environments. Its age is supposed on the basis of superposition. This formation is built of different rocks: white and red quartz sandstones, conglomerates and shales [3]. The red rocks prevail. Sporadically, there are the cavernous dolomite and siderite veins up to 40 cm. Thickness of the formation is 150 m.

Terrigenous - Carbonate Formation of the Lower and Middle Triassic

This formation lies transgressively and unconformably over various Carboniferous and Perm - Triassic units. It is developed up to periphery of the researched area. Generally, it is compounded out of two parts. Its age is confidently proven on the basis of fossils. Lower part belongs to the Werfen and is composed of an alternation of sandstones, shales, marlstones and some limestone. Sporadically, there are the limonite veins. Thickness of this part of formation is up to 300 m. The Upper part of formation started to form in the Upper Campilian and takes hold of the Anisian. It is built out of the bedded limestone and dolomites. Numerous occurrences of limonite, lead sulphides, zinc and mercury, then barite and fluorite were registered. Its thickness is 300 to 400 m.

Volcano - Sedimentary Formation

This formation is conformable over the previous rock formation and its roof was destroyed by erosion. It is best developed in a wider area of the Volar. It is actually well known the Dinaridic porphyrite-chert formation of the Ladinian age. It was built mostly of cherts and volcanogenic materials. Volcanic rocks are represented with elements of spilite-keratophyric association in it. In addition, it also has marlstones and micritic limestones with cherts. The thickness of the formation, due to the lack of roof, is found only in a part and is approximately 500 m. This formation is of a great metallogenic importance because in the whole Dinarides polymetallic mineralization (with local mineralization specialization) they are associated with it.

Triassic Terrigenous and Carbonate Formations

It was developed on the eastern periphery of the explored field and only a small part is shown on a map. It was built in the lower part of the terrigenous sediments, which probably belong to the Werfen. Then, in a column, there is a thick series of well bedded dolomite. Its age is determined super positionally. The thickness is about 1400 m.

Neogene - Quaternary Lake Sediments

These young sediments have been developed only in the Prijedor basin on the north and Kamengrad basin on the south. In particular, stand out poorly rounded fragments originating from neighboring Paleozoic formations. There are significant quantities of redeposited iron ore, which are largely exploited. Clastic material filled large pre - Neogene relief indentations in which the sediment thickness reaches up to 200 m [9].

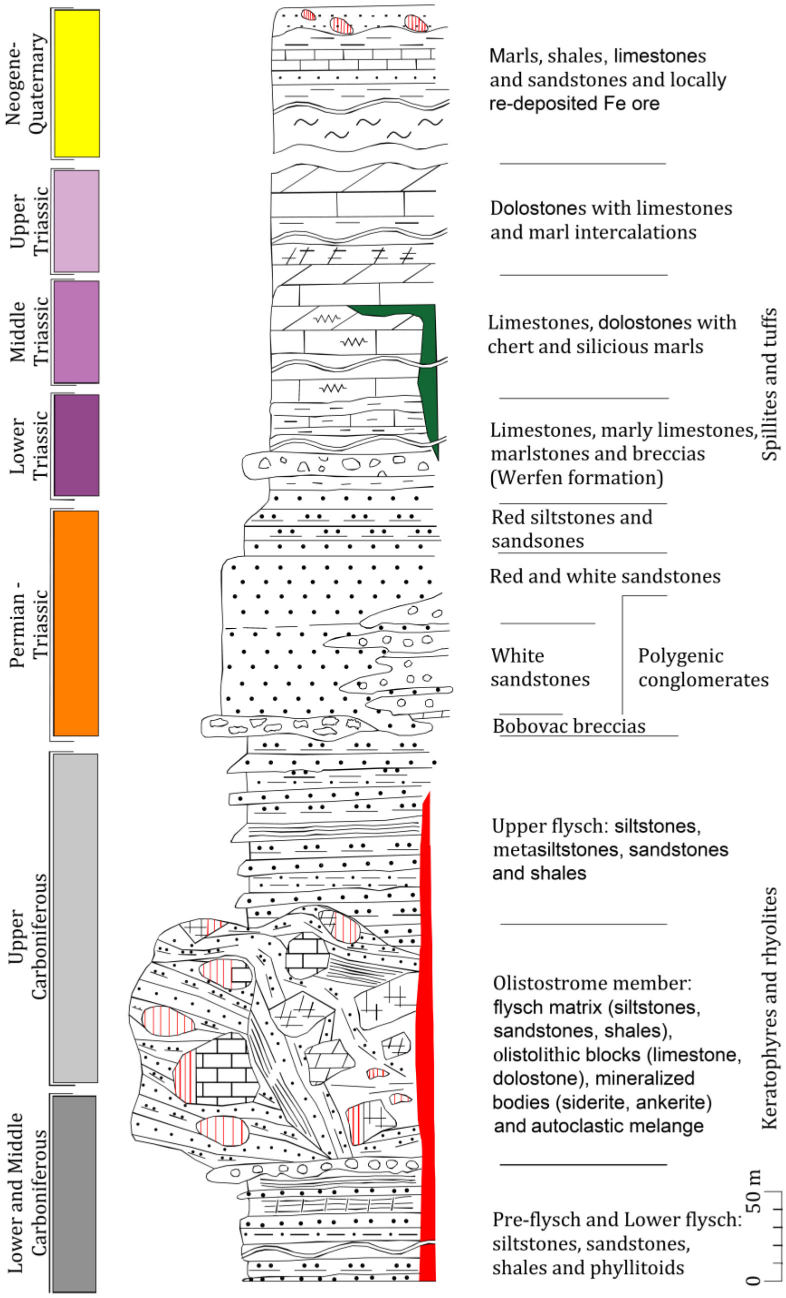

Figure 2 *Schematic lithostratigraphic column of the Ljubija ore region[7]*

3.1. Stratgraphic and Lithological Control Factors

In the geologic column of the Ljubija ore region, there are two ore - bearing formations: Javorik formation with their olistostrome members and Neogene - Quaternary formation in the Prijedor basin. The first contains primary siderite and ankerite ore bodies partly oxidized into limonite; in the second, there are only redeposited limonite [10]. Iron ore occurrences are also found in the other formations, but these are veins that have no significance for economic exploitation.

Regarding to lithology, the iron ore is associated with carbonate olistolithic blocks. Siderite and limonite are associated with limestone and, in dolomites, there are ankerite and limonite. Whole olistoliths or a portion could be replaced by the iron ore. Stratiform morphology of deposits are derived from the lensoid carbonate bodies, what were the confusing facts for hypothesis of iron ore genesis in this region.

4 MAGMATISM

Magmatic rocks have no wide distribution in the field. They occure in the wider area of Volar, in the north, and at Trnava, in the south. They are separately shown on the map although they are actually part of Triassic ie. Ladinian Volcano - sedimentary formation.

There are indentified: spilite, diabase, keratophyres and rhyolite - volcanic members that make Porphyrite - chert formation. Based on the analysis of their isotopic age (114 million years), the rocks are Cretaceous, which is not in accordance with the geological facts from the field. Therefore, it is assumed that this terrain in the middle of the Cretaceous was exposed to temperatures above 350^0C for a long time and that complete homogenization was achieved, ie "ideal rejuvenation" [11]. Magmatism in this zone of the Dinarides, based on the isotopic age of the rocks, took place from the Upper Permian to the Upper Triassic, but was still the strongest during the Ladinnian [12]. In Dinarides this Formation is an important magmatic control factor for polymetallic mineralization with specialization on mercury, iron, lead - zinc and manganese.

5. TECTONICS

Tectonics of studied terrain is very complex because it is the result of Hercynian, Kimmerian and Alpine deformation phases. Hercynian events have left their mark only on the Javorik formation as folds whose B - axis have azimuth from 10 to 40 ^{0} [6,13]. This dissipation of the B - axis is due to the Alpine folds, that is clearly identified by the Schmidt net of bedding with triclinic symmetry [6].

Of Kimmerian age is Sana dislocation, which was created during rifting in peripheral areas of the Apulia. As per its direction NW - SE Sana dislocation belongs to the south - west, supporting faults of rifting and opening of Dinaric ophiolitic belt. It cut through the entire lithosphere to mantle and were accompanied by ruptures of the lateral systems. It left her mark on the Javorik as well as younger formations. Through subsequent events it significantly influenced the change of Hercynian structural plan in Alpine terrain.

In Alpine tectogenesis were created fold structures with B - axis direction NW - SE (130 -140 degrees) and the corresponding longitudinal, transverse and diagonal ruptures. Sana dislocation was by the reverse transport turned into a nappe. Hercynian and Kimmerian structures are pre – ore - bearing structures and Alpine are post – ore – bearing.

5.1. Tectonic control factor

At the end of the Permian and in the Lower Triassic Sana dislocation cut the lithosphere to the mantle and became the supply channel for magmatism and circulation of hydrothermal fluids. So, it was a decisive impact on the orientation of Ljubija ore region, in a NW - SE direction, as a part of discontinued Triassic "metallogenetic zone of Central Dinarides"

Associated ruptures of the lateral systems at the studied terrain have predominantly NE - SW direction. They are well expressed in the field and in the metallogeny they had the role of distribution channels, which were significant for the circulation of hydrothermal fluids and today's distribution of ore deposits and mineral occurrences in the form of ore knots and ore fields.

This Cimmerian regional mega - framework made his mark in the meters field of view. In Adamuša and Southern Tomašica paleo splits of decimetere in size, filled with siderite and siderite with quartz, has exactly the same orientation. Their two conjugated systems that extends in NW - SE and NE - SW direction are also recorded. Alpine fault and split systems opened the pathways for descending meteoric waters that were rich with oxygen and over time gradually oxidized siderite and ankerite.

6 METALLOGENY

The first scientific researcher of the iron ore in the Ljubija ore region, F. Katzer, was of opinion that the iron ore was mostly of the hydrothermal - metasomatic origin and there was a possibility that some occurrence was of synsedimentary origin [5]. After him, all the authors supported the hydrothermal - metasomatic genesis. In the early sixties, M. Jurković suggested that all iron ore in this region were exclusively of synsedimentary origin [14]. He presented a variety of evidence for it. After him, such opinion on genesis were also shared by the authors of two doctoral dissertations, M. Jurić and M. Šarac [15].

During the nineties, after detailed studies of Adamusa and Southern Tomasica, A. Grubic and Lj. Protic assumed that there are two metallogenies in the region. The older one, the Carboniferous hydrothermal - sedimentary, sideritic, and the younger one, Triassic hydrothermal - metasomatic, ankeritic and polymetallic accompanied with sulphides [5].

It was not possible to do more with field, sedimentology, petrographic and ore-microscopic methods. For more reliable judgment, there had to be done very detailed and complex geochemical analysis and interpretation. That was done, at the end of the first decade of this century, by the Croatian geochemists for their own needs.

S. Strmic - Palinkas and others analyzed in the Swiss laboratories, sixty samples from the Adamusa, Southern Tomasica and other mines on: common elements, rare elements, isotopes of oxygen, sulphur and carbon, and hydrocarbons. All results and, in particular, the content of rare elements shown the hydrothermal metasomatic genesis of iron. In this regard, particularly indicative are the cerium (Ce) negative and europium (Eu) positive anomalies, which indicate that the ore could not be of the sedimentary origin [16]. These results were confirmed by V. Garasic and I. Jurkovic, but they left the question on genesis of threstratiform deposits opened [8].

After the first phase of this study, it was concluded that the first and main task in the next work was to check the geochemical characteristics of real (based on other geological features) stratiform siderite ore bodies. At the very beginning of work on the second phase of the study, samples were collected from the Adamusa and South Mines. The spectrochemical analysis of samples of the representative, verified stratiform body in Adamusa, showed an identical composition of rare elements that every hydrothermal - metasomatic deposits have. This was crucial evidence on the basis of which was completely abandoned working hypothesis about consedimentary and sedimentary, marine, Carboniferous origin of siderite and ankerite.

In the Ljubija ore region, there are the primary carbonate iron ore (siderite and ankerite) and the secondary oxidized (limonites). The limonite ore was formed from the first by long - term oxidation under hypergenetic conditions to depths of about 300 m. Apart from the iron ore, there are sulphides Pb, Zn, Cu, Hg, Ag and Au then, fluorite and considerable amount of barite in the region. It is a unique "siderite - polysulphide – barite ore formations", which consists of three sub-formations: a) siderite - ankeritic, partly limonitised; b) polysulfide and c) barite-fluoritic. Based on the mutual relations of members of mentioned sub-formations in the field, they should be formed in the following phases. In the first phase, siderite and ankerite were formed by the hydrothermal metasomatism of carbonate olistolithic blocks at moderate depths and at temperatures around 246 ^{o}C. In the second phase, sulphides in the form of veins were generated in almost all parts of geologic column. As it seems, in parallel with them, siderite veins were created too (at temperatures around 186 ^{o}C). Finally, in the third phase, barite was created in several places in the region in all formations except in the Neogene formations [16]. These were the fundamental data on the basis of which the Metallogenetic map of Ljubija Ore Region 1: 50.000 was made.

7 METALLOGENETIC REGIONALISATION AND CLASSIFICATION THE PERSPECTIVE AREAS OF THE LJUBIJA REGION

The all iron deposits are genetically related and close in age and have been developed in the framework of distribution the major, medium and minor deposits, and a large number of ore occurrences and widespread mineralization. Metallogenetic regionalization of the Ljubija area was carried outd. Smaller ore-bearing areas with the identified ore and mineralization, and favorable geological conditions for finding the other ones have been isolated and contoured. Smaller metallogenetic units are characterized not just by the individual geological position in the main structures of the Ljubija ore region and separation by smaller or bigger areas without ore, but also by different conditions of localization their ore formations and mineralization, and their affiliation to different ore formations. Smaller metallogenetic units within the Ljubija ore region are the ore zone, ore knot and ore field (Figure 3).

A prognostic map represents ranging of areas in the present level of exploration. Before current map, two - three accurate maps, similar to these maps of this area, were published. One of them was made by M. Šarac where the iron occurrences and deposits were plotted inside by his opinion, the overall ore - bearing Carboniferous rock layers of Sana - Una Paleozoic. According to this author, those are the prospective surfaces, and non-prospective would be all peripheral areas which are built of other stratigraphic units [5].

The different areas are marked on the Prognostic map of this study, according to the prospectivity, taking into account the quantitative (appearance and size of the ore bodies, excavated mass, potential resources...) and qualitative indicators (primarily chemical composition of the ore), followed by the control factors (stratigraphic, lithological, structural) and indications of mineralization (ore outcrops, alteration around the ore, indicator elements). In general, there are three major categories on the map as follows: prospective areas where exploration is justified with four groups of fields from the first instance fields to the insufficiently explored, followed by the are as where the additional exploration is not required at the present moment with two groups of fields and third non-prospective areas out of the ore zones and nodes. Isolated surface areas, most commonly, represent the geological units or units by the exploration level. They can be reclassified into the units of different prospectivity then they are at this stage of knowledge.

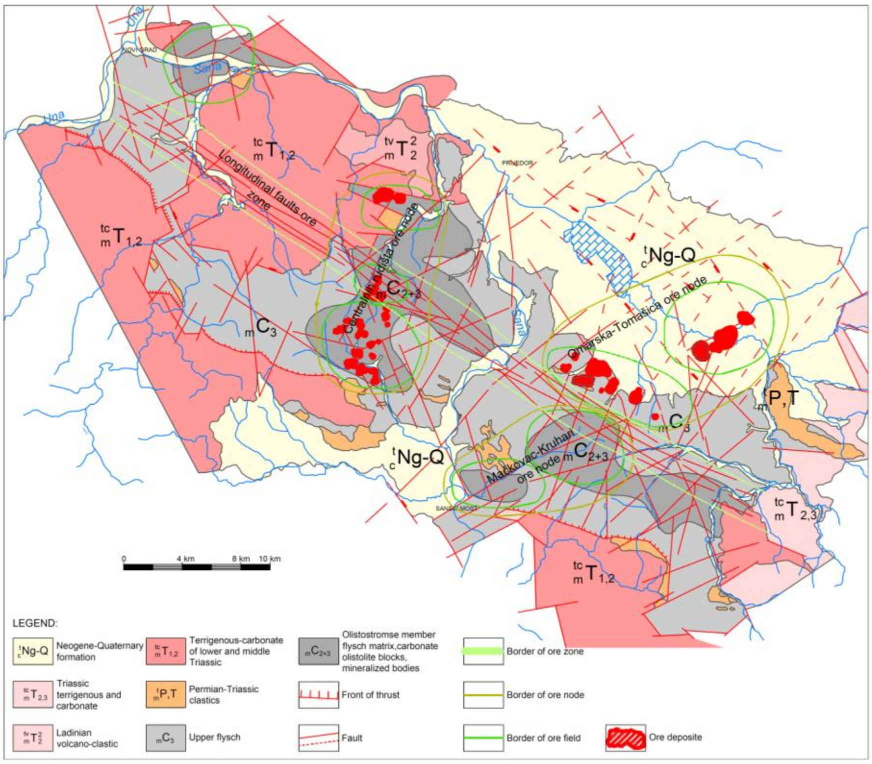

Figure 3 *Formation - geological map of the Ljubija ore region [4]*

REFERENCES

[1] Janković, S., Jelenković, R. (2000): Metallogeny of the Dinarides. Collection of Works Geology and Metallogeny of the Dinarides and Vardar Zone, p. 281- 305. Academy of Science and art of the Republic Srpska, Banja Luka (in Serbian)

[2] Janković, S. (1987): Interpretation of Test Data Obtained in the Period 1986/87, Faculty of Mining and Geology, Belgrade, p. 1-23. Ibid (in Serbian)

[3] Jurić, M. (1971): Geology of the Sanski Paleozoic Area in the

northwestern Bosnia. Special Editions of the Geological Gazette, Book XI. p. 1-146. Sarajevo (in Serbian)

[4] Grubić, A., Cvijić, R., Milošević, A. & Čelebić, M. (2015): Importance of Olistostrome Member for Metallogeny of the Ljubija Iron Ore Deposits. Arch. Techn. Sci., 13/1, p.1-8.

[5] Katzer, F. (1921): Geologische Uebersichtskarte von Bosnien-Herzegovina, 1:200.000 Drittes Sechstellblat: Banja Luka. Wien.

[6] Grubić, A., Protić, Lj. (2003): New Contributions to the Geology and Metallogeny of the Iron Mine Ljubija, p. 63- 137. Mining Institute. Prijedor (in Serbian)

[7] Milošević, A., Alekseev, A., Zaytseva, E., Novak, M., Kolar - Jurkovšek, T., Jurkovšek, B. (2021): Late Carboniferous Biota from the Ljubija Iron Mine Area, Bosnia and Herzegovina. Geologija, 64/1, p. 65 – 80. Ljubljana.

[8] Garašić, V. & Jurković, I. 2012: Geochemical Characteristic of Different Iron Ore Types from the Southern Tomašica deposit, Ljubija, NW Bosnia. Geol. Croat., 65/2: 255-270.

[9] Jurić, M. (1975): Interpreter of the Basic Geological Map of the SFRY, 1: 100 000 Sheet Prijedor. Federal Geological Survey, Belgrade: pp. 55 (in Serbian)

[10] Milošević, A., Grubić, A., Cvijić, R., Čelebić, M. (2017): Annexes the Knowledge of Metalogenia of the Ljubia mineral area. Proceedings, 7th Balkan Mine Congress. Prijedor, p. 57-68.

[11] Karamata, S. (1990): Report on the Study of Igneous Rocks in the Vicinity Ljubije - Prijedor in 1989. Faculty of Mining and Geology, Belgrade, p. 1-13. Ibid. (in Serbian)

[12] Pamić, J. and Lovrić, A. (1980): Geological and Isotopic Age of the Rift Magmatism of the Mesozoic Wilson Cycle. Ibid, p. 251-259. Belgrade (in Serbian)

[13] Mudrenović, V., Nenadić, D. (1996): Tectonics and Metamorphism of the Terrain Between Donje Ljubije and Majdan Mountains. Geological Annals of the Balkan Peninsula, Vol. 60, Book 1, p. 107-118. Belgrade (in Serbian)

[14] Jurković, I. (1961): Minerals of the Iron Ore Deposits of Ljubija near Prijedor. Geological Journal, No. 14, p. 161-220. Zagreb (in Serbian)

[15] Šarac, M. (1981): Metallogenetic Characteristics of the Ore-Bearing Area of Ljubija. Doctoral Dissertation Defended at the Faculty of Mining and Geology in Belgrade, p. 1-135. Zenica (in Serbian)

[16] Strmić-Palinkaš, S., Spangenberg, J. E. i Palinkaš, A. L. (2009): Organic and Inorganic Geochemistry of the Ljubija Siderite Deposits, NW Bosnia and Herzegovina. Min. Deposita, Vol. 44, No. 8, str. 893-913. Springer Verlag.

MINING AND METALLURGY INSTITUTE BOR
UDK: 622

ISSN: 2334-8836 (Štampano izdanje)
ISSN: 2406-1395 (Online)

UDK: 550.8.05:622(045)=111
DOI: 10.5937/mmeb2104017T

Received: 28.10.2021.
Revised: 29.11.2021.
Accepted: 28.12.2021.

Original Scientific Paper
Geotechnics

Dušan Tašić, Lidija Đurđevac Ignjatović*, Dragan Ignjatović*,
Vanja Đurđevac*, Sead Softić***

DETERMINATION OF SOIL DEFORMATION MODULUS USING THE STATIC AND DYNAMIC CIRCULAR PLATE LOAD TEST***

Abstract

The increase in mining activity in the Bor basin in recent years has also required the construction of new mining facilities. The construction of numerous embankments and dams, as parts of these facilities, required a constant control of compaction the coarse-grained and fine-grained materials from which they were built. The compaction check was performed using the static and dynamic circular plate test. The results of measurement and correlation of static and dynamic deformation modulus for multiple types of materials, used during construction, are presented.

Keywords: *circular plate test, deformation modulus, mining facilities*

1 INTRODUCTION

In situ geomechanical tests include checking the deformation modulus with a static and dynamic circular plate. Verification of the achieved compaction on the construction site is done in accordance to the technical specifications of the works, and it is based on the individual tests at a certain distance, certain area or depending on the amount of installed material. Standard tests of soil compaction, based on domestic technical regulations, are carried out according to the standard SRPS U.B1.046: 1968. Standard tests of soil compaction, on the basis of domestic technical regulations, are carried out according to the standard SRPS U.B1.046: 1968, which determines the static modulus of soil elasticity M_s. For this method of testing, it is necessary to provide a massive counter load for the load on plate, which significantly complicates the performance of experiment itself. In domestic practice, a non-standardized experiment with a dynamic circular plate (with a free-falling weight) has been used lately. A dynamic deformation modulus was obtained (E_{vd}) as a test result. The advantage of this method is on mobility of the testing device, and access to all parts of the facilities, as well as the fast measurement without the need for counterweight.

2 FIELD INVESTIGATIONS

In the field, at the locations planned for the construction of buildings, embankments or hydro-technical facilities, the tests were performed first with a static circular plate (Figure 1), and then a compaction control, on the same material, was

* *Mining and Metallurgy Institute Bor, Zeleni bulevar 35, 19210 Bor, Republic of Serbia*
** *International University of Travnik, Travnik, Bosnia and Herzegovina*
*** *This work was financially supported by the Ministry of Education, Science and Technological Development of the Republic of Serbia, Grant No. 451-03-9/2021-14/200052*

tested by the multiple dynamic circular plate tests (Figure 2).

The largest number of measurements was performed on the coarse-grained soil composed of crushed andesite, as the most dominant by-product of mining. The second tested embankment material consisted of a mixture of dusty-clay material and crushed stone, suitable for the construction of embankments, and can be found in the large quantities in near-surface parts of the terrain around Bor.

Figure 1 *Performing a test using the static load plate*

Figure 2 *Performing a dynamic plate load test (light falling weight device)*

3 CORRELATIONS OF THE TEST RESULTS

Recommended correlations relationships, according to the Austrian regulation, of dynamic (E_{vd}) and static (M_s) soil modulus, which can be used for different types of materials, are as follows:

- Cohesive soils
  $E_{vd} \leq 30$ MPa – $M_s = 1{,}75(E_{vd} - 10)$
- Granular soils
  – $E_{vd} \leq 30$ MPa – $M_s = 1{,}16E_{vd}$
  – $E_{vd} > 30$ MPa – $M_s =$
  $1{,}42\ (E_{vd} - 30) + 35$

Simultaneously with the tests of determining the modulus of soil elasticity for the most commonly used materials that were installed, the correlations, shown in Figure 3 and Figure 4, were obtained. Tests were performed for a wide range of required compaction conditions and construction stages.

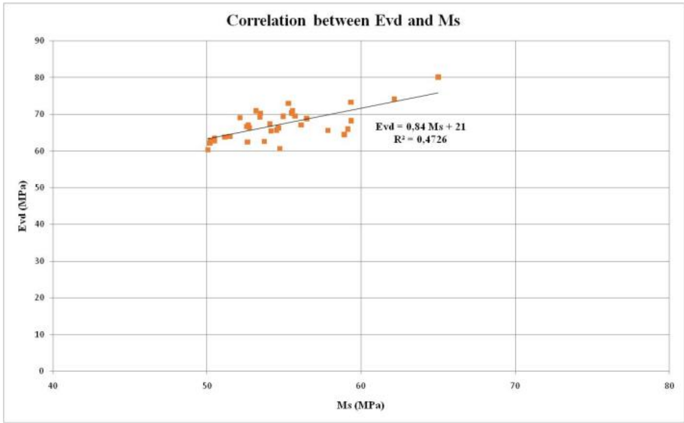

Figure 3 *E_{vd} - M_s correlations for crushed andesite material*

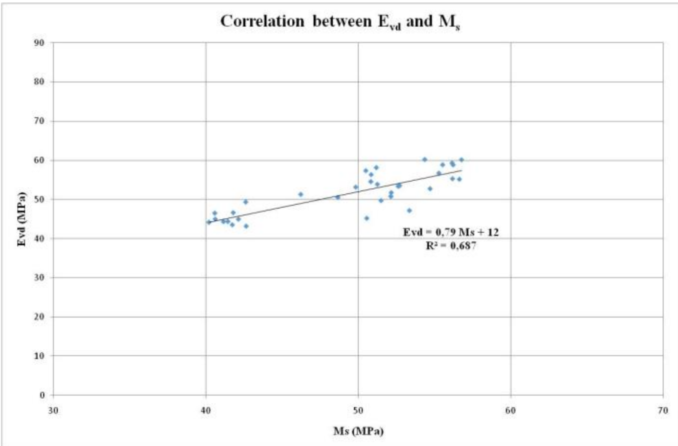

Figure 4 *E_{vd} - M_s correlations for mixed clay-stone material*

4 CONCLUSION

A large number of simultaneous measurements, i.e. checks of compaction the static and dynamic modulus of elasticity, were carried out on the most common materials used in construction the new mining facilities in Bor and its surroundings. The results of these parallel experiments and correlations of the obtained values for E_{vd} and M_s, can be considered sufficiently competent for these materials in further checking the compaction of these materials, because their use for similar purposes will continue in the future, and geomechanical practice will in the future strive to standardize the method with light falling weight device.

REFERENCES

[1] C. Adam, D. Adam, C. Kopf., I. Palmichl. Computational Validation of Static and Dynamic Plate Load Testing. Acta Geotehnica (2009) 4: 35-55 DOI 10.1007/s11440-008-0081-0

[2] S. Tošović, V. Vujanić, Classic and Modern Control of Materials Compaction during the Road Construction with Particular Reference to the Permanent Control, Highway Institute AD Belgrade, Serbia

[3] S. Samardaković, G. Šulović, M. Samardaković, C. Author., Correlations between Soil Deformation Moduli Measured by Dynamic and Static Circular Plate Load Test, TEIK 2010 Civil Engineering Geotechnics

MINING AND METALLURGY INSTITUTE BOR
UDK: 622

ISSN: 2334-8836 (Štampano izdanje)
ISSN: 2406-1395 (Online)

UDK: 622:669(497.11)"04/14"(045)=111
DOI: 10.5937/mmeb2104021N

Received: 13.07.2021.
Revised: 13.09.2021.
Accepted: 15.11.2021.

Original Scientific Paper
Metallurgy

Branislav Nikolić, Željko Kamberović**, Nikola Jovanović**,*
*Vesna Vujačić****

MINING AND METALLURGICAL ACTIVITY IN THE MEDIEVAL SERBIA

Abstract

The mining and metallurgical activity has a centuries-old tradition in Serbia. Copper, iron and gold are the basic metals in the ore of eastern Serbia. Lead, zinc, iron and silver ore are present in central Serbia, while antimony and lead ore are predominant at the location of western Serbia. The strength of Nemanjic's Serbia was mostly based on the development of this activity. With the arrival of the Turks, the mining and metallurgical activity weakened, and at the beginning of the 18th century it completely become extincted. Almost all current mines of polymetallic ores in Serbia appeared on the locations of medieval mines.

Keywords*: mining, metallurgy, foundry, medieval Serbia, gold, silver, copper, iron, lead, zinc*

1 INTRODUCTION

In the area of today's Serbia, south of the rivers Sava and Danube, there are several deposits of polymetallic ore that have been exploited since ancient times. The strength of the ancient Hellenes, Illyrians, Romans, Byzantines and then Nemanjić in the Middle Ages, was largely based on tools, weapons, money, jewelry and other metal products from these mines. There is a record that in the ancient times "Egyptian masters exploited gold from the source of the river Nile to the slope of the Carpathians" [1]. So, they exploited gold in the area of the current Bor - Majdanpek region, which is still one of the important producers of copper and gold. It is estimated that about 200 tons of gold were mined in Serbia in the period from 1250-1990 [1].

In central Serbia, from Avala, further south of Kosmaj, Rudnik, Kopaonik, Rogozna, Majdan mountain, Kriva Feja, in the east Bor-Majdanpek region, in the western Serbia Krupanj-Loznica region, all these are areas where there are several sites of nin-ferrous, precious, ferrous and other metals. Many of these deposits were exploited in the old century, and in addition to the mines, the smelters, mints, foundries and other metallurgical plants for metal processing were there.

Sočanica, a settlement between Zvečan and Leposavić, used to be the seat of Roman mining supervision, and the money of Alexander the Great and later Emperor Theodosius in the new century was minted on Kriva Feja and Blagodat [2]. Roman money was minted near Gračanica in the

* *Engineering Academy of Serbia, Belgrade, Serbia, Contact e-mail: nikolic_br@yahoo.com*
** *University of Belgrade, Faculty of Technology and Metallurgy, Belgrade, Serbia*
*** *University of Donja Gorica, Podgorica, Montenegro*

time of Emperor Trajan ("Metallum Ulpianum"), in Rudnik in the time of Septimius Severus, and in Medvedja (Lece) in the time of Emperor Constantine [2].

The invasions of the Huns and Avars, as well as the migration of peoples from the 5th to the 9th century, slowed down or stopped the exploitation of mines, and after this period, the mining and metallurgical activities developed as well as the power of the Serbian state strengthened. During the reign of Stefan Nemanja and other Nemanjićs, and especially during the reign of King Uroš I, until the arrival of the Turks, practically until the fall of Novi Brdo in 1455, the full development of mining and metallurgy in Serbia took place.

2 THE PERIOD UP TO THE FIFTEENTH CENTURY

After the 10th century, there was a constant development of mining and metallurgical activities. John of Ephesus wrote in the 6th century that the South Slavs "… have gold and silver, horse stables and many weapons ..." [2]. The Frenchman Brockier and the Byzantine Critovul wrote about the deposits of silver, gold and lead in Serbia in the 15th century [2]. In 1433, Brokier wrote that there were five gold and silver mines in Serbia.

The flourishing of mining and metallurgy in Serbia occurred, especially, after the arrival of the Sasa-Germans from Erdelj and the Romanian Banat during the reign of King Uroš (1243-1276) and Jelena Anžujska in the second half of the 13th century. At each mine there was a colony of foreign workers and merchants; Sasa, from Dubrovnik, Kotor, Greece and others. who lived according to their own autonomous laws and customs. Sasa formed the settlement of Janjevo near Gračanica, where they have survived to this day, so they are known as "Janjevci" and as hardworking and good craftsmen. The King Uroš I signed an agreement on trade with the people of Dubrovnik in 1276 for five years, and in 1281 this agreement was extended indefinitely.

The Lese ore deposit is mentioned in 1280 as a colony of Kotor and Dubrovnik [2].

In the Dubrovnik records "Trepca" was mentioned for the first time in 1303, and many Dubrovnik families who lived next to the mines of Serbia (Lukačević, Prodanović, Bobalević, etc.) were also recorded.

The Kopaonik mines and "Trepca" in Stari Trg had the greatest power in the 13th and 14th centuries, and Novo Brdo in the first half of the 15th century during the time of the despot Djuradj Brankovic (1427-1456). The Law of Emperor Dušan from 1346 defined the rules for exploitation, production and processing of metals. This law prescribed very strict rules, especially for gold and silver processors. Important centers had their own local law both before and after the Emperor Dušan: the Janjevo, Sasi, Novobrdo, Rudnik, Dubrovnik, Kotorand other laws. Despot Stefan Lazarević (1389-1427) passed the unique Mining Law in 1396, incorporated local laws into it, and supplemented and finally confirmed it on January 29, 1412 [3]. One of the signatories of this second law was Bogdan Jug, obviously the grandson of the old Jug Bogdan and probably the son of the oldest of the Jugović brothers, Boško Jugović, because according to the old and current Orthodox custom, the first grandson got his grandfather's name. The signatories of this law were Radič from Trepča, Lovren and Tripun from Rudnik and several craftsmen, what testified to the versatility of the issuer and author of this law. The first Serbian coins made of silver (electron) and copper (billon) appeared during the reign of King Radoslav (1228-1234), and the following kings also had their own coins: Vladislav (1234-1242), Uroš I (1242-1276), Dragutin (1276-1282), Milutin (1282-1321) and other rulers. There are records that the mint worked in Mojkovac during the reign of King Uroš I, in Trepča around 1400, and Prince Lazar had a mint and especially a mint of weapons.

Trepca and Janjevo are mentioned in 1303, Novo Brdo in the time of King Milutin, and Podrinje's Crnča in 1352, Bo(hor)rina in 1415 and Krupanj in 1422. In 1328, Janjevo is said to have iron ore and a foundry [3].

The main merchants were from Dubrovnik and in 1422 they exported 5672 kg of silver from Serbia. Their headquarters on Kopaonik were in 1426 in the settlement of Kovači, where there were several iron mines and smelters. Djuradj Brankovic leased 200,000 ducats a year to the people of Dubrovnik for Novo Brdo [3]. In 1422, there was an iron mine, smelter and foundry in Krupanj. Many called Kopaonik a "silver mountain", and in the 15th century, the Byzantine writer Kritovul described Serbia as "the seat of all countries and one Maidan of gold and silver". Many settlements were named after the type of activity present: Kopaonik, Rudnik (Majdan) Rudare, Rudnica, Kovači, Ljevoša (foundry, near Peć), Bakarnjača, Železnik (now Majdanpek).

In the 14t^{h} and 15th centuries, the lead ore was exploited on the Rogozma mountain, gold was washed in streams, and in Gluha Vas there was an iron mine and smelter that was processed in the neighboring Novi Pazar. In Stari Trg and its surroundings there were eight deposits of lead-zinc ore in the 14th century; the richest in silver were the ore of Novo Brdo, Rudnik and Stari Trg ("Trepča"), and with gold the Lece deposit (Medveđa), all mines as in today.

In the period 1426-1432, the Kabušić brothers, from Dubrovnik, exported 3,500 kg of silver from Novo Brdo, out of which about 93% was shipped to Italy [7].

There were several deposits of polymetallic ore in the Podrinje area, copper ore in Lipnik near Krupanj, and lead-copper ore in Kučajna and Rudnik. There are about 250 remains of the old smelters and metallurgical slags in Trepča and Kopaonik [3].

The main export of silver and other metals from Serbia was done by the people of Dubrovnik and Kotor with their caravans, and at the end of the 14th century, about one ton of gold was produced in Serbia annually. In the time of Nemanjić, many churches and monasteries were built in Serbia, which were covered with lead sheets, and this lead tin roof has survived to nowadays.

With the arrival of the Turks, the foreign workers and traders left and mining and metallurgical activities gradually weak. After the Battle of Kosovo, the despots Stefan Lazarević and Djuradj Branković, as well as Serbia, had the vassal autonomy. In the mining and metallurgical centers, there were mostly Turkish and Serbian officials, and the Turks incorporated the existing Serbian mining laws into their own, which they passed in 1520, 1536, 1566, and for Novo Brdo in 1494. [3] These laws of the Suleiman the Magnificent (1520-1566) were called the Canons and were based on the Muslim religious law.

The Serbian despotism was abolished by the Turks in 1459, four years after the fall of Novo Brdo, and after that, a completely Turkish period arose.

It is officially believed that the Middle Ages ended with the discovery of the "New World", i.e., the discovery of a new continent: America, discovered by Christopher Columbus (1492) and Amerigo Vespucci (1499 and 1501/02). America is also named after Amerigo. Some countries move that border of the Middle Ages, depending on their situation, and that was the time of great changes, renaissance, humanism, inquisition, etc.

This work also covers the time after 1500, because the mining and metallurgical activity in Serbia was intensive in the 16th century, and then it weakened and died out only at the end of the 17th century.

3 THE TURKISH ERA

Although it is officially considered that the Turkish time came immediately after the Battle of Kosovo in 1389, for the next 30 years the Turks did not appear much in Serbia. The Despot Stefan Lazarević fulfilled his vassal obligations towards Turkey, so as a vassal of Sultan Bayezid, he participated with his armored men in the famous battle near Angora (Ankara), in 1402, in which Khan Tamerlane defeated and captured the Sultan Bayezid. At that time, the Serbian armored men were the most elite soldiers, and Tamerlane respected knowledge; he was a top astronomer and his court was the world's strongest astronomical center. Tamerlan allowed Stefan Lazarevic and Djuradj Brankovic to return to Serbia with their army, but he previously singled out masters, masons, carpenters, foundries, miners and other craftsmen from the Serbian army and kept them in Turkey for his own needs. Serbian armored vehicles were known in the 14^{th} century and in the battle of Kosovo, but primarily thanks to highly developed metallurgy, i.e., high-quality manufacturing of armor, shields, spears, sabers and other weapons. There were various types and shapes of armor: plate, wire (mesh), for people, horses, etc. And that is a specific field of metallurgy that had a long tradition in Serbia. In other words, the foundry and metal processing were highly developed activities in Serbia in the period 1200-1700.

In the middle of the 15^{th} century, the mining and metallurgical town of Novo Brdo, which is about 20 km east of Pristina, had about 40,000 inhabitants and was one of the largest European centers. At that time, for example, London had only about 5,000 inhabitants. The Turks had already conquered Belgrade and the area up to Belgrade, and Novo Brdo was still independent, under the Serbian rule. The had its own mine, foundries, production of weapons, money, food and its own economy. For two years, the Turks unsuccessfully attacked and besieged it, but they did not capture it until 1455. Outraged by the resistance of the people of Novo Brdo, the Turks destroyed Novo Brdo in 1455, and in 1456, 50,000 Serbian prisoners from Novo Brdo and the surrounding area were sold at the Constantinople Slave Market. After this, the Novo Brdo area never recovered, and that was a breakdown for the Serbian mining and metallurgical activity, as well as for the Serbian state.

The Turks occupied Rudnik in 1438, and in the period from 1442-1518 the people of Dubrovnik mined silver and copper from Rudnik. The 743 kg of pure silver was produced in Rudnik in 1516, and in the period 1476-1523, 740-820 kg of silver was produced [3]. In the middle of the 16^{th} century, the iron ore was exploited, from which the cannon balls were cast.

In the village of Ba (Suvobor), in the second half of the 16^{th} century, the smelters and foundries operated in which weapons, cannonballs and mining tools were produced.

In the Takovo region and on Kosmaj, there are still landfills of foundry slag. The Turks captured Kučajna and Braničevo in 1439, and in 1553 Kučajna became the center of the Cadillac and the main mining and metallurgical center of this region [3]. In 1829, Otto Pirch wrote that there was a mine in Kučajna in the time of Prince Lazar. The Trepca mine, foundry and market in Stari Trg had 521 households at the end of the 16^{th} century, and only 50 households at the end of the 17^{th} century, during the Austro-Turkish wars.

In Turkish times, the wealthier Serbs leased certain mines in Podrinje, Rudnik and Kopaonik until 1540, but the Turks took power and control, taking metal and metal products to Constantinople, and the Sasi, Germans, people from Dubrovnik, Kotorans and others foreigners left Serbia, which meant a decline in mining and metallurgical activities in Serbia.

The Austro-Turkish wars at the end of the 17th century and in the first third of the 18th century resulted in great migrations of Serbs in 1690 and 1735, after the defeat of Austria, on whose side the Serbs fought. Then, in 1690, the fleeing from Turkish revenge and terror, 37,000 Serbian families from Kosovo, Metohija and other parts of Serbia crossed the rivers Sava and Danube and settled in Austro-Hungary. Apart from the Serbs, the foreign craftsmen and merchants also left Serbia, so after these wars and migrations, the exploitation of mines in Serbia practically stopped, that is, the mining and metallurgical activity stopped.

In Serbia, on the sites of former smelters and foundries, there are a large number of landfills of their slag with a significant content of useful metals. These slags can be processed in modern production under certain conditions. This is the case, for example, in the "Trepca" lead smelter in Zvečan, in the period 1968-1975, 800-1200 t of old slag were processed annually, which in practice are called the "Roman slag" and which contained 8-9% lead, 2-3% zinc, 30-40% iron, 1-2% antimony, 0, 02-0.05% silver, etc. Metal slag recycling is an integral part of modern production. These slags are still present in the village of Babe, near Ralja.

4 FOUNDRY

Casting and processing of money and jewelry, mints and filigree have always been present in the mining settlements. Casting of church bells, cannon pipes and cannons belongs to a specific and highly professional metallurgical field. Due to the mass construction of churches and monasteries during the Nemanjić's time, there was a need to manufacture the church bells, which also contributed to the development of foundry. The quality of metal, size, mass and dimensions of a bell, as well as the specific properties of a pendulum, affect the quality, type and power the sound propagation of a particular bell.

The two oldest preserved medieval church bells in Serbia are the two Rhodope bells, which were cast in August 1432 [5]. Little is known about the Rhodopes, it is only known that he was one of the prominent lords in the time of Djuradj Branković, with whom he participated on the side of Sultan Bayazit in the battle of Angora, in 1402.

The first, the older bell, donated by the lord Rhodope, was donated to the Monastery of the Mother of God Hvostanska, which was also called Mala Studenica, and it was the seat of the episcopate in the 12th century and since 1381 the seat of the metropolitanate in the parish Hvosno [5]. This monastery was located in the present village of Studenica, near Pećka Banja, in the north of Metohija in the municipality of Istok, about 15 km east of Peć. It is written that, before the arrival of the Turks, this monastery received milk through ceramic pipes from the mountain Kopaonik, which is above this monastery. In this monastery, Saint Sava reconciled the brothers Stevan and Vukan and persuaded them not to fight against each other. After the migration of Serbs 1690-1735, the monastery was demolished, and from the stones of the monastery walls, the settlers Arnauts built houses and a mosque in the middle of the present village. There are still many remains of the monastery walls, but the Serbs never researched anything, so they did not even restore this archeological site. When the Arnauts excavated and took stone from the monastery walls in 1891, they also excavated a bell that read: “Most Holy Mother of God, receive this small contribution from the many sinful slaves of your Rhodopes in the summer of 1432, on the 2nd day of August, very sinful Rhodope” [5]. This bell was bought by the then Vice

Consul of Serbia in Pristina T. Stanković with the help of Nikola Pašić, Minister of Foreign Affairs of Serbia. This bell is soprano in sound, Figure 1.

Figure 1 *The older Rhodope bell*

The second Rhodope bell, Figure 2, was found in the village of Banje about 15 km east of the previously described Monastery in the village of Studenica. Before 1432, Rhodope built the church of St. Nicholas, in the village of Banje as his endowment, and in Turkish times this church was destroyed. When the inhabitants of the village of Banje wanted to renovate this church in the 19th century, they found and excavated another, younger, Rhodope bell. Banje is still a purely Serbian village. The Turks did not allow the reconstruction of this destroyed church, so the Serbs from Banja buried the bell to hide it from the Turks, who then melted the church bells and made weapons out of them. In the First World War, in 1916, the Austro-Hungarian soldiers searched for buried Serbian cannons and ammunition in the entire Spa, found and excavated this Rhodope bell and transferred it to the Patriarchate of Peć, where it is still kept in the treasury. This younger bell bears the cast date of August 11, 1432, it sounds like an alto, and the donor dedicated it to the church of St. Nicholas in the village of Banje, and on it is the figure of St. Nicholas. This church was destroyed until 1930, when the locals began to rebuild it, and then, next to the south wall of the church, they discovered Rhodope's tombstone with an epitaph on which it says that Rhodope died on February 7, 1436.

There is little information about Rhodope, and it is only known that he had brothers Nikola and Stefan and that he was married to Olivera with whom he had two sons, Jovan and Stepan.

The people of Dubrovnik made cannons in the 15th century. In addition to the master casters from Italy, the masters from Serbian areas were also engaged in casting cannon tubes and making cannons. In the 15th century, Ivan Ognjenović, Marko Progonović, Radoje, Milorad, and Domko Nikolić worked in Dubrovnik as the "bombers". Many historians write about these masters that they are from Dubrovnik, however, their origin and reality are different. There are still a lot of Ognjenovićs in Montenegro and Serbia. Progonovićs is mentioned in "Gorski vijenac" and it is a settlement in Montenegro. The Nikolićs then lived from Popovo Polje to Nikšić (Zahumlje). Radoje and Milorad are Serbian names, not Dubrovnik, Latin. A bell was excavated near Čačak, which says that it was made in 1454 by the caster Radoje Milišić. It is obvious that this is the same Radoje who also worked in Dubrovnik as a foundryman. That Serbia had developed this activity is evidenced by the letter of Alfonso the Beautiful, King of Aragon and Naples, despot Djuradj Brankovic, in 1455, to send him 6 masters "... because it is known that you have excellent and experienced people to find and clean silver wires and gold ... “.

Figure 2 *The younger Rhodope bell*

5 CONCLUSION

Exploitation and processing of polymetallic ores in the area of present-day Serbia has a centuries-old and even millennial tradition. The golden age of the mining and metallurgical activity in Serbia in the Middle Ages was in the 13th, 14th and the first half of the 15th century. The production and processing of lead, copper, silver and gold decreased after the arrival of Turks, and finally stopped after the Austro-Turkish wars and the migration of Serbs at the end of the 17th and in the first half of the 18th century.

In Karadjordj's time, the renewal of mining began, especially at Rudnik, but only after the internal autonomy of the hatisherifs in 1830 and 1833, the conditions were created for the renewal of this activity.

With the formation of the Technical Faculty in 1863 and enactment the Mining Law in 1866, the conditions were created for the actual renewal of mining and metallurgical activities in Serbia.

Each country bases its development on its own natural potential. Mining and metallurgy have always been one of the key carriers of Serbia's development. When this activity was intense, strong, Serbia was also strong, and the development of this activity in the time of Nemanjić coincides with the development of the Serbian state.

The current mines of polymetallic ores of non-ferrous and precious metals are practically based on the medieval mines of these metals.

REFERENCES

[1] B. Nikolić, Increasing the Use of Precious Metals, Study for the MMC Combine "Trepca" Kosovska Mitrovica, 1969 (in Serbian)

[2] M. Janjušević, Lj. Božović, F. Agoli, Lead and Zinc Combine "Trepca". Kosovska Mitrovica, Jubilee Monograph, 1974 (in Serbian)

[3] P. Jovanović, Mining on the Territory of Serbia I, Publisher JINA, Belgrade, 2007 (in Serbian)

[4] S. Ristić, Decani Monument, Belgrade, 1864 (in Serbian)

[5] Z. Antonijević, Sinful Rhodope Casted the Oldest Church Bell, 04/01/2009 (in Serbian)

[6] B. Nikolić, Radoje livac and the people of Dubrovnik, "Express Politics", Belgrade, January 29, 2002 (in Serbian)

[7] B. Nikolić, Ž. Kamberović, V. Nikolić, Silver in the Medieval Serbia, Technology - Mining, Geology and Metallurgy, 57 (3) (2006) 15-18 (in Serbian)

MINING AND METALLURGY INSTITUTE BOR
UDK: 622

ISSN: 2334-8836 (Štampano izdanje)
ISSN: 2406-1395 (Online)

UDK: 622.271/.68:662.75(045)=111
DOI: 10.5937/mmeb2104029J

Received: 29.10.2021.
Revised: 29.11.2021.
Accepted: 29.12.2021.

Original Scientific Paper
Mining

Jasmin Jamaković, Sunčica Mašić***

FUEL CONSUMPTION OF THE BELAZ DUMP TRUCKS ON AN EXAMPLE OF THE OPEN PIT "TURIJA" OF THE BROWN COAL MINE BANOVIĆI

Abstract

This work sets out the methodology and presents the calculation results of fuel consumption of the BelAz dump trucks at the Open Pit "Turija" of the Brown Coal Mine Banovići itd. based on monitoring data. Properly determined fuel consumption allows the preventive measures and selection of strategy to reduce it. Data collection took six months, the data were analyzed, and thus the results by month of all dump trucks were presented.

Keywords: *dump truck, BelAz, fuel, open pit, coal, overburden, maintenance, Brown Coal Mine Banovići*

1 INTRODUCTION

The main activity of the Brown Coal Mine "Banovići" Ltd. Banovići is the production, processing and trade of brown coal, which is based on the balance reserves of about 165,249,697 million tons of brown coal. Most of these reserves are intended for excavation by the underground mine exploitation (about 95 million tons), and the rest (of about 70 million tons) by the open pit exploitation. Coal is produced by the open pit and underground exploitation in two mines that operate within this company, namely: the Mine "Open Pit Exploitation of Coal" (with two open pits) and Mine "Underground Exploitation" (with one underground mine"Omazići").

After the period of delayed exploitation, reactivation was started at the Open Pit "Turija", while at the Open Pit "Grivice", a continuous exploitation is carried out from the day of opening starting from the northern outcrop to the deepest coal reserves on the south side.

The open pit "Turija" was selected for the subject research. A total of 14 dump trucks are used for transport at OP Turija, namely: 12 diesel-electric trucks BelAz 75131 with a capacity of 136 t and 2 diesel-electric trucks BelAz 75137 with a capacity of 136 t. The BelAz trucks are with diesel-electric DC traction.

By a comprehensive research and collection of data on the parameters of truck transport at a specific location, it was necessary to conclude which parameters have the greatest impact on fuel consump-

* *RMU "Banovići"d.d. Banovići, B&H*
** *University in Tuzla Faculty of Mining, Geology and Construction Engineering, B&H*

tion at constant load in driving of useful and useless minerals. In order to perform the subject analysis, it was necessary to deter-mine the average monthly fuel consumption for each considered transport unit (dump truck). For dump trucks in the conditions of work at the OP "Turija" of the Brown Coal Mine Banovići, taking into account all relevant influencing factors, the average fuel consumption can be defined as well as measures to reduce it.

2 METHODS OF DATA COLLECTION AND PROCESSING

2.1 Methods of data collection

In the long-term practice of the BCM "Banovići", the method of data collection on the work and downtime of dump trucks is established. The mode of operation in the production facilities of the BMC Banovići is a three-shift eight-hour system. The data used in preparation of this work were taken from the database of the Department of Mining Technical and Operational Preparation of the Mine "Open Pit Coal Exploitation". The data were processed using Microsoft Excel licensed by the BCM "Banovići".

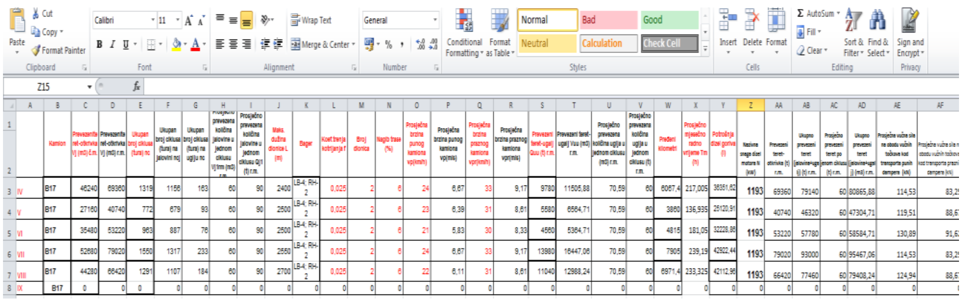

Figure 1 *Layout of a Microsoft Excel Sheet with inserted data for processing*

2.2 Methods of data processing

The most accurate method for determining the truck fuel consumption is to obtain data from actual mining operations. However, if such a possibility does not exist, various equations and data published by the original equipment manufacturer for trucks can be used for estimation purposes. Hourly fuel consumption FC (l/h) can be determined from the following equation [1]:

$$FC = P \times 0.3 \times LF \qquad (1.1)$$

where P is the engine power (kW), 0.3 is the unit conversion factor (l/kW/h) and LF is the engine load factor (part of the full power required by the truck). Values for the truck engine load factors according to some authors in the relevant literature range from 0.18 to 0.50, while the others state values between 0.25 and 0.75, depending on the type of equipment and level of use. [1]

For different engine load factors LF, the hourly fuel consumption FC (l/h) is shown in Table 1.

Table 1 *Hourly fuel consumption FC for engine power of 1193 (kW) and 1176 (kW) and various load factors LF*

Engine power 1176 (kW)		Engine power 1193 (kW)	
LF	**FC (l/h)**	**LF**	**FC (l/h)**
0.18	63.504	0.18	64.422
0.2	70.56	0.2	71.58
0.25	88.2	0.25	89.475
0.3	105.84	0.3	107.37
0.35	123.48	0.35	125.265
0.4	141.12	0.4	143.16
0.45	158.76	0.45	161.055
0.5	176.4	0.5	178.95
0.6	211.68	0.6	214.74
0.7	246.96	0.7	250.53
0.75	264.6	0.75	268.425
1	352.8	1	357.9

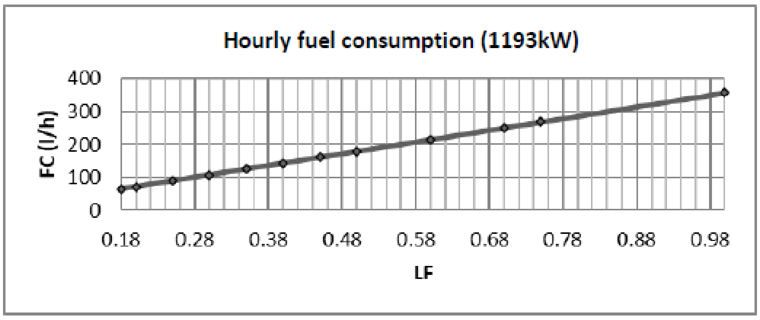

Figure 2 *Fuel consumption FC (l/h) for engine load factor values (part of full power required by truck) LF = 0.18 to 1 for engine power P = 1193 (kW)*

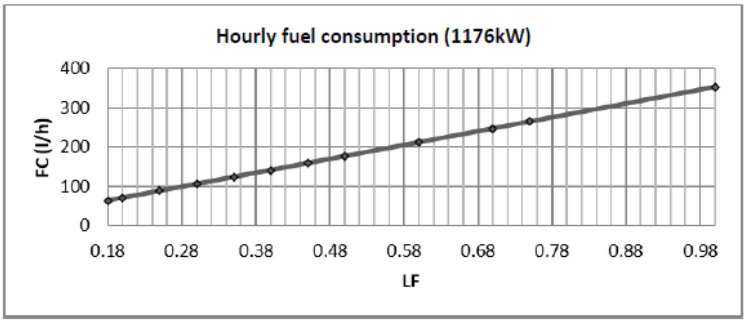

Figure 3 *Fuel consumption FC (l/h) for engine load factor values (part of full power required by truck) LF = 0.18 to 1 for engine power P = 1176 (kW)*

A similar equation for fuel consumption has been proposed in literature [1]:

FC = (CSF × P × LF) / FD (1.1)

where CSF is the specific fuel consumption for the engine at full power (0.213 - 0.268 kg/kW/h) (0.35-0.44 lb/HP per hour), P is the power (kW), LF is the engine load factor, and FD is the fuel density (0.8318 kg/l for diesel purchased by the mine). The following values for engine load factors are ecommended in literature: 25% (light working conditions), 35% (average working conditions) and 50% (difficult working conditions) [1].

Table 2 *Fuel consumption FC (l/h) for different SCF and LF (P = 1176kW)*

	FC (l/h)	**FC (l/h)**	**FC (l/h)**
LF	CSF=0.213 (kg/kW/h)	CSF=0.268 (kg/kW/h)	CSF=0.230 (kg/kW/h)
0.25	75.28492	94.72469	81.29358
0.35	105.3989	132.6146	113.811
0.5	150.5698	189.4494	162.5872
1	301.1397	378.8988	325.1743

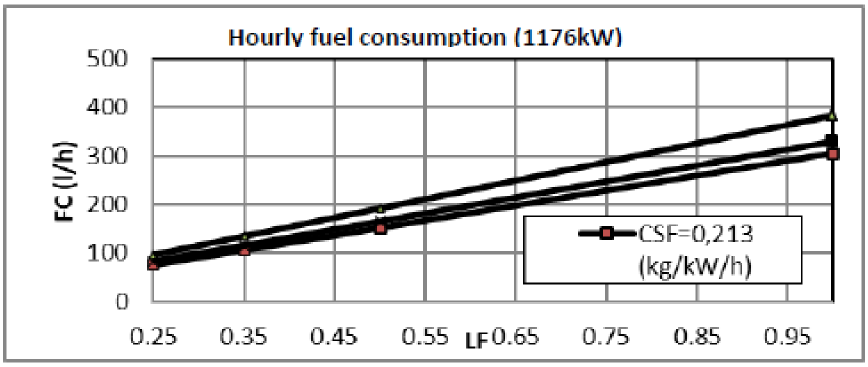

Figure 4 *Fuel consumption FC (l/h) for engine load factor values (part of full power required by truck) LF = 0.25, 1.35, 0.5 and 1 for engine power P = 1176 (kW) and specific CSF fuel consumption for the engine at full power*

Table 3 *Fuel consumption FC (l/h) for different SCF and LF (P = 1193kW)*

	FC (l/h)	**FC (l/h)**	**FC (l/h)**
LF	CSF=0.213 (kg/kW/h)	CSF=0.268 (kg/kW/h)	CSF=0.230 (kg/kW/h)
0.25	76.37323	96.09401	82.46874
0.35	106.9225	134.5316	115.4562
0.5	152.7465	192.188	164.9375
1	305.4929	384.3761	329.875

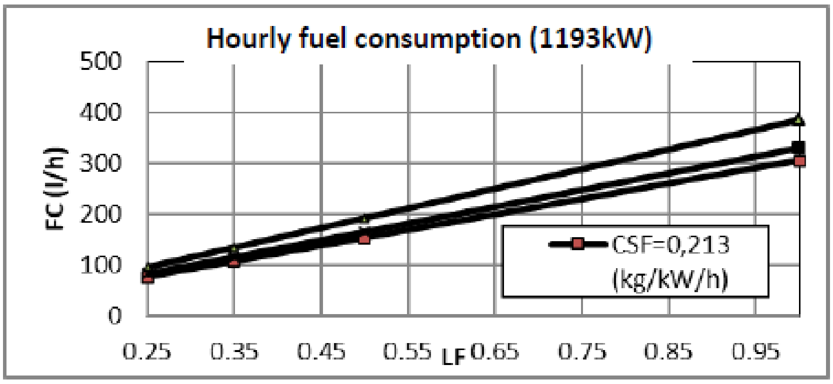

Figure 5 *Fuel consumption FC (l/h) for engine load factor values (part of full power required by truck) LF = 0.25, 1.35, 0.5 and 1 for engine power P = 1193 (kW) and specific CSF fuel consumption for the engine at full power*

Based on the collected and processed data, it was found out that the dump truck at the OP "Turija" worked in difficult working conditions, and the load factor of the LF engine had value of 45 to 50%.

Liebherr developed a method for determining the truck fuel consumption per hour. According to this method, the rate of fuel consumption is directly proportional to the delivered power [1]. Assuming that LF = 100%, the obtained fuel consumption would be 352.8 (l/h) for 1176 kW engine and 357.9 (l/h) for 1193 kW engine.

3 FUEL CONSUMPTION OF THE BELAZ DUMP TRUCK AT THE OPEN PIT "TURIJA"

Based on the data of the Operational Technical Preparation Service, the operating parameters of the BelAz dump truck with internal markings B-1 were calculated; B-2; B-4; B-5; B-6; B-7; B-8; B-9; B-10; B-11; B-15; B-16; B-17 and B-21. The BelAz dump trucks at the OP "Turija" transport both overburden and coal during their work. The average volume mass of the overburden in the solid state is ρ_{rmj}=2.25 (t/m^3), the average bulk density of the overburden in the loose state is ρ_{rmj}=1.5 (t/m^3), and the average looseness coefficient for overburden k_{rj}=1.5.

As an illustration of the calculated operating parameters of all dump truck individually, Table 4 and Figure 6 are highlighted for BelAz of internal code B-1.

Table 4 *Operating parameters of BelAz internal code B-1*

Month	Truck	Transported load- waste Vj (m^3) č.m.	Transported load- waste Vj (m^3) r.m.	Total number of cycles (tour), n_c	Total number of cycles (tour) on waste, n_{cj}	Total number of cycles (tour) on coal, n_c	Average amount of waste transported in one cycle, Vj1rm (m^3) r.m.	Average amount of waste transported in one cycle, Qj1 (t) r.m.	Maximum length of a section, L (m)	Excavator	Rolling friction coefficient f	Number of route sections	Slope of route (%)	Average speed of a full truck, v_p (km/h)	Average speed of a full truck, v_p (m/s)	Average speed of an empty truck, vpr (km/h)	Average speed of an empty truck vpr(m/s)	Cargo-coal transported Quu (t) r.m.
IV	B1	46920	70380	1253	1173	80	60	90	2400	LB-4; RH-2	0.025	2	6	24	6.67	33	9.17	4800
V	B1	35880	53820	947	897	50	60	90	2500	LB-4; RH-2	0.025	2	6	23	6.39	31	8.61	3000
VI	B1	37840	56760	978	946	32	60	90	2500	LB-4; RH-2	0.025	2	6	21	5.83	30	8.33	1920
VII	B1	37800	56700	1000	945	55	60	90	2550	LB-4; RH-2	0.025	2	6	24	6.67	33	9.17	3300
VIII	B1	29080	43620	805	727	78	60	90	2700	LB-4; LB-2	0.025	2	6	22	6.11	31	8.61	4680
IX	B1	34440	51660	1000	861	139	60	90	2600	LB-4; LB-2	0.025	2	6	24	6.67	33	9.17	8340

Transported cargo-coal Vuu (m^3) r.m.	Average transported amount of coal in one cycle (m^3) r.m.	Average transported amount of coal in one cycle (t) r.m.	Traveled km	Average monthly working time Tm (h)	Diesel fuel consumption (l)	Rated power of diesel engine N (kW)	Transported cargo-discovery (t) r.m.	Total transported cargo (waste + coal) (t) r.m.	Average transported cargo per one cycle (t) r.m.	Total transported cargo (waste + coal) (m^3) r.m.	Average traction force at circumference of traction wheels in transport of full dump trucks(kN)	Average traction force at circumference of traction wheels in transport of empty dump trucks (kN)	Average cycle time (h)	Average cycle time (s)	Average transported cargo per cycle (m3) r.m.	Average distance traveled for one cycle Lu = 2L (km)	Average driving time of a full truck tp (s)	Average driving time of an empty truck tpr (s)	Average transported cargo per one cycle (m^3) r.m.
5647.06	70.59	60	6014.4	230.01	39107.13	1176	70380	75180	60	76027.06	112.90	82.11	0.18	660.84	60.68	4.8	360.00	261.82	60.68
3529.41	70.59	60	4645	178.245	33045.41	1176	53820	56820	60	57349.41	117.80	87.40	0.19	677.59	60.56	4.904963	391.30	290.32	60.56
2258.82	70.59	60	4890	188.7	32289.6	1176	56760	58680	60	59018.82	129.02	90.32	0.19	694.60	60.35	5	428.57	300.00	60.35
3882.35	70.59	60	5100	192.78	34341.76	1176	56700	60000	60	60582.35	112.90	82.11	0.19	694.01	60.58	5.1	382.50	278.18	60.58
5505.88	70.59	60	4347	155.295	28165	1176	43620	48300	60	49125.88	123.16	87.40	0.19	694.49	61.03	5.4	441.82	313.55	61.03
9811.76	70.59	60	5200	176.46	27252.48	1176	51660	60000	60	61471.76	112.90	82.11	0.18	635.26	61.47	5.2	390.00	283.64	61.47

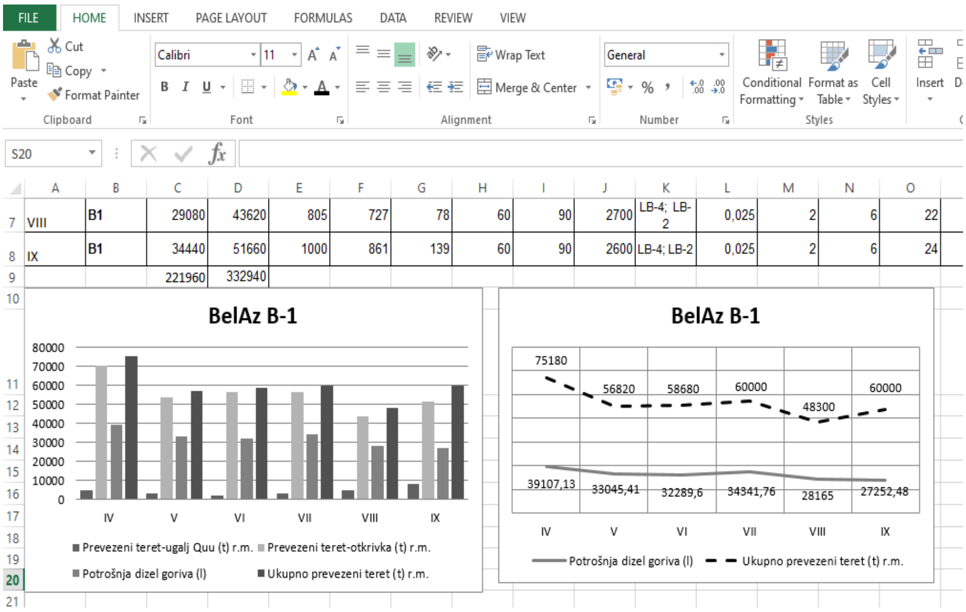

Figure 6 *Transported cargo-coal (t) r.m., waste(t) r.m., total transported cargo (t) r.m. and consumption of diesel fuel (l) in IV, V, VI, VII, VIII and X months of BelAz internal code B-1*

Figures 7 and 8 show the total transported cargo (t) r.m. and diesel fuel consumption (l) in IV, V, VI, VII, VIII and IX months of all BelAz at the OP "Turija".

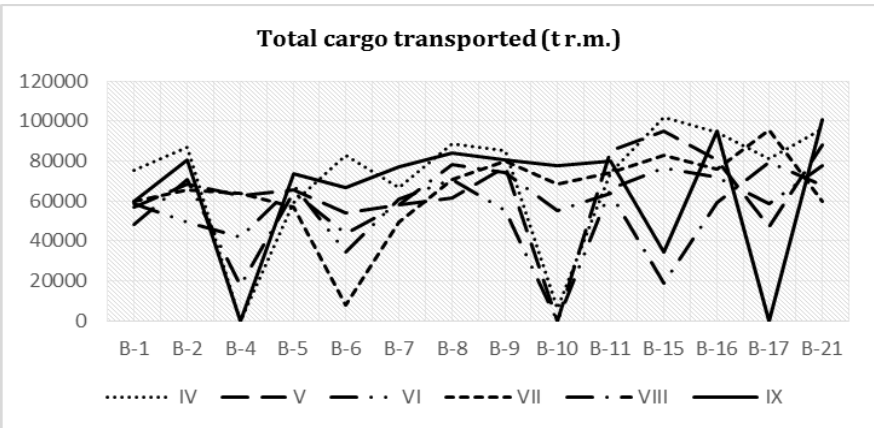

Figure 7 *Total transported cargo (t r.m.) in IV, V, VI, VII, VIII and IX months*

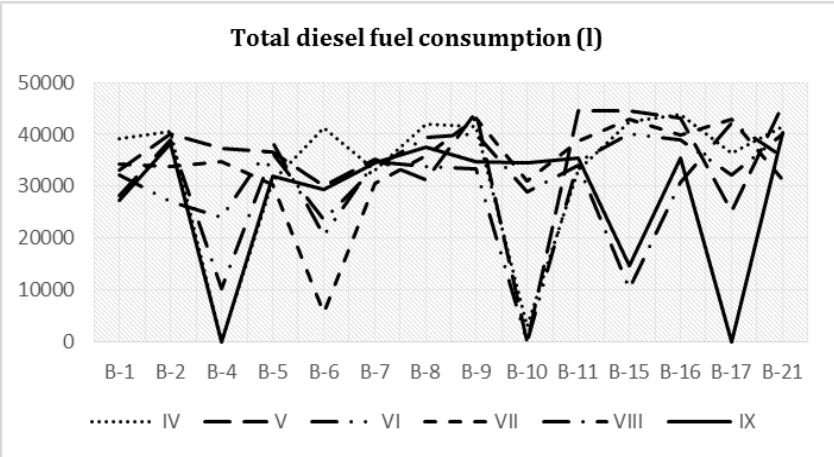

Figure 8 *Total diesel fuel consumption (l) in IV, V, VI, VII, VIII and IX months*

During six months of monitoring, the dump trucks traveled a total of 443692 (km). Analyzing the relationship between the amount of transported cargo and consumption of diesel fuel, it was found that in the same working conditions, the transport of a larger amount of cargo requires higher consumption of diesel fuel and vice versa. For the same amount of transported cargo, changes in working conditions affect the fuel consumption. Lack of auxiliary equipment and climatic conditions (precipitation, storm) cause the production to be difficult, so that even in the case of increasing the number of effective hours for transporting the same amount of cargo, leads to more fuel consumption, and it happens that more fuel is used for transport smaller amounts of cargo. In some cases, due to bad weather (heavy rain), it is necessary to move the dump truck to the other sites. By transferring the Liebher and Terex RH 120E excavators from the lower floors of the E – 252 base terrain E - 360 base, i.e. on the first floor, the length of waste transport to the landfill has decreased, as well as the slopes (ascents) of the route.

In case of excavator failure, the dump trucks are transferred to the other excavator sites, and in case of lack of excavator capacity at the existing open pits, the dump trucks are transferred to open pits, and this procedure reduces the productivity of the dumper. The organizational part in the production process is very important due to the productivity of the open pit. Poor work organization leads to a decline in coal production and overburden, and production costs rise. Poor passability of transport units due to narrowing of transport routes, poorly demined floors, maintenance problems, lack of spare parts, as well as failure to fulfill orders for the purchase of parts for dump trucks are just some of the elements that affect the diesel fuel consumption.

Based on the collected data, the average diesel fuel consumptions per hour traveled (l/h), per kilometer traveled (l/km) and the transported ton of loose cargo (l/t r.m.) were calculated, and shown in Figures 9 and 10.

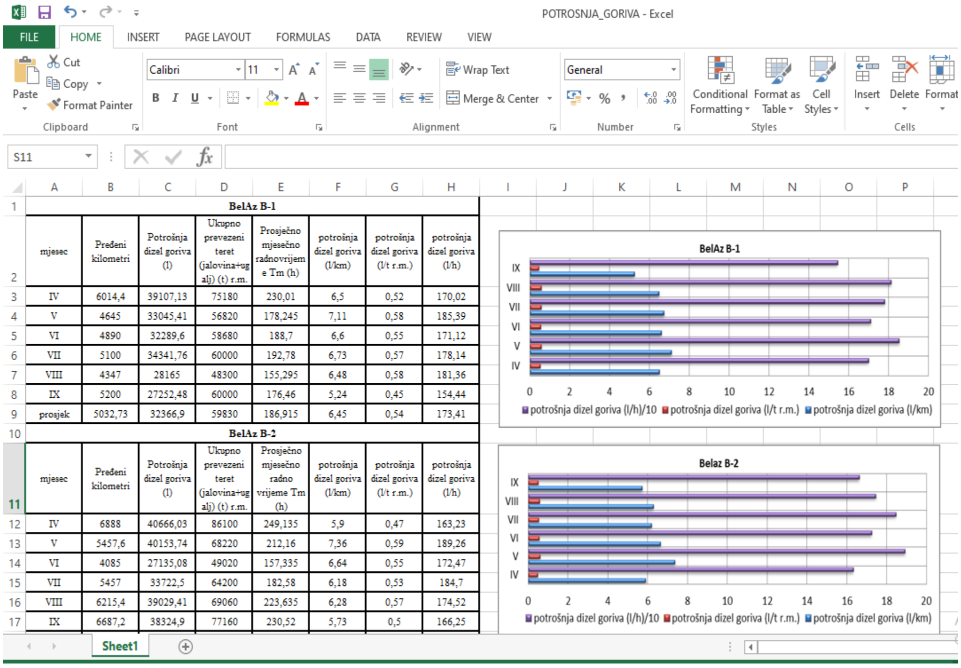

BelAz B-1							
mjesec	Pređeni kilometri	Potrošnja dizel goriva (l)	Ukupno prevezeni teret (jalovina+ugalj) (t) r.m.	Prosječno mjesečno radnovrijeme Tm (h)	potrošnja dizel goriva (l/km)	potrošnja dizel goriva (l/t r.m.)	potrošnja dizel goriva (l/h)
IV	6014,4	39107,13	75180	230,01	6,5	0,52	170,02
V	4645	33045,41	56820	178,245	7,11	0,58	185,39
VI	4890	32289,6	58680	188,7	6,6	0,55	171,12
VII	5100	34341,76	60000	192,78	6,73	0,57	178,14
VIII	4347	28165	48300	155,295	6,48	0,58	181,36
IX	5200	27252,48	60000	176,46	5,24	0,45	154,44
prosjek	5032,73	32366,9	59830	186,915	6,45	0,54	173,41

BelAz B-2							
mjesec	Pređeni kilometri	Potrošnja dizel goriva (l)	Ukupno prevezeni teret (jalovina+ugalj) (t) r.m.	Prosječno mjesečno radno vrijeme Tm (h)	potrošnja dizel goriva (l/km)	potrošnja dizel goriva (l/t r.m.)	potrošnja dizel goriva (l/h)
IV	6888	40666,03	86100	249,135	5,9	0,47	163,23
V	5457,6	40153,74	68220	212,16	7,36	0,59	189,26
VI	4085	27135,08	49020	157,335	6,64	0,55	172,47
VII	5457	33722,5	64200	182,58	6,18	0,53	184,7
VIII	6215,4	39029,41	69060	223,635	6,28	0,57	174,52
IX	6687,2	38324,9	77160	230,52	5,73	0,5	166,25

Figure 9 *Consumption of diesel fuel per kilometer (l/ km) in the IV, V, VI, VII, VIII and IX months*

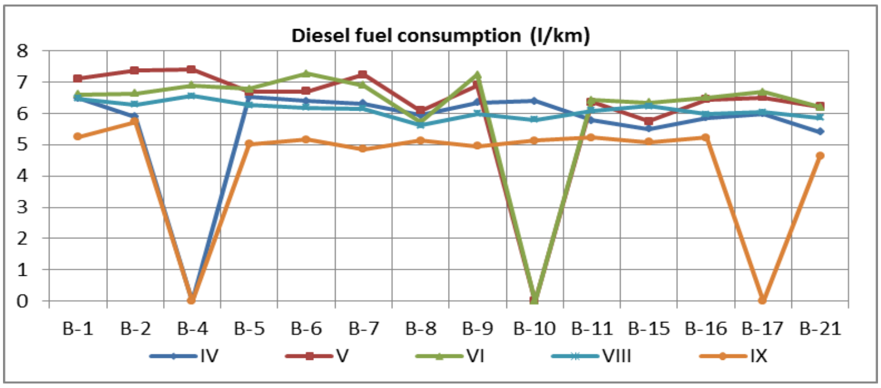

Figure 10 *Consumption of diesel fuel per kilometer (l/ km) in the IV, V, VI, VII, VIII and IX months of the BelAz dump truck at the OP "Turija"*

The first dump trucks of the type BelAz B-1, B-2, B-3, B-4, B-5, arrived at the BCM Banovići on March 15, 2006 and as such are among the dumpers of older production, and they have made over 70,000 engine hours. The average values of diesel fuel consumption per kilometer (l/km) of a dump truck in operation at the OP "Turija" are shown in Table 5.

Table 5 *The average values of diesel fuel consumption per kilometer (l/km) for the IV, V, VI, VII, VIII and IX months of all BelAz dump trucks that were in operation*

Month	Average diesel fuel consumption per kilometer traveled (l/km)
IV	6.065385
V	6.7125
VI	6.668333
VII	6.331538
VIII	6.126923
IX	5.118333

In the VII and VIII months, all dump trucks were working and the average monthly consumption of a BelAz dump truck ranged from 6.13 to 6.67 (l/km).

Older BelAz trucks, driven by drivers with less experience, had the highest consumption in cargo transport, while relatively newer BelAz trucks used less fuel. With the BelAz B-8, the replacement of t engine showed a reduction in diesel fuel consumption, which was to be expected.

The greatest impact on fuel consumption has the quality of road surface, weather conditions, and operation of auxiliary machinery. The transport of overburden took place to the inner western landfill with an average route length of 2500 m. Coal was loaded occasionally, and the average length of the route was 2500 m.

The analysis can generally conclude that the ratio of the amount of transported waste to the amount of coal $\left(\frac{\text{t waste}}{\text{t coal}} \text{r.m.}\right)$ does not significantly affect the consumption of diesel fuel (l/t rm) of the BelAz dump truck at the OP "Turija". The reason is in the fact that there were the same length of sections for waste and coal transport, and approximately road surfaces of the same quality.

In the dry period, the minimum fuel consumption for similar operating conditions can be expected from 6.13 to 6.67 (l/km), while in winter it increases by 12%. As the dump truck ages, a higher consumption can be expected than the obtained one.

4 PREVENTIVE MEASURES AND SELECTION OF MAINTENANCE STRATEGY

Based on the knowledge after research, suggestions can be made to improve and reduce the fuel consumption. Fuel consumption is affected by adequate maintenance and servicing of BelAz dump trucks, and it is necessary to do it on time. Simplify access to the regular service points, because it simplifies service and reduces the amount of time spent on regular maintenance procedures. It is still necessary to check the tire pressure regularly. Too little tire pressure worsens the lateral guidance of tires, prolongs the braking distance and thus reduces the driving safety. Also, a low tire pressure increases the rolling resistance, thereby increasing the fuel consumption. Checking the condition of tires and pressure in them is very important for safety and consumption. The tire is the only contact surface between the vehicle and ground, and has the task of withstanding carrying, movement, shock absorption, braking and acceleration, while the rolling resistance has a direct impact on fuel consumption. Maintenance and improvement of the road surface can significantly reduce the fuel consumption. When designing, take into account the lengths of routes intended for transport and their slopes. Reducing the length of route and its slope enables a shorter cycle of dump trucks and transport of larger quantities of cargo with lower fuel consumption. Apply adequate organization of the technological process, because it has a significant impact on the fuel consumption.

CONCLUSION

Many parameters, such as age and maintenance of the vehicle, load, speed, cycle time, layout at the open pit, work schedule, idle time, tire wear, rolling resistance, engine operating parameters and gear change patterns can affect the fuel consumption at the open pit excavation. The fuel consumption of the BelAz dump truck during the six months was discussed at the OP “Turija”. Analyzing the results of processed data, it was found out which parameters and circumstances affect the amount of fuel consumed.

Analyzing the relationship between the amount of transported cargo and diesel fuel consumption, it can be concluded that in the same working conditions, the transport of larger quantities of cargo requires higher diesel fuel consumption and vice versa. Lack of auxiliary equipment and climatic conditions (precipitation, storm) cause that the production is difficult. In the months when the technological process was difficult, the fuel consumption was increased compared to the consumption in stable working conditions. In such conditions, and in the case of increasing the number of effective hours for transporting the same amount of cargo, the fuel consumption was higher for transportting smaller amounts of cargo. Changes in route length as a result of moving the excavator to a new location and changes in route slope due to the increased length of transport route and inadequate organization of technological process, poor working conditions, some dump trucks recorded higher fuel consumption when transporting smaller quantities of cargo. It can be concluded that the dump truck at the OP "Turija" worked in difficult working conditions. Older manufactured BelAz had the highest consumption in transport, served by drivers with less experience, while relatively newer BelAz used less fuel. With BelAz B-8, the replacement of engine showed a decrease in diesel fuel consumption, which was to be expected. The greatest impact on the fuel consumption has the quality of road surface, weather conditions, and operation of auxiliary machinery.

The presented method of processing, analysis and extraction of important information on the parameters of operation and consumption of diesel fuel in this way in our area was done for the first time, and it can be repeated at the other open pits that use dump trucks to transport cargo. The contribution of this work to the professional literature is that for the first time the fuel consumption at one open pit was determined on the basis of collected data and the method used. Determining fuel consumption is used to determine the preventive measures and maintenance strategies for the transport system in order to reduce it, as well as the emission of exhaust gases into the atmosphere.

REFERENCES

[1] V. Kecojević, D. Komljenović (2010) Haul Truck Fuel Consumption and CO_2 Emission Under Various Engine Load Conditions, https://www.researchgate.net/publication/261214668_Haul_truck_fuel_consumption_and_CO2_emission_under_various_engine_load_conditions, 19.10.2020.

[2] Ali Soofastaei (2016) Efficiency of Haul Trucks in Surface Mines, PhD Project, DOI:10.13140/RG.2.2.18587.67365, https://www.researchgate.net/publication/309176186_Development_of_an_Advanced_Data_Analytics_Model_to_Improve_the_Energy_Efficiency_of_Haul_Trucks_in_Surface_Mines , 10.12.2020.

[3] S. Mašić (1999) Collection of Solved Problems from Transport in Mining, Faculty of Mining, Geology and Civil Engineering, Textbook, University of Tuzla (in Serbian)

[4] S. Hodžić, S. Mašić (2005) Collection of Solved Problems from Continuous Transport in Mining, Faculty of Mining, Geology and Civil Engineering, Textbook, University of Tuzla (in Serbian)

[5] Sadudin Hodžić, Sunčica Mašić (2008) Cyclic Transport, Faculty of Mining, Geology and Civil Engineering, Textbook, University of Tuzla (in Serbian)

[6] Law on Environmental Protection, Official Gazette of FB&H, No. 15/2021 (in Serbian)

[7] https://www.researchgate.net/publication/309176186_Development_of_an_Advanced_Data_Analytics_Model_to_Improve_the_Energy_Efficiency_of_Haul_Trucks_in_Surface_Mines, 10.12.2020.

[8] https://www.researchgate.net/publication/309176186_Development_of_an_Advanced_Data_Analytics_Model_to_Improve_the_Energy_Efficiency_of_Haul_Trucks_in_Surface_Mines, 10.12.2020.

MINING AND METALLURGY INSTITUTE BOR
UDK: 622

ISSN: 2334-8836 (Štampano izdanje)
ISSN: 2406-1395 (Online)

UDK: 622.271/.68(045)=111
DOI: 10.5937/mmeb2104041S

Received: 01.10.2021.
Revised: 01.11.2021.
Accepted: 01.12.2021.

Original Scientific Paper
Mining

Nikola Stanić[*], Miljan Gomilanović[*], Saša Stepanović[*], Sead Softić[**]

SELECTION OF A RATIONAL TRUCK MODEL FOR WASTE TRANSPORT AT THE OPEN PIT GACKO USING THE AHP METHOD[***]

Abstract

This work presents the principle of optimal model truck selection for waste transport at the open pit Gacko. The analysis was performed for three types of trucks: Belaz 7555, Belaz 75491 and Belaz 75135. Selection of the optimal model was done using the AHP method from the group of multicriteria decision-making methods. The work presents the analysis results of the technological procedure of waste transport at the open pit Gacko and evaluation the most important criteria for an optimal type truck selection. In selection the important criteria and assessment the degree of their impact, a questionnaire method was used that was conducted among the mining engineers at the open pits Gacko, Pljevlja, Šuplja Stijena and Mining and Metallurgy Institute Bor. Testing and calculations were done for the truck types and models that have been in long-term use at the open pits. The research pointed out that the best results, according to a number of criteria, are shown by the trucks with a carrying capacity of 55 tons (Belaz 7555), which are also the smallest carrying capacity that was tested.

Keywords: *transport, truck model selection, AHP method, open pit*

INTRODUCTION

Selection of equipment in the system of open pit exploitation is an issue that is placed in the center of the study of mining issues with the basic aim to optimize the technical and economic parameters of system. The most commonly used methods are the modeling methods, case studies and application of numerous methods from the group of multi-criteria decision-making in order to optimize the selection of mining equipment.

Selection of equipment is a constantly current task in mining, in accordance with the frequent technical and technological improvements in the field of production, automation, application of information technology and various optimization models.

Considering the research on this issue in our country, we can single out the Study of Selection the Excavation-Transport-Landfill Equipment in the Selective Excavation of Coal Series (Prof. Dr. Vladimir Pavlović, Prof. Dr. Dragan Ignjatović, Faculty of Mining and Geology, Belgrade, 2010) can be singled out. This Study has defined the methodology and criteria for selection the basic equipment complex in the specific conditions of the lignite deposits of the Electric Power Industry of Serbia.

[*] *Mining and Metallurgy Institute Bor, Zeleni bulevar 35, 19210 Bor, Serbia, e-mail: nikola.stanic@irmbor.co.rs*
[**] *International University of Travnik, Travnik, Bosnia and Herzegovina*
[***] *This work was financially supported by the Ministry of Education, Science and Technological Development of the Republic of Serbia, Grant No. 451-03-9/2021-14/200052*

Among the foreign examples are the significant results of the project of international cooperation between Germany (EU) and the University of Mining and Technology of Mongolia (Deutsch-Mongolische Hochschule für Bergbau und Technologie (GMIT) (DAAD), 2013)), in which the coal mining system at the open pits in Mongolia. During the project period, the coal production was increased from about 5.5 Mt of coal to over 30 Mt. The project was implemented under the coordination of Prof. Dr. Carsten Drebenstedt (Freiberg Technical University), one of the leading experts in the field of geotechnics and selection of mining equipment.

The basic characteristic of technological procedures in the open pit exploitation is its dynamic character, both in terms of changing the exploitation parameters related to the variability of workspaces and variability of the characteristics of the working environment and surroundings (urban, meteorological and environmental conditions). Therefore, the optimization of selection the equipment at the open pits is an attempt to achieve the optimal technological and economic parameters of exploitation in the longest possible period and shortest in the service life of equipment being selected. This means that the optimal parameters can be achieved only in the total time of analysis and not in each individual moment. Another important feature is that the selection of equipment is made in relation to the most important technological process, which refers to the largest amount of mass and has the largest share in the total costs. On the example of the open pit Gacko, and which is characteristic for other open pits, it is the technological process of waste transport. In the current century of this open pit mine, there is a tendency for equipment to be procured primarily according to the available economic possibilities and current offer on the market, and not in accordance with the long-term needs and more complex view of this issue. In this work, the aim was to define one of the possible systemic approaches to the selection of discontinuous equipment for waste transport, which would include the assessment of the most important influencing factors. This implies both defining the influencing factors and objectively assessing the degree of their influence.

The open pit of lignite Gacko-Centralno polje is characterized by a large number of sites for overburden and coal excavation with different materials, distance from the place of landfilling and disposal and transport conditions. A continuous, combined and discontinuous waste transport system is also in use. As a key segment for achieving the stable and reliable coal exploitation, the system of exploitation in the roof coal zone has been singled out, where the overburden, layer and interlayer waste are transported by a discontinuous equipment. Due to this reason, the subject of optimizing the selection of trucks is the waste transport from the roof exploitation zone for a maximum annual capacity of 1,500,000 m^3/year.

The main goal of research in the field of selection the optimal transport equipment is to determine the possibility of application and change the existing structure of complex transport mechanization for specific working conditions at the open pit Gacko-Centralno polje. Apart from this, an important factor in the success of entire system is the determination of conformity of operation the excavation-loading and transport equipment for different conditions that are expected at this open pit in a longer period. In order to realize these two most important goals, it was previously necessary to determine the method of objective characterization and assessment the influence degree of numerous factors that define the techno-economic indicators of the system.

MATERIAL AND WORKING METHOD

The open pit Gacko-Centralno polje provides lignite as a solid fuel for electricity production for the Gacko Thermal Power Plant. The basic requirements for the mine are in terms of total quantity, average quality, stability and reliability of production. [1] In order to meet these requirements, two coal mining sites have been developed at the open pit, the Central and Roof Exploitation Zone, which differ significantly in terms of exploitation conditions. Lignite production in the Roof Exploitation Zone is characterized by a favorable coefficient of overburden, small depth of exploitation, overburden and waste of unfavorable physical and mechanical characteristics and low quality of coal. In this zone, the exploitation is carried out with the basic goal of providing a sufficient amount of lignite for the Thermal Power Plant, which together with coal of the Central Exploitation Zone will form a mixture of satisfactory quality. [2] The excavation and transport of waste from the roof zone is discontinuous and is currently carried out by trucks with a capacity of 100 tons, which are the only ones currently available. The current planning and project documentation envisages the procurement of trucks and other capacities, but without a detailed consideration of the working environment conditions, but on the basis of experiential criteria. [3]

As a rule, transport at the open pits is the most important technological process and has the largest share in the cost structure. Considering transport at the open pits, the basic characteristic is that it is a matter of dislocation the large quantities of material, striving to shorten the transport routes, construction the quality roads and selection the most efficient equipment for given conditions. [4,5,6] Factors that affect the success of this technological process are: relief, hydrographic, meteorological, structural geological and others, often beyond the possibility of influencing them, but also those whose management can achieve more favorable results. A survey method was used to determine the important influencing factors as well as to assess the degree of their influence. The survey was conducted at the open pits where the long-term use of discontinuous transport is present, as well as at the Scientific Institution, among employees who have been dealing with the issue of open pit mining for many years.

Engineers from the open pit Gacko, open pit Potrlica-Pljevlja and open pit Šuplja stijena Pljevlja participated in the survey. The survey involved 57 engineers who evaluated the criteria for selection a rational truck model according to the importance defined by the weighting factor. Respondents were asked to rate from 1 to 5 the 5 criteria selected from a wider set shown in Table 2. The survey results are shown in Table 1.

Table 1 *Survey results*

Criterion /R.B.	1	2	3	4	5	6	7	8	9	10	11	12	13	14	15	16	17	18	19	20	21	22	23	24	25	26	27	28	29
Regulatory costs	4	5	5	4	5	5	5	5	5	5	5	4	4	4	3	3	5	5	5	5	4	4	4	5	5	5	3	3	3
Capital costs	5	4	4	5	3	4	4	4	4	4	3	5	2	3	4	4	4	4	3	4	3	5	5	3	4	4	4	2	5
Labor costs	3	3	3	3	4	3	3	3	3	3	4	1	3	1	1	1	1	3	4	3	5	1	3	4	3	3	5	4	4
Road maintenance costs	2	1	2	1	1	1	2	2	2	2	2	3	5	2	5	2	2	2	1	1	1	2	1	2	1	1	1	5	1
Coefficient of compliance the excavator and truck capacity	1	2	1	2	2	2	1	1	1	1	1	2	1	5	2	5	3	1	2	2	2	3	2	1	2	2	2	1	2

Criterion /R.B	30	31	32	33	34	35	36	37	38	39	40	41	42	43	44	45	46	47	48	49	50	51	52	53	54	55	56	57
Regulatory costs	2	5	5	5	2	4	4	4	5	5	5	5	4	4	5	4	5	5	4	4	4	3	4	4	4	5	5	5
Capital costs	4	4	3	3	3	3	3	5	4	4	4	4	5	5	4	5	4	4	5	3	5	4	5	5	5	4	4	4
Labor costs	5	2	4	1	5	1	5	3	1	3	2	3	3	3	3	3	3	3	3	5	3	5	3	3	3	3	3	1
Road maintenance costs	3	3	2	2	4	5	2	1	2	2	3	2	2	2	1	2	1	1	2	1	2	2	2	1	2	2	2	3
Coefficient of compliance the excavator and truck capacity	1	1	1	4	1	2	1	2	3	1	1	1	1	1	2	1	2	2	1	2	1	1	1	2	1	1	1	2

Based on the survey results, the average weighting factors of criteria as the arithmetic mean of the survey scores were calculated and shown in Table 2.

Table 2 *Weighting factors of the criteria based on the survey results*

Criterion/evaluation	Regulatory costs	Road maintenance costs	Capital costs	Labor costs	Coefficient of compliance between the excavator and truck capacity
Total number of points of the weighting factor	247	115	227	170	96
Average weight factor	4.33	2.02	3.98	2.98	1.68

The aim of the survey is to define the most important influencing factors and to assign each of the factors an appropriate weight rating in accordance with the expected relative impact. These weighting factors are the most important element in the process of determining the optimal type of truck for waste transport in the Roof Exploitation Zone of the open pit Gacko.

To determine an optimal type of truck, a method from the group of multicriteria decision-making methods, a subgroup of methods of analytical hierarchical processes (AHP method) was chosen. The group of multicriteria decision-making methods includes both optimization and non-optimization methods. [7] These are a wide range of methods that were often used in specific situations and whose common feature is that they can combine a large number of, by their nature, diverse criteria. The selection methods from the AHP group are essentially not optimization methods, but are often used for the practical needs of selection the mechanization complexes at the open pits, in order to select the most favorable from the limited set of available production units. [8] Due to these properties, it was used in this case. Each of the methods from the AHP subgroup contains the weighting factors and satisfaction factors as a key element. [9] These factors are related to the selected criteria and can be of different nature, different limits, descriptive or numerical, etc. There are a number of methods to reduce weight and satisfaction factors to a common denominator, but the end result is always largely related to the magnitude of weight and satisfaction factors. [10] Therefore, the accuracy of results is largely dependent on objectivity when choosing these two factors. In this particular case, the survey method was used in order to ensure this objectivity as much as possible.

Selection of the optimal truck type was made in relation to the possible truck types characteristic for the given capacity, transport lengths, working environment characteristics and loading equipment characteristics previously defined from the capacity conditions and possibility of selective coal exploitation. Based on the above, the offered set of truck types has been reduced to trucks with a carrying capacity of 100, 80 and 55 tons, and which are more often used at the open pits of similar capacity.

Truck transport calculation

The Talpac software was used to calculate the excavator-truck system. The Talpac software package is a simulation model of loading and transport process at the open pits. This software enables optimization of the transport fleet, calculation of technical and economic parameters of equipment operation, such as a cycle length, capacity, number of trucks in the system, effective operating time, etc. In the specific case, this program was used to determine the parameters in waste transport from an open pit to an external landfill.

The input data used in calculation are:

- Total possible number of shifts per year: 1,095 shift/year
- Shift duration: 8 h
- Number of working hours per year: 8,760 h
- Available shift work time: 5.5 h
- Available working hours per year: 3,500 hours

The calculation was made for an annual capacity of 1,500,000 m^3. Komatsu PC 1250 bucket hydraulic excavator with a bucket volume of 6 m^3 was chosen for a loading unit, while three truck models of different capacities were chosen for the transport equipment, shown in Tables 3 and 4.

Table 3 *Characteristics of loading machinery [11]*

Komatsu PC 1250				
	Parameters			
	Bucket volume (m^3)	6	Engine power (kW)	363
	Speed (km/h)	4.2	Speed (rpm)	1800
	Digging depth (m)	8.45	Weight (kg)	75200
	Mean soil pressure (N/cm^2)	12.2	Length arrow (mm)	7500
	Crawler width (mm)	610	Overall length (mm)	14405
	Crawler stand width (mm)	4110	Branch height	4690
	Crawler stand length (mm)	5810	Cabin height	3670
	Bucket width (mm)	2200	Total width	4110

Table 4 *Characteristics of transport mechanization [12,13,14]*

			
	Belaz 7555	**Belaz 75491**	**Belaz 75135**
	37.5	46	71.2
Engine power (kW)	522	630	895
Load capacity (t)	55	80	110
Max. speed of movement (km/h)	55	50	50
Shaking angle (^{o})	47	46	47
Weight (kg)	41000	72500	100100
Total height (mm)	4610	5350	5900
Total width (mm)	5240	5420	6400
Total length (mm)	8890	10300	11500
Price (€)	400 000	700 000	900 000

Based on the entered data, the hourly capacities of a truck for the transport route from the open pit to the external landfill were calculated and expressed in m^3/h when working in conjunction with the loading machinery. The number of trucks required in the appropriate period was calculated on the basis of the total required time of truck engagement for the waste amount from the open pit and specific transport length. The truck capacity calculated in the Talpac software package is shown in Table 5.

Table 5 *Truck capacity calculated in the Talpac software package*

Truck model	**Capacity (m^3/h)**
Truck Belaz 7555	304.07
Truck Belaz 75491	343.44
Truck Belaz 75135	340.79

Operating costs

The truck capacity served as the basis for calculation the operating costs given in Table 6.

The price of operating costs for all types of analyzed trucks was calculated with the calculated standards and prices of drive material.

Table 6 *Operating costs*

Material	Prices (€)	Belaz 7555	Belaz 75491	Belaz 75135
Fuel standard (l/cm^3)	1	0.287034	0.306709	0.434907
Lubricant standard (kg/cm^3)	5	0.028703	0.030671	0.043491
Oil standard (l/cm^3)	2.5	0.031574	0.033738	0.04784
Tire standard (pcs.)	900	0.000013	0.000013	0.000013
Spare parts standard (kg/cm^3)	10	0.01	0.01	0.01
€/m^3		0.614685	0.653508	0.88366

Capital costs

Capital costs are given on the basis of purchase prices, estimated total lifespan and estimated capacity, and thus ex pressed as the unit costs per m^3. Table 7 shows the investments in transport equipment.

Table 7 *Investments in transport equipment - capital costs*

	Belaz 7555	Belaz 75491	Belaz 75135
Number of trucks	5	4	3
Price of one truck (€)	400,000	700,000	900,000
Total price (€)	2,000,000	2,800,000	2,700,000
€/m^3	0.188	0.233	0.226

Labor costs

Labor costs were calculated on the basis of data on salaries of the Gacko Mine. The costs for the four-brigade work system have been calculated. Table 8 shows the labor costs.

Table 8 *Labor costs for the four-brigade system*

	Belaz 7555	Belaz 75491	Belaz 75135
Number of trucks	5	4	3
Gross salary	800	800	800
Net salary	1,280	1,280	1,280
Number of shifts	4	4	4
Monthly salary costs	25,600	20,480	15,360
Annual salary costs	307,200	245,760	184,320
€/m^3	0.205	0.164	0.123

Road maintenance costs

Road maintenance costs are calculated based on the road area determined by the length of transport and width of transport means and amounts to:

Road area = road width * road length

Road width = truck width * 2 + 4m

The road maintenance costs per m^2 are 0.5 €, and the price is determined based on the price list of works on construction and modernization the roads of the official public company. [15]. Road maintenance costs are shown in Table 9.

Table 9 *Road maintenance costs per m^2*

	Belaz 7555	Belaz 75491	Belaz 75135
Truck width	5	6	7
Road area	58,838	66,898	72,540
eur/year	29,419	33,449	36,270
Eur/m^3	0.0196	0.0223	0.0242

Coefficient of compliance of loading and transport equipment

Coefficient of compliance of loading and transport machinery is a measure of compliance the excavator capacity and number of trucks in the system, i.e. the ratio between the optimal and required capacity of a truck in the system. Table 10 shows the coefficient of compliance for the truck models that are the analysis subject.

Table 10 *Coefficient of compliance*

	Belaz 7555	Belaz 75491	Belaz 75135
Coefficient of compliance	0.850	0.699	0.778

Evaluation and ranking methods of variant solutions

The assumption is that it is necessary to decide on one of several variants, in this case the three shown models of trucks.

There are the following stages that are necessary to set up a scoring model:

I Stage:

Set a list of criteria to be considered. Criteria are important factors for evaluating any decision.

II Stage:

Determine the weight of each criterion that shows its relative importance:

wi = weight of criterion i

III Stage:

Determine the measure of each criterion that shows how well each alternative meets each criterion:

r_{ij} = measure for criterion i and decision j

IV Stage:

Calculate the value for each decision alternative:

S_j = value for decision alternative j

The equation for calculating the value of Sj is:

Sj = ∑i wi*rij

V Stage:

The order of selected alternatives from the highest to the lowest value is at the same time ranking according to the scoring model for alternative decisions. The decision is made for an alternative with the highest number of points and it is recommended for implementation.

According to this method, selection of a truck model was made in five stages, with the first defining a list of criteria, the second the weighting criterion, the third the satisfaction level measure, the fourth calculating the value of alternatives for decision making and the fifth the ranking variants.

TESTING RESULTS

The application of described method for the specific truck models and fr specific working conditions led to a definition of the rank for each of the offered models. The practical procedure was carried out through the following stages.

I Stage: List of criteria

- Regulatory costs
- Capital costs
- Labor costs
- Road maintenance costs
- Coefficient of compliance between the excavator and truck capacity

II Stage:

A scale is used to determine the weight, depending on the importance of criteria, and in this case, considering the selected list of criteria, a five-point scale is used:

Importance	**Weight** (w_i)
Very important	5
Somewhat important	4
Medium important	3
Somewhat unimportant	2
Very unimportant	1

The weighting factors, shown in Table1, represent the result of expert assessment and as such were used in the further procedure, where the relative ratio of weight factors for individual criteria is more important than its absolute value. Based on the weighting factors, the used criteria were ranked and their order is given in Table 11.

Table 11 *Decision criteria, importance and weight of criteria*

Ord.No.	Criterion	Weight
1	Regulatory costs	4.33
2	Capital costs	3.98
3	Labor costs	2.98
4	Road maintenance costs	2.02
5	Coefficient of compliance between excavator and truck capacity	1.68

III Stage:

Each alternative decision is evaluated from an aspect of meeting each criterion. The following levels of satisfaction were selected for selection a possible variant:

Satisfaction level	Measure (r_{ij})
Extremely high	9
Very high	8
High	7
Almost high	6
Medium	5
Almost low	4
Low	3
Very low	2
Extremely low	1

The calculation process must be completed for each combination of alternative decisions for each criterion. Since there are five criteria and three alternatives for decision making (5*3 = 15), 15 measures for alternative decisions are obtained, which are given in the following Table 12.

Table 12 *Measures for decision-making alternatives*

Criterion	**Belaz 7555**	**Belaz 75491**	**Belaz 75135**
Regulatory costs	7	5	2
Capital costs	7	3	4
Labor costs	2	5	8
Road maintenance costs	6	5	3
Coefficient of compliance between excavator and truck capacity	6	3	4

IV Stage:

It is necessary, according to the given weight, to calculate the values of each alternative for decision making. Thus, for example, for alternative 1, its value is:

$$S_j = \sum_i w_i * r_{ij} = 4.33*7 + 3.98*7 + 2.98*2 + 2.02*6 + 1.68*6 = 86.386$$

Based on the determined values, the values of decision-making alternatives, given in Table 13, are obtained.

Table 13 *Values of decision-making alternatives*

Criterion	**Weight**	**Belaz 7555**		**Belaz 75491**		**Belaz 75135**	
		Measure	**Value**	**Measure**	**Value**	**Measure**	**Value**
	(w_i)	(r_{i1})	(w_i*r_{i1})	(r_{i2})	(r_{i3})	(w_i*r_{i3})	(w_i*r_{i2})
Regulatory costs	4.33	7	30.333	5	21.667	2	8.667
Capital expenditures	3.98	7	27.877	3	11.947	4	15.930
Labor costs	2.98	2	5.965	5	14.912	8	23.860
Road maintenance costs	2.02	6	12.105	4	10.088	3	6.053
Coefficient of compliance	1.68	6	10.105	8	5.053	4	6.737
Total value			**86.386**		**63.667**		**61.246**

V Stage: Ranking

1. Belaz 7555 = 86.386
2. Belaz 75491 = 63.667
3. Belaz 75135 = 61.246

DISCUSSION

On the basis of conducted procedure and ranking of alternatives, a truck model with the lowest load capacity, the Belaz 7555 model with a load capacity of 55 tons, was chosen as the most favorable.

In the criteria selection and their ranking, on the basis of the obtained average grade, the order and relative ratio of individual criteria is in line with expectations and coincides with literature data. Most often, considering a discontinuous transport at the open pits, the operating costs are singled out as the most significant and are often the subject of consideration, given that the highest savings can be achieved on them. The capital costs are at the second place in terms of importance, which is also common, and their reduction is more often the subject of economic than technical parameters. Other criteria show a significantly lower degree of influence on the final result.

Considering that the standard costs are highlighted as the most significant, their verification and improvement was performed with the previous transport costs monitored at the open pit and difference from the average realized total costs indicates that the costs obtained by applying the presented model are realistic.

In the process of optimizing the transport process at the open pits and in general in the other technological processes, there is a constant increase in capacity, which should result in lower unit costs. This approach often neglects the specific conditions, and for the case under consideration, it is primarily the need to apply a selective coal exploitation in the roof exploitation zone. The structural assembly of the deposit in this zone is such that there is a frequent change of seams and interlayers of coal and waste of small thicknesses. This limits the possibility of using the excavation equipment of large dimensions of the working body. For the specific case, volume of an excavator bucket of $6m^3$ represents the upper limit of application in the conditions of selective exploitation. This is the result of practical experience and monitoring the quality of run-of-mine coal at the open pits in the region and in the world. This is precisely the reason why, according to the criterion that had the lowest weight factor, the coefficient of conformity of loading and transport equipment, the selected model has showed the same rank.

CONCLUSION

The methods of multi-criteria decision-making and optimization are often used in mining because they allow a number of different criteria to be compared with each other and, based on them, to rank or select the optimal solution. The results of applying the AHP method in selection the optimal model of waste transport truck at the open pit Gacko Centralno polje show similar results as the determination of the Gacko mine experts and confirms experiences from the other open pits in the region. Therefore, it can be said with a high reliability that the applied method is appropriate, that the ranking determines the optimal model of a truck and that the considered criteria are sufficient for its selection. As the expected result is the choice of one model from the limited domain of available transport means, the method itself, although not intended for that, can be applied as an optimization. In order for the result to be as favorable as possible from the user point of view, it is necessary to expand the domain of possible results, i.e. to analyze a larger number of truck models from different manufacturers. It is also possible to have a multidisciplinary approach with experts in the field of maintenance and automation of equipment and inclusion the new criteria and indicators of success in the application of a particular model in these two aspects. This is especially important in the case of the transport process automation, which has consequences for more efficient, safer work and increased utilization of available time.

REFERENCES

[1] Aleksandar D., N. Stanić., M. Gomilanović. Mining and Metallurgy Engineering Bor.4 (2016), 19-28.

[2] N. Stanić, S. Stepanović, D. Bugarin, M. Gomilanović. Mining and Metallurgy Engineering Bor 1-2, (2017), 23-34.

[3] S. Stepanović, N. Stanić, D. Bugarin, M. Gomilanović, Mining and Metallurgy Engineering Bor 3-4 (2017), 155-164.

[4] S. Vujić S, Selective Excavation and Disposal of Overburden in a Function of Reclamation the Coal Open Pits, Faculty of Mining and Geology, Belgrade. (2006) (in Serbian)

[5] R. Borović, Truck Transport at the Open Pits, Faculty of Mining and Geology Belgrade (1995) (in Serbian)

[6] S. Nurić, Truck Transport at the Open Pit Mining, Mikro krik Banovići, Banovići (2009) (in Serbian)

[7] C.Stojanović, Methods of Model Choice Assessment and Criteria for Investment Projects Selection, 11th International Opencast Mining Conference, OMC Zlatibor 2014, 385- 394.

[8] M. Crnogorac, D. Danilović, V. Karović Maričić, B. Leković. Tehnika 67, (2016), 381-388.

[9] R. Karim, C. L Karmaker, Journal of Industrial Engineering 1, (2016), 7-13.

[10] D. Bogdanovic, D. Nikolic, I. Ilic, Anais Da Academia Brasileira de Ciências 84, (2012), 219-233.

[11] Technical Specification Excavator KOMATSU PC1250, Komatsu Europe International N.V., Vilvoorde, Belgium.

[12] Technical Specification Mining Dump Truck BELAZ-7555 B, Management Company of Holding “Belaz-Holding”, Minsk, Republic of Belarus.

[13] Technical Specification Mining Dump Truck BELAZ-74591, Management Company of Holding “Belaz-Holding”, Minsk, Republic of Belarus.

[14] Technical Specification Mining Dump Truck BELAZ-75135, Management Company of Holding “Belaz-Holding”, Minsk, Republic of Belarus.

[15] Price List of Works on Construction and Modernization of Roads, Public Company Roads of Serbia Belgrade (2019) (in Serbian)

MINING AND METALLURGY INSTITUTE BOR ISSN: 2334-8836 (Štampano izdanje)
UDK: 622 ISSN: 2406-1395 (Online)

UDK: (045)=111
DOI: 10.5937/mmeb2104053S
Received: 25.10.2021.
Revised: 25.11.2021.
Accepted: 24.12.2021.
Original Scientific Paper
Material Science

Jelena Stefanović, Silvana Dimitrijević*, Sandra Filipović*, Jelena Đorđević**

EVALUATION OF THE CORROSION RESISTANCE OF STEEL ELEMENTS IN THE INDUSTRIALLY AGGRESSIVE ENVIRONMENTS USING THE ACCELERATED CORROSION TESTING METHODS**

Abstract

This work presents the methods for testing the resistance of materials due to corrosion of structural steel, in the presence of corrosion agents in the immediate vicinity of the industrial complex RTB in Bor. General corrosion testing was performed near the Sulfuric Acid Plant, Electrolytic Refining Plant and next to the automatic air quality monitoring station in Bor for 6 months, as well as in the salt chamber for 120h and 240h and by immersion of samples in electrolyte solution from the Electrolytic Refining Plant for of a month. The results were compared with the standard samples stored in the laboratory. A method based on measuring the loss of mass was used to evaluate the material corrosion resistance. Samples are rectangular, dimensions adopted according to the standard EN 10002-1. The steel used is S235, and its mechanical characteristics were obtained from the tensile test.

Keywords: *corrosion, corrosion resistance, mass loss, comparative analysis*

INTRODUCTION

Methods, based on measuring the loss of mass or measuring the depth of corrosion destruction of samples that have been exposed to an aggressive environment for a certain period of time, are most often used to evaluatethe corrosion resistance of metals. The corrosion resistance degree of metals can be very reliably determined by testing the mechanical properties of metals. The procedure is reduced to comparing the individual mechanical characteristics of two groups of samples: groups of samples exposed to the action of certain aggressive agents, and groups of samples not exposed to this action. [4]

Research on corrosion in the industrially polluted environments is very important, since corrosion is a factor that affects the load-bearing capacity and durability of steel structures, which causes the huge costs for the maintenance of structures. The corrosion process develops the fastest during the winter months due to the increase in concentration of pollutants in the air, such as SO_2, CO_2, chloride ions and dust. Various combinations of these factors are typical of the industrial environment. The most important climatic factors that affect the corrosion process are relative humidity, number of sunny hours, air and metal

* *Mining and Metallurgy Institute Bor, jelena.stankovic@irmbor.co.rs*
** *This work was financially supported by the Ministry of Education, Science and Technological Development of the Republic of Serbia, Grant No. 451-03-9/2021-14/200052*

surface temperature, wind speed and duration and frequency of rain, dew and fog. Condensation is considered as an important cause of metal corrosion, especially indoors. Its formation depends on relative humidity and temperature changes.

The character and speed of corrosion, in addition to the above factors, are greatly affected by the stress state of an observed metal element. Tests have shown that the tensile stresses in particular have a great effect on the acceleration of corrosion process. This is explained by a destruction of protective oxide coating and formation of microcracks. In such cases, the stress corrosion is referred to.

There are a number of corrosive destructions, namely: surface uniform corrosion, surface uneven corrosion, local corrosion-shallow, local corrosion-deep, point corrosion, subsurface corrosion, selective corrosion, intercrystalline corrosion and transcrystalline corrosion. The cases of simultaneous action of several types of corrosion are also possible, with a particularly dangerous combination within which the stress corrosion is also present.

All corrosion destructions affect the load-bearing capacity of steel structures, and thus increases the maintenance costs. Laboratory tests have a task of giving approximate results as well as corrosion tests on atmospheric cells, only for accelerated weather.

The subject of this paper research is the physical and mechanical properties of structural steel due to the corrosion propagation caused by the presence of corrosion agents in the industrial environment of RTB Bor. General corrosion testing is performed in the field, in selected atmospheric corrosion stations, near the Sulfuric Acid Plant, Electrolytic Refining Plant (Electrolysis) and next to the automatic air quality monitoring station in Bor (Figure 1). Also, a number of samples, steel tubes, were tested in chambers for accelerated aging and by immersion in electrolytes. All samples were compared to the standard samples stored in the laboratory conditions. Methods, based on measuring the loss of mass and testing the mechanical properties of samples exposed to the aggressive environments over time, will be used to evaluate the corrosion resistance of metals.

EXPERIMENT

Tests were performed on steel tubes of adopted dimensions on the basis of the standard EN 10002-1 (Figure 1). The material used is the commercial steel S235. Chemical composition was tested on a standard measuring, size 30x40x8mm, by the use of optical emission spectrometry and is given in the following Table (Table 1):

Table 1 *Chemical composition of tested steel*

Steel designation	C	Si	Mn	Cr	Mo	Ni	P	S
	0.12	0.012	0.27	0.012	0.003	0.013	0.005	0.008
S235	Al	Cu	B	Nb	V	Ti	Sn	Fe
	0.036	0.041	0.0003	<0.004	<0.0005	<0.001	0.0006	99.40

In this paper, 8mm thick samples were analyzed. All tested samples, from all places, were previously measured, exposed to the appropriate aggressive environments, cleaned and then measured again. In general, after 6 months of exposure [3], all tubes were 100% covered with corrosion.

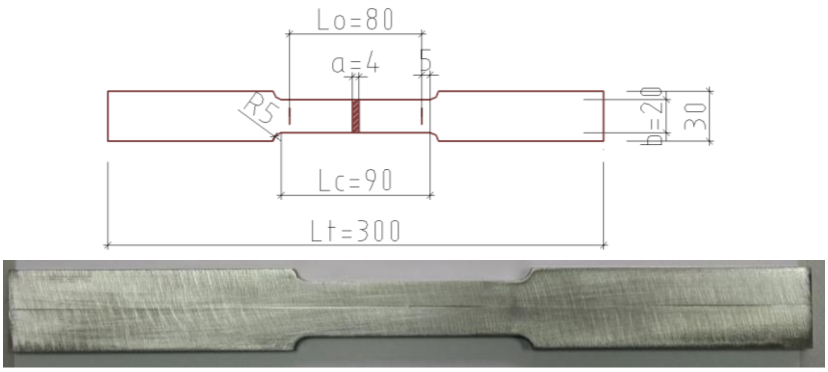

Figure 1 *Dimensions and appearance of sample before exposure*

Mechanical characteristics were obtained by the tensile testing of all tubes. Tensile testing is performed on the universal testing machines or torches with hydraulic or mechanical drive. The main parts of tensile testing machines are: stand (or frame), loading device, force measuring device and device for automatic drawing of force-deformation diagrams. A "Servo-hydraulic Universal Testing Machine Instron 1332 with FastTrack8800control system" was used in the experiment. The maximum tensile force is 100 kN.

ACCELERATED METHODS FOR CORROSION TESTING

It is desirable that the corrosion resistance tests are performed in the real operating conditions or on the atmospheric corrosion stations. These are specially selected places, most often with an industrial atmosphere, where samples are exhibited and changes in them and monitored due to corrosion. Atmospheric corrosion stations perform not only the tests of resistance of metals, alloys and their welded joints to the general corrosion, but also the tests of other types of corrosion (pitting, selective corrosion, stress corrosion, etc.). Tests on corrosion stations are long-lasting, so the accelerated laboratory tests are often used, during which corrosion destruction occurs in a relatively short time. Acceleration of corrosion processes is achieved by the action of aggressive components, imposition of a certain electrode potential, increasing temperature and degree of humidity, etc. The corrosion testing methods used in this paper are explained below.

Continuous immersion in solution

This is technically the simplest method. The time required to reach the desired level of corrosion damage to material depends on the chemical composition of solution and corrosion resistance of t sample. During these tests, the acceleration of corrosion process is achieved by continuous or alternating immersion of samples in solutions of a certain composition, at certain temperature. The tests are most often performed in chloride solutions (NaCl, $FeCl_3$), usually with the addition of an oxidizing agent (H_2O_2, $KCrO_4$). In this way, not only the general corrosion of metals, alloys and their welded joints is tested, but also the other types of corrosion (pitting, stress corrosion, etc.).

In this work, electrolyte solutions from the Electrolysis were used as a corrosive medium, which fulfilled the condition that solution corresponds to the industrial environment. The immersion was continuous, lasting for a month.

Accelerated aging chambers

In the chambers for corrosion tests, the acceleration of corrosion process is done increasing the temperature and relative humidity of air, with introduction the aggressive components into the atmosphere of chamber. The most important tests are in a wet chamber, chamber with SO_2 and in salt chamber (NSS, ASS and CASS method). All these methods are used to test not only the general corrosion of metals and alloys and their welded joints, but also to test the other types of corrosion, such as pitting, corrosion in gaps, stress corrosion, etc. In this experiment, a test was performed in the salt chamber "Industrial filter" with an external compressor according to ISO 9227, with neutral spray (NSS test) for 120h and 240h. The concentration of sodium chloride solution is 5% (pH 6.5 ÷ 7.2), at a temperature of 35°C (± 2°C).

Scab test

This method is used for accelerated testing in the external field conditions, in selected atmospheric corrosion stations. In this experiment, locations near the Sulfuric Acid Plant, Electrolytic Refining Plant (Electrolysis) and next to the automatic air quality monitoring station in Bor were selected (Figure 1). Exposure of samples (steel tubes) lasted 6 months. Samples are placed on a wooden frame so that they rest on it with the smallest surface. They are placed at an angle of 45 ° to the ground, as a horizontal, and facing south, which in many tests is considered as the position in which the largest surface of sample is affected by corrosion in the longest time interval [2]. The Scab test is the subject of ISO 11474: 2014, which defines repeated spraying of salt solutions. In this experiment, the standard in terms of spraying was deviated, because an attempt was made to obtain the material degradation due to corrosion with real agents in the industrially aggressive environments, with atmospheric conditions in winter months between November and May.

CLEANING OF SAMPLES FROM CORROSION PRODUCTS

Corrosion products from all samples, after exposure, as well as from control, standard, were removed according to the standard SRPS C.A5.005. This standard specifies procedures for removal the corrosion products from metals and alloys, which are created on samples for corrosion testing during their exposure to the corrosive media. The procedures set out in this standard are intended to remove corrosion products without significant removal of the parent metal. This enables accurate determination the loss of metal mass or alloy, which occurs during exposure to the corrosive environments.

An ideal cleaning method involves removing only the corrosion products, while the base metal remains intact. To determine the mass loss of parent metal when removing the corrosion product, the parallel uncorroded, control sample is cleaned by the same procedure as sample under test. By measuring the mass of control sample before and after cleaning, the value of mass loss, caused by cleaning, is obtained and this value is used to correct the mass loss for sample from which the corrosion products are removed.

Figure 2 *Placement of samples in the field*

Chemical cleaning methods involve exposing of samples for corrosion testing to a specific chemical solution that removes corrosion products with minimal dissolution of any parent metal. Chemical cleaning is often performed with prior light brushing of test specimens to remove bulky corrosion products that do not adhere to the substrate. Periodical removal of samples from solution for easy brushing can facilitate the removal of corrosion products that adhere firmly. On the test tubes exposed to the atmospheric effects, first the products were removed mechanically, and then chemically, for duration defined in standard. The reference samples were followed by the same method, according to the recommendations of standard, in order to take into account the mass losses, due to the effect on the base material.

ANALYSIS OF THE RESULTS

The degradation level of mechanical properties and changes in mass due to the corrosion on samples after 6 months of exposure to the atmospheric effects in Bor, at three sites, then on samples exposed 120 h and 240 h in a salt chamber, samples immersed in electrolyte solution for one month and samples stored in the laboratory conditions, are shown in Table 2. Designation E indicates standard samples, A immersed in electrolyte solution, EF samples placed in the Electrolytic Refining Plant, MP samples next to the station of automatic air quality monitoring (in order to further correlate the corrosion level and percentage content of corrosion inhibitors in the air). The AF samples were placed in the immediate vicinity of the Sulfuric Acid Plant. SSI is a designation of samples exposed to the NSS test for 120 hours, and SSII exposed to 240 hours.

Table 2 *Comparative values of change in mass and breaking force on samples from standard, immersed in solution, exposed to the atmosphere and in a salt chamber*

Sample designation		**Exposure period**	**Mass before exposure (g)**	**Mass after exposure (g)**	**Mass loss in percent**	**Breaking force (N)**
E	E5	6 months	521.467	521.440	0.005	63597.00
	E6	6 months	513.088	513.056	0.006	62120.00
A	A5	1 month	521.264	489.223	6.147	57798.00
	A6	1 month	518.690	485.432	6.412	57479.00
EF	EF5	6 months	521.256	520.341	0.176	63154.00
	EF6	6 months	503.781	502.714	0.212	61382.00
AF	AF5	6 months	519.034	511.258	1.498	61680.00
	AF6	6 months	521.248	513.691	1.450	61972.00
MP	MP5	6 months	521.210	518.870	0.449	63303.00
	MP6	6 months	513.096	511.491	0.313	62127.00
SSI	SSI5	120h (5 days)	522.374	521.100	0.244	62563.00
	SSI6	120h (5 days)	521.472	520.077	0.268	62126.00
SSII	SSII-5	240h (10 days)	507.020	505.051	0.388	60053.00
	SSII-6	240h (10 days)	510.228	508.441	0.350	60791.00

All of the above samples were pre-measured, exposed to the appropriate aggressive media and re-measured to determine the change in mass. Corrosion products from all samples, as well as from control, standard, were removed according to the standard SRPS C.A5.005 in a solution of hydrochloric acid, hexamethyl tetraamine and distilled water. The standard samples, as expected, have negligible weight losses, compared to the other samples that have been exposed to the corrosive agents.

From the above results (Table 2), it is noticeable that the percentage mass loss of samples near the Sulfuric Acid Plant is far higher than on samples located next to the measuring station, which is 4 kilometers away from the plant. Also, the mass loss samples immersed in electrolyte solution from electrolysis is much greater than the mass loss of samples that were placed in the Electrolysis Plant. Therefore, the force that these test tubes can receive is less.

Furthermore, it can be seen from this Table that the weight loss in the test tubes exposed to the atmospheric effects is significantly higher than in the same samples exposed to the effect in salt chamber, for approximately the same values of breaking force that these tubes can receive. This data unequivocally shows that the uniform corrosion is emphasized in samples exposed to the atmospheric effects, which is expected, while the other types of corrosion are present in samples from salt chamber, such as pitting or spot corrosion, which is noticeable on the surface of samples. [1]

However, based on the breaking forces, it can be concluded that the exposure time of 6 months in the industrial environment with increased CO_2 content in the air corresponds to the exposure period in a salt chamber with neutral solution (NSS test) between 120 h and 240 h, since between these values can be reported good correlation. This proves that in accurately conducted laboratory conditions, with greater or lesser accuracy, the atmospheric corrosion of industrial environments can be simulated, thus simplifying and acelerating the experimental process.

CONCLUSION

When comparing samples from different places, one must be very careful. The chosen methods cause different types of corrosion. Those that cause the non-uniform types of corrosion are more complex and require more careful analysis in order to approach the real conditions in the exploitation of steel elements.

The obtained results and data from this work should contribute to the perception and study of bearing capacity and durability of corrosion - weakened steel structures in the industrial environments, where there are many inhibitors of atmospheric corrosion. First of all, it is necessary to check the laboratory accelerated corrosion methods in the real operating conditions, which would reduce the time required to perform the experiments.

REFERENCES

[1] J. Stanković, Z. Mišković, M. Pavlović, D. Jevtić, Z. Marković, The Effect of Corrosion Propagation in the Industrially Aggressive Environments and Salt Chamber on the Bearing Capacity of Axially Tensioned Elements, International Conference YuCorr, Tara, Serbia, 2017, 128-133 (in Serbian)

[2] S. P. Parekh, A. V. Pandya, H. K. Kadiya, Progressive Atmospheric Corrosion Study of Metals Like Mild

Steel, Zinc and Aluminum in Urban Station of Ahmedabad District, International Journal of ChemTech Research, CODEN (USA), Vol. 4, No. 4, Oct-Dec 2012, 1700-1774

[3] Mendoza, F. Corvo, Outdoor and Indoor Atmospheric Corrosion of Carbon Steel, Corrosion Science 41 (1999) 75-86

[4] M. Pavlović, D. Stanojević, S. Mladenović, Corrosion and Protection of Materials, 1st Ed., Faculty of Technology Zvornik, 2012 (in Serbian)

MINING AND METALLURGY INSTITUTE BOR
UDK: 622
ISSN: 2334-8836 (Štampano izdanje)
ISSN: 2406-1395 (Online)

UDK: 621.38:681.586(045)=111
DOI: 10.5937/mmeb2104061P
Received: 01.10.2021.
Revised: 01.11.2021.
Accepted: 01.12.2021.
Original Scientific Paper
Electronics

Marijana Pavlov-Kagadejev[*]

DIFFERENT WAYS FOR VISUALIZATION OF DATA OBTAINED FROM AN ARDUINO UNO MICROCONTROLLER BOARD[**]

Abstract

Arduino microcontroller platforms are frequently in use in the last few years. The reason is their simplicity, low cost, and availability of a large number of ready-made solutions on the Internet. The Arduino Integrated Development Environment itself has a Serial Monitor and Serial Plotter tools for data presentation. The Serial Monitor displays the textual and numeric values of the data obtained through the serial port. By using the Serial Plotter, measurement results from the Arduino serial port can be seen in the form of Real-Time diagrams. The deficiency of such a way of data visualization is that it does not provide many opportunities for change and adaptation to the user needs. This paper presents examples of several different programming environments which provide the good opportunities for presentation the results generated by the Arduino boards. Some hardware modules used to display data from the Arduino boards are also described in this paper.

***Keywords**: Arduino, visualization, measurement, sensor, graph, Real-Time*

1 INTRODUCTION

The Arduino-based microcontroller boards are very popular in the last few years due to their low cost, simplicity, and functionality. It is very often used to measure various parameters, as a research tool, or for entertainment [1, 2, 3]. There are a number of low-cost sensors, which can be easily connected to Arduino boards. The obtained results can be archived and later used for various purposes. There are different versions of the Arduino boards like the Arduino Uno, Arduino Mega, Arduino Leonardo, etc. The all are affordable, but due to their price, the most common is the Arduino Uno microcontroller board. The Arduino Uno is easy to operate and there are a number of ready-made software solutions on the Internet that works with this platform.

For the users, who only need to monitor the current value of measured parameters, without archiving data, and with no need for better visualization, it is enough to connect some sensors to the Arduino board, and load the appropriate program (which is easy to find online and modified if needed) using the Arduino IDE (Integrated Development Environment). In such cases, by the use of the IDE tool Serial Monitor, and sending the measured values to the serial port, the results of measurements will appear in the format defined by the program. Another Arduino IDE tool, the Serial Diagram, provides an on-screen presentation of measurements results in the form of time diagrams. Such a way of presenting data is very limited and hardly usable for further

[*] *Mining and Metallurgy Institute Bor, Zeleni bulevar 35, 19210 Bor, Serbia*
[**] *This work was financially supported by the Ministry of Education, Science and Technological Development of the Republic of Serbia, Grant No. 451-03-9/2021-14/200052*

research and analysis. To overcome this problem, different programming environments and hardware modules are used.

In this paper, different ways of data visualization will be shown on a simple example of temperature and humidity measurements using the Arduino Uno microcontroller and DHT22 sensor. Measured data were displayed using the programs created in different programming environments (Processing, Node-red, LabVIEW, and Visual Studio C #) and hardware modules (LCD, 7-segment display, LED, and OLED display). The aim of this paper is to facilitate the selection of programming environments for working with an Arduino board and to give their advantages and disadvantages. Also, the paper aims to display various hardware modules, which are suitable for the self display of data without a PC. This is especially suitable for portable measuring devices development.

2 ARDUINO UNO AND DHT22 SENSOR CHARACTERISTICS

a) *b)*

Figure 1 *a) Arduino Uno microcontroller board, and b) DHT22 sensor*

The Arduino Uno (Figure 1a) is a microcontroller board with the 14 digital input/output pins (6 can be used as PWM outputs), 6 analog inputs, 16 MHz ceramic resonator (CSTCE16M0V53-R0), USB connection, power jack, ICSP header and reset button. It is based on the ATmega328P microcontroller. This board contains the USB port for simply connection to a computer, or powers it with an AC-to-DC adapter or battery to get started. The Arduino Uno board is the first in a series of USB Arduino boards, and reference model for the Arduino platform. The main characteristics of the Arduino Uno microcontroller are given in the Table 1 [4].

Table 1 *Technical characteristics of the Arduino Uno microcontroller*

Microcontroller	ATmega328
Operating Voltage	5V DC
Input Voltage (recommended)	7-12V
Input Voltage (limits)	6-20V
Digital I/O Pins	14 (6 provide PWM output)
Analog Input Pins	6
DC Current per I/O Pin	40 mA
DC Current for 3.3V Pin	50 mA
Flash Memory	32 KB (ATmega328) (0.5 KB used by bootloader)
SRAM	2 KB (ATmega328)
EEPROM	1 KB (ATmega328)
Clock Speed	16 MHz

The DHT22 is a digital sensor module (Figure 1b) that consists of a thermistor, for temperature measurement, and capacitive sensor, for determining the relative air humidity. The DHT22 working temperature is from -40°C to + 80°C, and the relative air humidity range is from 0 to 100%. Temperature and humidity measurement accuracy are 0.5° C and 2%, respectively [5]. The DHT22 sensor module with 3 pins has been used in this research. The first pin (shown in Figure 2) is for ground (GND), the second for power supply (VCC), and the third for data transfer (DATA) [6].

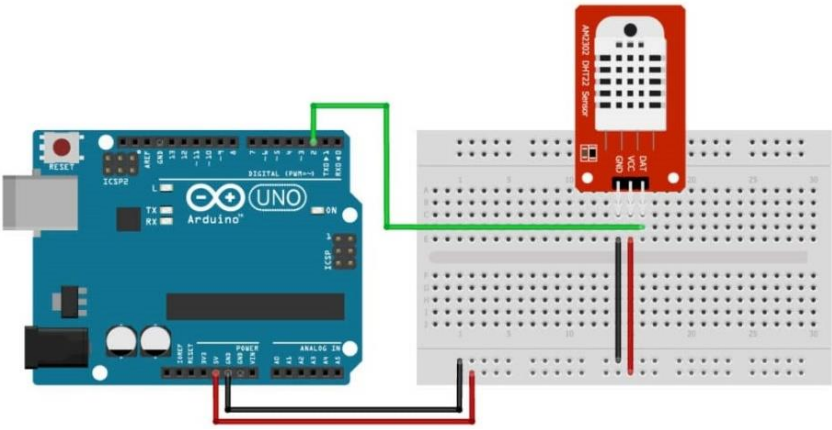

Figure 2 *Wiring DHT22 sensor module to Arduino Uno board*

For the DHT22 sensor module programming, the DHT sensor library has to be installed by the Arduino Library Manager. Also, an adequate code has to be written and uploaded on the Arduino Uno. After that, the measured values of temperature and relative air humidity will appear on the Adriano Serial Monitor and Serial Diagram. On the Serial Monitor, the measured values appear in the format defined by the code, and time diagrams of the measured parameters appear on the Serial Diagram (Figure 3).

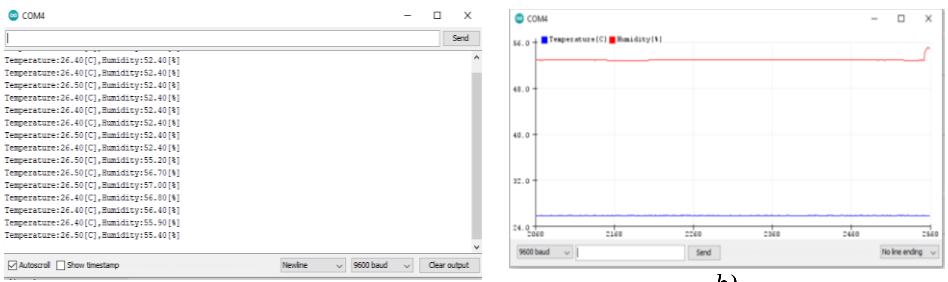

a) *b)*

Figure 3 *Data displayed on a) Serial Monitor and b) Serial Plotter on Arduino IDE*

3 SOTFWARE TOOLS FOR DATA PRESENTATION

In order to improve the presentation of data obtained by an Arduino board, a large number of different programming environments may be used. These environments are very different, both in terms of programming, capabilities, and price. Some of them are free, while some are very expensive. In this paper, we will present data measured with Arduino Uno and DHT22 sensor using the programs created in the Processing, Node-red, LabVIEW, and Visual Studio C # programming environments.

3.1 Processing 3

The Processing 3 is an open-source environment, a flexible software sketchbook and language for learning how to code within the context of visual arts [7]. It has been promoting software literacy in visual arts and visual literacy in technology since 2001. Processing is used for learning and prototyping.

In terms of structure, the Processing IDE is similar to the Arduino. It has setup function and draw function like the Arduino has a setup and loop function. The Processing IDE can communicate with the Arduino IDE via serial communication. In this way, we can send data from the Arduino to the Processing IDE, and also from the Processing IDE to the Arduino. The Processing IDE layout is shown in Figure 4.

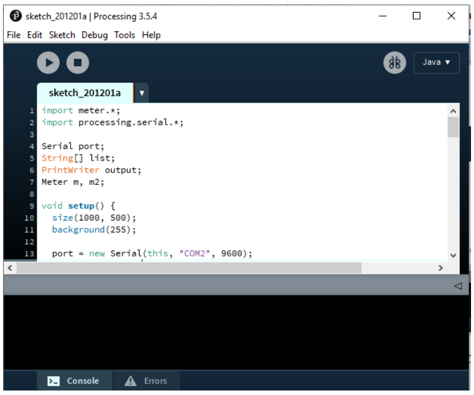

Figure 4 *Processing code*

The Arduino board communicates with the PC using the serial port. Processing sketch can be used to read data from the Arduino board via serial communication by importing a Serial library (Figure 5). This library is already built-in Processing.

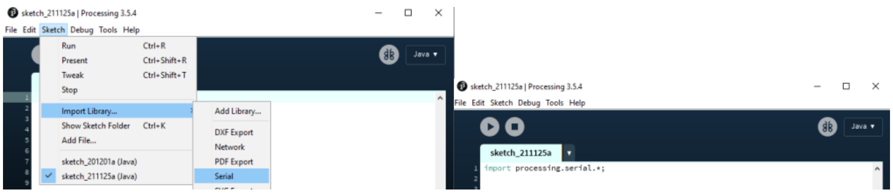

Figure 5 *Importing Serial Library in Processing sketch*

The methods used by the serial communication protocol are described below:

To Import Serial library: `import processing.serial.*;`

To create an object from Serial class: `Serial myPort;`

To list all available serial ports: `println(Serial.list());`

To define port number connected to Arduino board:

`String portName = Serial.list()[0];`

To open the used port and define the Boud Rate:

`myPort = newSerial(this,portName,9600);`

Figure 6 presents an example of displaying data from athe Arduino Uno board and DHT22 sensor module by a program written in the Processing IDE.

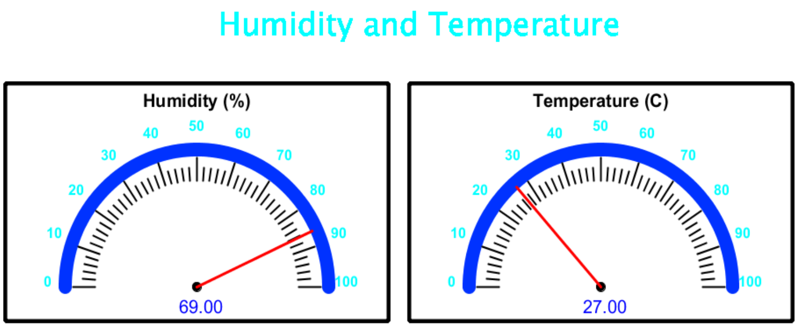

Figure 6 *Arduino data visualization by using Processing script*

3.2 Node-red

The Node-RED is a programming tool that connects hardware devices, APIs, and online services in new ways [8]. It has a browser-based editor that makes it easy to wire together flows using the wide range of nodes in the palette. Flows can be deployed to the runtime in a single click. The JavaScript functions can be created within the editor using a rich text editor. Useful functions, templates, or flows for re-use can be saved using the built-in library.

The lightweight runtime is built on the Node.js. This makes it ideal to run on a low-cost hardware such as the Raspberry Pi as well as in the cloud. There are over 225,000 modules in the Node package repository. That makes it easy to extend the range of palette nodes to add the new capabilities.

The Node-RED does not have preinstalled nodes for the Arduino, Serial port, and Dashboard. So, these nodes have to be installed with the following commands on the Command Prompt:

```
npm install node-red -node-arduino
npm install node-red -node-serialport
npm install node-red -dashboard
```

The Serial port node (Figure 7a) is used to enable the Node-RED serial communication with the Arduino board. It has to be dropped from the Nodes palette into the flow section. By double click on the node, a pop window will appear. The correct number of COM port has to be chosen. The other parameters like the Boud Rate have to be defined in this window (Figure 7b).

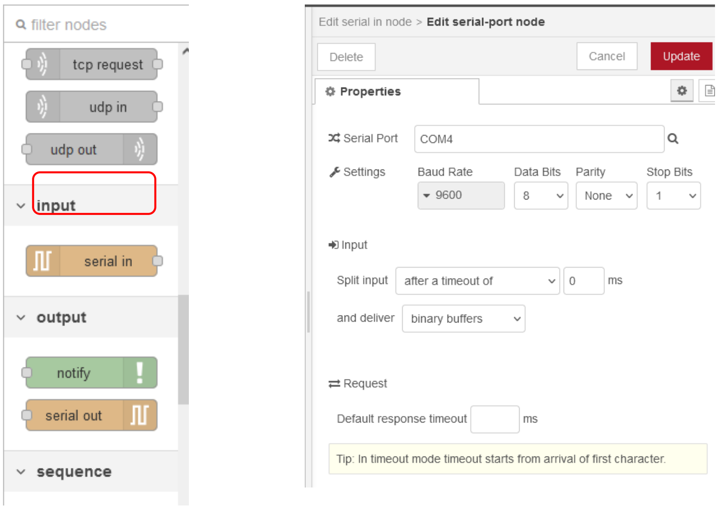

a) *b)*

Figure 7 *Serial port node object properties in the Node-RED programming environment*

Figure 8 shows an application that displays data from the Arduino Uno board and DHT22 sensor module. The flow dashboard is shown on the left, and the values and graphs of temperature and relative air humidity, obtained from the sensor, are shown on the right side.

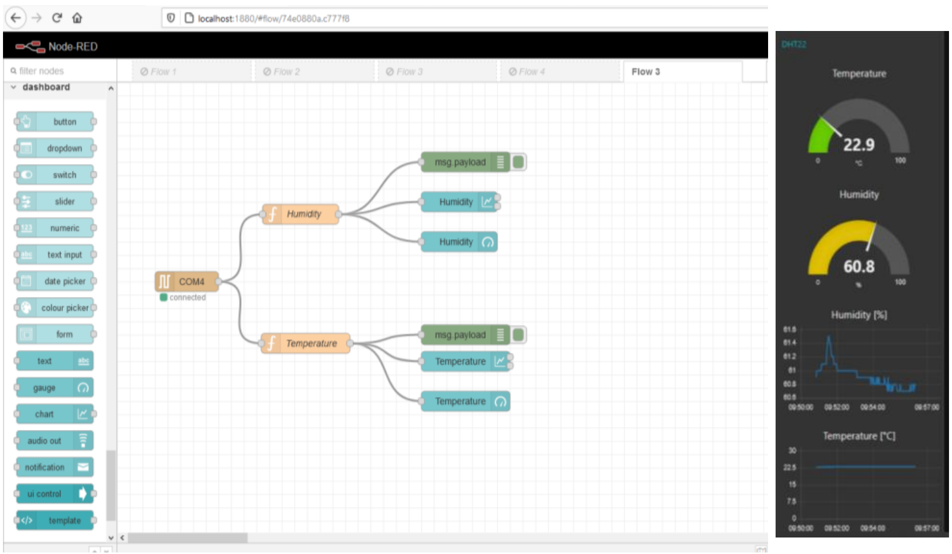

Figure 8 *Node-RED application for data visualization from Arduino board*

3.3 LabVIEW

The LabVIEW is a software dedicated to the measurement applications that require test, measurement, and control with rapid access to the hardware and data insights [9]. It offers a graphical programming approach that helps to visualize every aspect of an application, including hardware configuration, measurement data, and debugging. This makes it simple to integrate measurement hardware from any vendor, represent complex logic on the diagram, develop data analysis algorithms, and design custom engineering user interfaces.

With LabVIEW and adequate hardware, it is easy to build a custom measurement solution to visualize and analyze real-world signals and to make data-driven decisions. Flexible test applications that control multiple instruments can be created with the LabVIEW. Industrial equipment and smart machines can be built faster using the LabVIEW. The LabVIEW can be used for teaching students in the classroom or lab, too.

In our example, the Virtual Instrument Software Architecture (VISA) is used to connect the Arduino board with the LabVIEW. The required object has to be selected from the Block Diagram window as follows: Data Communication > Protocols > Serial (as shown in Figure 9).

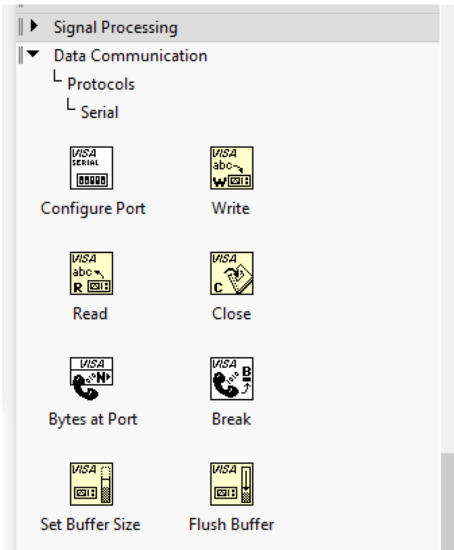

Figure 9 *Virtual Instrument Software Architecture objects window*

A VISA Configure Serial Port object allows users to choose which serial port to use and to set up the Baud Rate. The default Baud Rate is 9600.

An example of a LabVIEW application is shown in Figure 10. Figure 10a shows the Front Panel, and Figure 10b a the Block Diagram of this application. Controls, bar graphs, diagrams, and parameter values obtained from the Arduino Uno board and DHT22 sensor module are shown in the Front Panel. The Block Diagram shows the elements that make up the LabVIEW application.

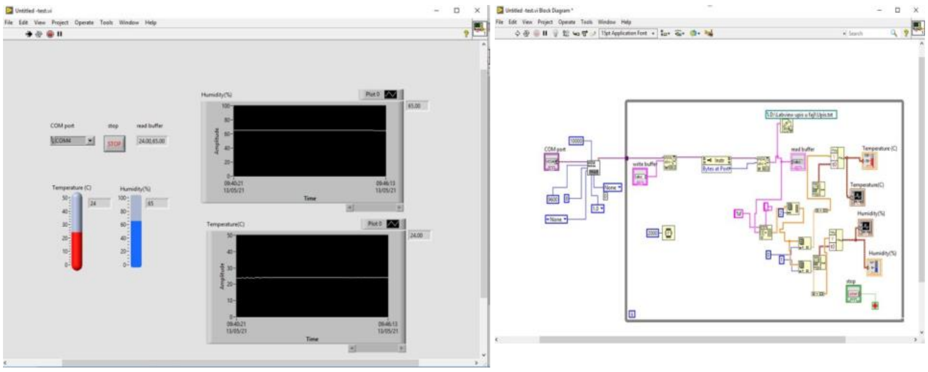

a) *b)*

Figure 10 *LabView application: a) Front Panel, and b) Block Diagram*

3.4 Visual Studio IDE | C#

The Visual Studio IDE is a creative launching pad that can be used to edit, debug, and build code, and then publish an app. Such IDE can be used for many aspects of software development. Visual Studio includes compilers, code completion tools, graphical designers, and many more features to ease the software development process [10]. Visual Studio IDE| C# is shown in Figure 11.

The Visual Studio Code is a powerful source code editor which runs on a desktop and is available for Windows, macOS, and Linux. It comes with a built-in support for the JavaScript, TypeScript, and Node.js and has a rich ecosystem of extensions for other languages (such as C++, C#, Java, Python, PHP, Go) and runtimes (such as .NET and Unity).

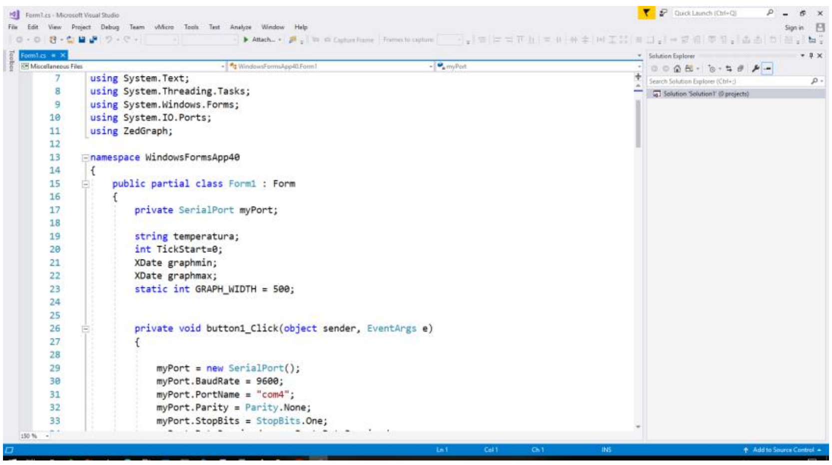

Figure 11 *Visual Studio IDE | C#*

The using statements at the top of code define links to the libraries (called namespace). Using System.IO.Ports has to be written to the top of code. After that, the SerialPort class can be used in the program for serial communication with the Arduino board. This class provides a framework for synchronous and event-driven I/O, access to the pin and break states and access to the serial driver properties [11].

Figure 12 shows how the SerialPort tool can be added to the Windows Form Application. From Toolbox, the Serial Port tool has to be dropped to Form. Properties of this tool will appear by the right click on it.

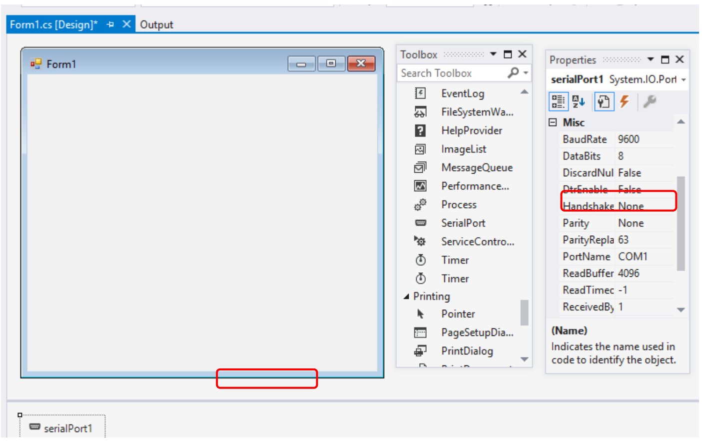

Figure 12 *SeralPort tool with serial port object properties in C#*

The Visual Studio programming IDE is available for Windows and Mac OS. An application for data visualization, obtained from the Arduino board, is developed in the Visual Studio C#. Real-time diagrams and numerical values, obtained from the Arduino Uno board and DHT22 sensor board, are shown in Figure 13.

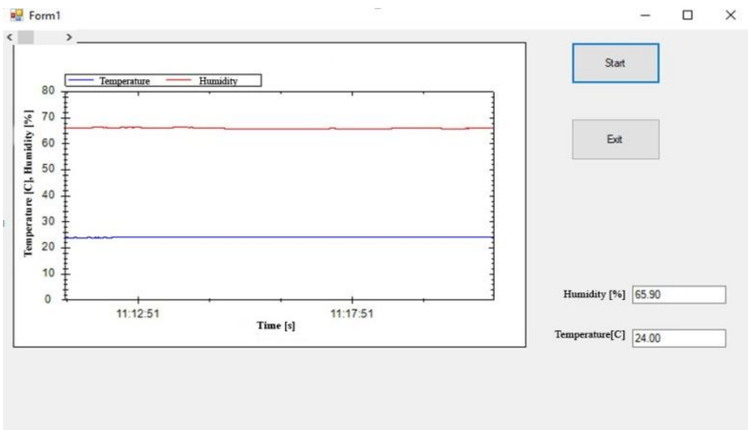

Figure 13 *Visual Studio C# application for data visualization from Arduino board*

4 HARDWARE MODULES FOR DATA DISPLAYING FROM THE ARDUINO BOARDS

There are different types of hardware modules that are used to display data from an Arduino microcontroller. Some of them are the 7 segments, LED, OLED, and LCD displays (Figure 10). The advantage of this way of displaying data is that a PC is not necessary after code has been uploaded to the Arduino.

The measured values are shown on display. This way of displaying data is suitable for the portable measurement devices [12, 13].

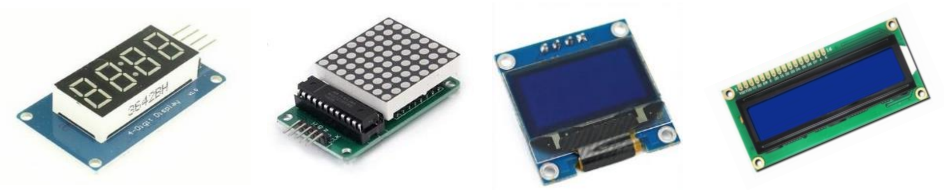

a) *b)* *c)* *d)*

Figure 10 *Different types of displays: a) 7 segment, b) LED, c) OLED, d) LCD*

The most popular way for displaying information from the Arduino boards is made using the LCD displays. The LCD displays can be divided into two generic types: characters and graphics. Character LCD is the cheapest and simplest display. It consists of several rows and columns. 1602 LCD Display Module has 2 rows and 16 columns and can display 32 characters. This display is simple and has full compatibility with the all Arduino microcontrollers and processor boards. The 16x2 Arduino LCD Keypad Shield is very popular. It includes and 6 push buttons. Figure 11 shows an example of measurement results presentation by using the 1602 LCD Keypad Shield Module connected on an Arduino Uno board.

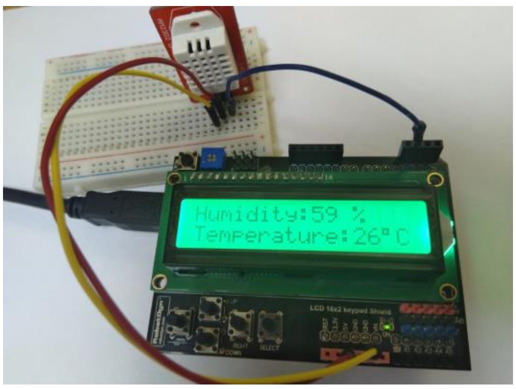

Figure 11 *Measurement results presentation by using the 1602 LCD Keypad Shield Module*

The LCD displays are frequently used for measurement the results presentation in portable measurement devices. An example of using the LCD2004 module (4x20 characters display) in a portable measuring device is given in Figure 12. In addition to the DHT22 sensor, this device has a sensor module for measuring the PM_{10} and $PM_{2.5}$ particle concentrations.

Figure 12 *Using the LCD display in a portable measurement device*

CONCLUSION

This paper presents the different ways for data visualization obtained with an Arduino board. Four different programming environments are used: Processing 3, Node-red, LabVIEW and Visual Studio C #. Processing 3 and Node-red are open-source free environments and there are numerous free examples on the Internet that can make their use easier for users who are not professional software developers. The LabVIEW environment provides a lot of possibilities, but it is necessary to know how this specific environment works, in order to develop the applications. In addition, the LabVIEW is an expensive package and is not affordable to everyone, after a trial period. The Visual Studio C # provides the biggest freedom for developers. However, the cost of the Professional and Enterprise version of this programming IDE is not negligible. For students and for non-commercial purposes, a Community version is available for free. There are many other different programming tools that can be used to display data obtained by the Arduino boards that are not mentioned in the paper. All users will choose the visualization method that suits them the best, based on their personal requirements, needs, and possibilities. If the user priority is to read the measured values without a PC, then it is most convenient to use the hardware modules to display data from the Arduino boards. Such display modules are the low-cost and their implementation is not so complex for the common user of the Arduino IDE.

REFERENCES

[1] Bist´ak P., Arduino Support for Personalized Learning of Control Theory Basics, IFAC-PapersOnLine ELSEVIER Volume 52, Issue 27, 2019, Pages 217-221

[2] Louis L., Working principle of Arduino and Using it as a Tool for Study and Research, International Journal of Control, Automation, Communication and Systems (IJCACS), Vol.1, No.2, April 2016 DOI: 10.5121/ijcacs.2016.1203 21
[3] Organtini G., Arduino as a Tool for Physics Experiments, IOP Conf. Series: Journal of Physics: Conf. Series 1076 (2018)
[4] https://www.arduino.cc/en/Main/ArduinoBoardUnoSMD
[5] Bogdan M., How To Use The DHT22 Sensor For Measuring Temperature And Humidity With The Arduino Board , Acta Uiversitatis Cibiniensis – Technical Series Vol. LXVIII 2016
[6] https://www.makerguides.com/dht11-dht22-arduino-tutorial/
[7] www: https://processing.org
[8] www: https://nodered.org
[9] www: https://www.ni.com
[10] www: https://visualstudio.microsoft.com
[11] https://docs.microsoft.com/en-us/dotnet/api/system.io.ports?view=dotnet-plat-ext-6.0
[12] Tasić V., Cocić M., Radović B., Božilov A., Apostolovski-Trujić T., Assessment of the Impact of External Pollution by Suspended Particles on the Indoor Air Quality at the Technical Faculty in Bor, Copper, Vol.45., 2 (2020) 19-28 (in Serbian)
[13] Tasić V., Božilov A., Lazović I., Mirkov N., Measurement of CO2 concentrations in the Indoor Air Using the Low-Cost Sensors and Monitors, Copper, Vol.45., 2 (2020) 11-18 (in Serbian)

MINING AND METALLURGY INSTITUTE BOR
UDK: 622

ISSN: 2334-8836 (Štampano izdanje)
ISSN: 2406-1395 (Online)

UDK: 66.017:541.183(045)=111
DOI: 10.5937/mmeb2104073M

Received: 15.10.2021.
Revised: 15.11.2021.
Accepted: 15.12.2021.

Original Scientific Paper
Material Science

Vesna Marjanović[*], Radmila Marković, Vesna Krstić[*,**]*

DIFFERENT TYPES OF ADSORBENTS FOR SELENIUM (Se) REMOVAL FROM WATER: A REVIEW

Abstract

Development of adsorption materials based on metal oxides, silicon dioxide, carbon, biosorbents and adsorbents, obtained from natural waste, can be used to remove selenium from water. Research on some of these materials is at the laboratory level, while the others were tested in the pilot plants, and a few have found a commercial application. The high adsorption capacities show a possibility of their application for selenium removal from water. This paper presents a literature review of different types of adsorbents for the removal of selenium (Se) from water.

Keywords: *selenium, adsorption, adsorbents, adsorption capacity*

1 INTRODUCTION

Selenium (Se) is naturally present in rocks and soils in the environment in the form of selenite, selenate, selenide, and elemental Se. It is a trace element in the natural ore deposits that contain minerals, such as heavy metal sulfides [1]. In addition to the naturally occurring Se, its increase of concentration in the environment is caused by human activities, especially mining, coal combustion, pesticide production, agricultural use, etc. [2]. Selenium occurs in water and wastewater from natural sources, but also due to anthropogenic activities, such as agriculture, mining, oil refineries, and coal combustion, the concentrations range from a few micrograms per liter to 30 mg L^{-1}.

Selenium is nutritionally important in small amounts, but higher amounts are associated with certain diseases and potential side effects in humans, and can also be toxic to aquatic organisms, birds, and other animals, which is shown to be a worldwide problem.

In accordance with the principles of green chemistry, it is necessary to take preventive measures to reduce the release of selenium, and then the necessary methods for removal from water should be considered and evaluated. Various methods for the treatment of selenium-containing water and wastewater have been investigated [3,4]. Some are still in the laboratory research phase, others have already been tested in the pilot plants, and a few have been applied on a commercial scale. It is difficult to define the best cost-effective option, given the different characteristics of water and wastewater that need to be treated, which requires specific approaches and different costs. The impact of any technology should be assessed, optimized and demonstrated on the basis of a case study [5]. Selenium removal can be achieved by application physical, chemical, and biological methods. Therefore, the prevention, control and removal of selenium from water are very important.

[*] *Mining and Metallurgy Institute Bor, Zeleni bulevar 35, 19210 Bor, Serbia, vesna.marjanovic@irmbor.co.rs, radmila.markovic@irmbor.co.rs*
[**] *University of Belgrade, Technical Faculty Bor, VJ 12, 19210 Bor, Serbia, vesna.krstic@irmbor.co.rs*

2 ADSORPTION

Special attention is paid to the removal of selenium in the scientific literature, where the application of adsorption, development and efficiency of different types of adsorbents having a special significance. Conventional and alternative materials have been explored as the potential adsorbents for Se, in order to find the cheap strategies for water and wastewater treatment. Until now, the scientific literature has mostly published series of laboratory tests, using the standard selenium solutions. The adsorption materials are classified into organic resins, oxides and minerals (including single and mixed oxides and hydroxides), carbon-based adsorbents (activated carbon and graphene), biosorbents and adsorbents derived from the natural waste.

The obtained experimental data are modeled by the well-known Langmuir and Freundlich isotherms. The parameters, obtained by the Langmuir isotherm (especially Q_m), can be directly correlated with the adsorption properties of an adsorbent. The maximum adsorption capacity (Q_m) represents the maximum amount of adsorbate that a solid can retain to achieve a single layer coverage. In addition, the Langmuir isotherm also provides a qualitative agreement with the experimental data obtained for the values (Q_m) [6].

It is important to note that the adsorbed amounts of Se depend on the experimental conditions (pH, concentration, ionic strength of solution, temperature, ions in solution, etc.). It is clear that the maximum adsorption capacity (Q_m) is not the only criterion to estimate the adsorbent potential, but it may be the first. Many other aspects must be considered such as the adsorption kinetics, effect of various factors on adsorbent performance, suitability for continuous treatment, separation of solid and liquid phases, leaching results, availability and cost of procurement, regeneration and disposal after use.

2.1 Adsorption materials based on organic resins, metal oxides and silicon dioxide

Thiourea-formaldehyde (TUF) chelating resin was synthesized and used in the adsorption of selenite (SeO_3^{2-}) and selenate (SeO_4^{2-}) ions. The effect of the initial acidity of the solution and the initial concentration of selenium on adsorption was investigated. Selenite and selenate ions were found to be adsorbed on TUF resin under strongly acidic conditions (3–5 M HCl). The adsorption capacity of TUF resin was 833.3 mg g^{-1} for selenite and 526.3 mg g^{-1} for selenate. All the obtained adsorption data for selenite and selenate ions fit well into the Langmuir isotherm. Mechanisms of adsorption are the reduction of selenite or selenate to elemental selenium, Se (0) [7], Table 1.

Oxides of aluminum, iron and silicon dioxide, in natural or synthesized forms, can be used to remove selenium. In addition to the large specific surface area, the oxides generally have a high zero charge point (pH_{ZPC}), which means that the solid surface will be positively charged over a wide range of pH values, and have a higher affinity for the oxyanion adsorption [25]. Many studies of oxyanones and oxides were conducted to explain the type of interaction between the adsorbate and adsorbent, Table 1. The type of interaction between selenite species and selenate with mineral oxides was studied using the X-ray adsorption spectroscopy (XRD), and it was shown that selenate forms a weakly bound complex with the outer-sphere, and that selenite forms a tightly bound complex with the inner-sphere [26].

Table 1 *Adsorption capacities (Q_m) listed in literature for Se (IV) and Se (VI) for oxides, minerals and organic synthetic resin*

Adsorbent	Se Species	C_{in} (mg L^{-1})	m/v (g L^{-1})	pH[a]	T (°C)	Q_m (mg g^{-1})	Ref.
Organic synthetic resin							
Thiourea–formaldehyde resin	Se (IV)	50-1000	0.4	*	-	833.2	[7]
	Se (IV)	100-500	0.4	*	-	526.3	
Oxides and minerals							
Commercial FeOOH	Se (IV)	0.5-20	0.5	5	25	26.3	[8]
Commercial hydroxyapatite	Se (IV)	0.005-0.020	-	5	30	0.82[c]	[9]
Anatose nanoparticles	Se (IV)	10-54	5.0	5	20	7.71	[10]
Magnetite	Se (IV)	0.24-40	-	4	25	0.22	[11]
	Se (VI)	0.24-40	-	4	25	0.25	
Binary oxide Al(III)/SiO_2	Se (IV)	0-237	-	5	25	32.7	[12]
	Se (VI)	0-237	-	5	25	11.3	
Binary oxide Fe(III)/SiO_2	Se (IV)	0-237	-	5	25	20.4	
	Se (VI)	0-237	-	5	25	2.4	
Fe-Mn hydride oxides based adsorbents	Se (IV)	5-500	2	4	22	41.02	[13]
	Se (VI)	5-500	2	4	22	19.84	
Mn_3O_4 (non-microwave- assisted aged)	Se (IV)	0.25-10	2.5	4	25	0.507	[14]
	Se (VI)	0.25-10	2.5	4	25	1.00	
Mn_3O_4 (microwave- assisted aged)	Se (IV)	0.25-10	2.5	4	25	0.800	
	Se (VI)	0.25-10	2.5	4	25	0.909	
Magnetic Fe/Mn oxide nanomaterial	Se (IV)	0.25-10	2.5	4	25	6.57	[15]
	Se (VI)	0.25-10	2.5	4	25	0.769	
Mg-Al LDH	Se (IV)	0-1000	4	9[a]	25	120	[16]
Zn-Al LDH	Se (IV)	0-1000	4	9[a]	25	99	
Mg/Fe HTlc	Se (IV)	~0-80[b]	1	6	30	2.9	[17]

*C_{in} - initial concentration range; m/v – adsorbent dosage; T - temperature, [a]initial pH; [b]equilibrium concentrations (estimated from the graphs); [c]maximum adsorption amount obtained experimentally, at the higher equilibrium concentration (20 µg L^{-1}); *3mol L^{-1}. HCl; **5 mol L^{-1} HCl.*

The studies have confirmed the observations [27, 28, 13], that the activated alumina (AA), mainly composed of aluminum-oxide (Al_2O_3), is a good material for adsorption and catalysis. It is prepared by dehydration of aluminum hydroxide at high temperatures and has the good physical properties, well-developed macro and meso porous structure, and a large specific surface area. The pH_{ZPC} value of activated alumina ranges from 8.4 to 9.1 [29, 30]. AA has been shown to be ineffective for Se (VI), and adsorption and performance for Se (IV) depend on pH, and are affected by silicon dioxide, arsenic, and vanadium in solution [30, 31]. For the initial Se (IV) concentrations in the range of 10–94 mg L^{-1}, the maximum adsorption is between pH 2 - 7, with a significant decrease above pH 7 [30]. The maximum adsorption efficiency was observed at pH values of 2.5 to 4 for a Se (IV) concentration of 440 mg L^{-1}. However, this dependence on pH is not a problem for the wastewater from flue gas desulfurization (FGD) and mine wastewater due to their typically acidic pH, but is not suitable for the agricultural water because its pH is around 8 [32].

Oxyhydroxides and iron oxides, such as magnetite (Fe_3O_4) [33, 34, 11, 35], hematite (α-Fe_2O_3) [36], maghemite (γ-Fe_2O_3) [37], FeOOH commercial adsorbent [8] and iron nanoparticles oxides/hydroxides [38] have been studied as selenium adsorbents. The adsorption of Se (VI) to maghemite was found to be dependent on the pH and ionic strength of solution [36]. Examination of the influence of pH value was done in the range of 3.5 - 8.0, and the best degree of removal is at pH 3.5; complete removal is at an ionic strength of 0.01 M NaCl and about 70% for 0.1 M NaCl (from an initial concentration of approximately 790 mg L^{-1} and using a 1 g L^{-1} dose of adsorbent).

Titanium dioxide (TiO_2) has been shown to adsorb different types of selenium [27, 39, 10]. Anatase is one of the polymorphic forms of titanium dioxide, which is a non-toxic mineral, with the high chemical stability, large specific surface area and ability to oxidize and reduce the absence of numerous pollutants. The isoelectric point of anatase pH_{ZPC} was found to be 6.3 (at 25°C) [36] and the adsorption of both selenium species on anatase gradually decreased with increasing pH [27, 37, 39, 10], with less efficient removal of selenates [39], with adsorption becoming negligible for the pH value above 6 [27, 37].

The kinetics of selenium (IV) adsorption on anatase is described by a pseudo-second order kinetic model, with the rate constants depending on pH and sorbate concentration [39, 18]. Ionic strength did not affect the adsorption of Se (IV) [39], but its increase caused a decrease in the removal of Se (VI) [27]. At pH 5 and temperatures in the range 273–313 K, the maximum adsorption capacities, according to the Langmuir model, were between 7.3 and 8.5 mg g^{-1} [10]. At pH 3.5, more than 90% of selenate was removed from an initial concentration of 0.8 mg L^{-1}, using an anatase dose of 0.46 g L^{-1}, and NaCl concentration of 0.01 mol L^{-1} [27], removal of Se (VI) selenate using anatase is not effective. The binary metal oxides, Al(III)/SiO_2 and Fe(III)/SiO_2, were prepared in order to improve the adsorption capacity of SiO_2 for anionic species [40]. The binary oxide Al(III)/SiO_2 showed the adsorption capacities for Se (IV) and Se (VI), 32.7 and 11.3 mg g^{-1}, respectively; higher than Fe(III)/SiO_2, 20.4 and 2.4 mg g^{-1}, respectively, due to a stronger association between Al(III) and surface of SiO_2 and its total specific surface area which is positively charged. After a contact time of 2 hours, more than 95% of Se (IV) was adsorbed and equilibrium was reached.

Szlachta and Chubar (2013) [13] developed an ion exchange adsorbent based on the oxides of hydrate Fe(III) and Mn(III) (ratio 1:1). The adsorption equilibrium isotherms were performed at 22°C and different pH values, which had a constant value during the experiments. The maximum adsorption capacity (single layer), calculated according to the Langmuir isotherm for Se (IV), was 41.02, 26.71 and 18.45 mg g^{-1}, at pH 4, 6 and 8, respectively. The predicted maximum adsorption capacity for Se (VI) is 19–20 mg g^{-1}.

2.2 Carbon-based adsorbents

Activated carbon (AC) is the most commonly used commercial adsorbent for water treatment. Its efficiency in removing numerous organic pollutants is well known, but its adsorption capacity for metals is not always satisfactory. Granular Activated Carbon (GAC) is used in continuous processes. The treatment of AC with iron has been investigated to improve its ability to remove oxyanions, although the iron treatment usually reduces the specific surface area and volume of pores [41, 42, 43, 18]. The pH_{ZPC} of modified AC and iron content itself have been shown to be determinants of AC performance for the arsenic oxyanone adsorption [44].

Zhang et al. (2008) [18] synthesized the granular activated carbon (Fe-GAC) and reported significant removal of selenite in a wide pH range (2–8) and reduction in removal efficiency at pH values greater than 8. The adsorption kinetics followed the second-order pseudo model and it took 48 hours to reach the equilibrium (more than 90% is adsorbed in 6 h). The adsorption isotherms are generally well described by the Langmuir model. The adsorption capacities ranged from 2.5–2.9 mg g^{-1} with different ionic strengths and temperatures (25–45°C). Phosphate, at a concentration of 5 mmol L^{-1}, completely suppressed the adsorption of selenite on the Fe-GAC. At concentrations between 0.1 and 5 mmol L^{-1}, sulfate did not show a significant effect on selenite adsorption on the Fe-GAC, Table 2.

Table 2 *Adsorption capacities (Q_m) listed in literature for Se (IV) and Se (VI) for carbon-based adsorbents*

Adsorbent	**Se Species**	**C_{in} (mg L^{-1})**	**m/v (g L^{-1})**	**pH [a]**	**T (°C)**	**Q_m (mg g^{-1})**	**Ref.**
Carbon-based adsorbents							
Fe-GAC	Se (IV)	2	0.3-2.8	5	25	2.58	[18]
Magnetic nano-particle-graphene oxide composites	Se (IV)	0-100	1	6-9	25	23.81	[19]
	Se (VI)	0-100	1	6-9	25	25.51	

C_{in} - initial concentration range; m/v – adsorbent dosage; T - temperature, [a]initial pH

Different graphene-based adsorbents were studied for different types of pollutants, including heavy metals, anions, dyes, and other organic pollutants [45, 46, 47]. The hydrophilic monolayer graphene oxide has a large specific surface area, so that it is easy to change the hydroxyl and carboxyl functional groups on the surface.

Modification of graphene oxide sheets with magnetic iron oxide nanoparticles was performed and this material (magnetic nanocomposite of graphene oxide) was used to remove selenium (IV) and (VI) from water [19]. The adsorbent is dosed in the amount of 1 g of L^{-1}, the percentage of removal is from 80% to almost 100% at concentration of 300 mg of L^{-1} Se (IV) and Se (VI) in solution. In the pH range of 2–10, it did not have a significant effect on Se (IV) adsorption, but at pH 11, a drastic drop in percentage of removal was observed. However, in the adsorption of Se (VI), a gradual decrease in the percentage of removal with increasing pH value along the entire studied range was observed. By the equilibrium tests performed at pH values from 6 to 9, the adsorption capacity of 23.8 mg g^{-1} and 15.1 mg g^{-1} for Se (IV) and Se (VI), respectively, was shown. Important advantages of adsorption by the magnetic nanocomposite graphene oxide are a high percentage of removal for both Se oxyanions, high rate of desorption and rapid separation of solid / liquid components (external magnetic field),k Table 2

3 BIOSORBENTS AND ADSORBENTS OBTAINED FROM NATURAL WASTE

In addition to the commercial and synthetic adsorbents, many other materials were investigated as the unconventional adsorbents to remove contaminants from water. The aim of this research is to find a cheap (low-cost) alternative to the traditional adsorbents, avoiding the costs of their preparation (and regeneration) and taking advantage of waste and natural readily available materials. Some studies have reported the use of raw materials, but further treatments were carried out to produce the adsorbents with improved properties [48].

Agricultural waste, used to prepare the carbon sorbent by treatment with hot sulfuric acid are: peanut shell [20, 21] and rice shell. This treatment partially oxidizes cellulose and hemicellulose and creates functional groups (-COOH and -OH) on the surface of adsorbent. Increasing the pH value from 1.5 to 7, leads to a gradual decrease in the adsorption of Se (IV) in both adsorbents. The maximum sorption capacities were in the range of 24 - 43 mg g^{-1} for adsorbent obtained from peanut shell and 26 - 41 mg g^{-1} for adsorbent obtained from rice shell [20, 21], at pH 1.5 and different temperatures (25-45°C), with higher adsorption at higher temperatures. The scanning electron microscopy (SEM) and XRD analysis showed the presence of elemental selenium as particles on the sorbent surface, indicating the reduction of Se (IV) to Se (0), which is developed on the sorbent surface. The physico-chemical tests indicate that the carbon oxidation has occurred on the surface of peanut shells and rice shells treated with sulfuric acid, Table 3.

Table 3 *Adsorption capacities (Q_m) listed in literature for Se (IV) and Se (VI), on waste materials and biosorbents*

Adsorbent	Se Species	C_{in} (mg L^{-1})	m/v (g L^{-1})	pH^a	T (°C)	Q_m (mg g^{-1})	Ref.
Waste materials and biosorbents							
Sulfuric acid-treated peanut shells (dry)	Se (IV)	25-250	2	1.5	25	23.76	[20]
Sulfuric acid-treated rice husk (dry)	Se (IV)	25-250	2	1.5	25	25.51	[21]
Cladophora hutchinsiae (green algae)	Se (IV)	$\sim$0-300^b	8	5	20	74.9	[22]
S. cerevisiae dried biomass	Se (IV)	$\sim$0-120^b	2	5	25	39.02	[23]
Fish scales	Se (IV)	0.005-0.02	-	5	30	0.67	[9]
Hydroxyapatite (fish-scale)	Se (IV)	0.005-0.02	-	5	30	1.58^c	
G. lucidum mushroom	Se (IV)	$\sim$0-40^b	7	5	20	127	[24]
Chitosan	Se (IV)	0.005-0.02	-	5	30	1.92^c	[9]

C_{in} - initial concentration range; m/v – adsorbent dosage; T - temperature, ^{a}initial pH; ^{b}equilibrium concentrations (estimated from the graphs); ^{c}maximum adsorption amount obtained experimentally, at the higher equilibrium concentration (20 µg L^{-1}).

Another natural waste, fish scales, was used as a precursor for the preparation of hydroxyapatite nanocrystals by the alkaline heat treatment [9]. This material showed pH_{ZPC} of 7.86 and a higher specific surface area and pore volume than commercial hydroxyapatite. Selenite adsorption was favored in the pH range between 3 and 6. The maximum adsorption capacity is 1.94 mg g^{-1} at 30 °C, according to the Langmuir model. The results of studies concerning the use of fish scales (untreated), chitosan and commercial hydroxyapatite showed that for these adsorbents the adsorption equilibrium is better described by the Freundlich model than by the Langmuir model. However, the Freundlich model did not give very good matches for chitosan and fish scales.

Nettem and Almusallam (2013) [49] studied the adsorption of Se (IV) by red fungus (*Ganoderma lucidum*). Biosorption was rapid (completed in 90 minutes), and the best effect was achieved at pH 5. At the initial Se concentration of 10 mg L^{-1}, the adsorbent was dosed in the amount of 7 g L^{-1} and optimal pH value of 5, and the removal of Se decreased with increasing temperature by 97% (20°C) at 74% (40°C). The data obtained by the Langmuir and Freundlich models matched well with the experimental data on adsorption equilibrium. The Langmuir model predicted a single-layer and adsorption capacity of 126.99 mg g^{-1}, although the maximum experimental adsorbed amount is about 70-80 mg g^{-1} for the studied equilibrium states, Table 3.

The mushroom (*Ascomicota*) was tested for removal the both types of selenium, Se (IV) and Se (VI) [50], where the removal efficiency was 78% for selenite and 28% for selenate.

Biomass obtained from water weeds: water hyacinth (*Eichhornia crassipes*) and small lentils (*Lemna minor*) were tested for the removal of Se (VI) from very dilute solutions (20 mg L^{-1}) [51]. The maximum adsorption capacity was at pH 4 (estimated under static conditions). Also, the biosorption capacities of *Eichhornia crassipes* and *Lemna minor*, when tested in the horizontal flow columns, were 0.135 and 0.743 mg g^{-1}, respectively.

A dried biomass - baker's yeast (*Saccharomices cerevisiae*) was tested for selenium removal. It is widespread and used in food and beverage production, easy to grow (without complicated fermentation techniques), and also occurs as a by-product from the fermentation industry [51]. Khakpour et al. (2014) tested *Saccharomices cerevisiae* as an adsorbent for Se (IV) and found that the optimal pH value was 5 (test range 2–8), adsorption capacity 12.5 mg g^{-1} (initial Se concentration 50 mg L^{-1}, adsorbent dose 2 g L^{-1}, temperature 25°C. The maximum adsorption capacity was 39.0 mg g^{-1}, calculated by the Sips model, which is a combination of the Langmuir - Freundlich isotherm parameters. The authors proposed a two-step process to improve percentage of Se (IV) removal from aqueous solution and improved biomass utilization. On the basis of the initial Se concentration of 50 mg L^{-1}, the total removal efficiency of 96% is expected in this two-step process, Table 3.

Algae treatment can be performed by two methods as follows: adsorption on the biomass of inanimate and living algae. The use of algae treatment for selenium biosorption is a promising biotechnology, after obtaining the successful results for heavy metals (such as zinc, lead, cobalt, cadmium, nickel). Tests on green algae (*Ulva rigida* and *Cladophora sericea*) from the Romanian Black Sea coast for Se removal have shown that the removal rate ranges between 80 and 95% within 5-7 h, with the initial Se concentration of 25 mg L^{-1} [52]. The adsorption capacity of algae for selenite and selenate is 0.5 mg g^{-1} and 0.2 mg g^{-1}, respectively.

Green microalgae (*Chlorella vulgaris*) were used in testing the biological treatment of selenate and selenite removal, and showed a high removal efficiency of 89%, for the initial Se concentration of 1580 mg L^{-1}, while the concentration of selenate and selenite in wastewater was 20 and 10 ppb [53].

Marine algae biosorption has shown to be effective in removal the heavy metal cations from wastewater. The high binding capacity of metals to the marine algae is the result of presence the polysaccharides, proteins or lipids on the cell wall surface, which contain functional groups such as amino, hydroxyl, carboxyl and sulfate, which act as binding sites for metals

Marine macroalgae are classified into three species: brown (*Phaeophita*), red (*Rhodophita*) and green (*Cladophora hutchinsiae*) [54]. By studying the biosorption of Se (IV) of green algae (*Cladophora hutchinsiae*), the removal efficiency was obtained between 70 and 96%, the biosorbent was dosed in the amount of 8 g L^{-1}, the initial concentration of Se of 10 mg L^{-1}, temperature 20°C, the pH value is in the range of 2 to 8, with maximum removal at pH 5. In acidic conditions, low selenium biosorption is explained by the fact that neutral species (H_2SeO_3) cannot undergo electrostatic interaction with algae. The increase in temperature showed a decrease in removal efficiency, from 96% (20°C) to 60% (50°C). The kinetics of biosorption were quite well described by a pseudo model elsewhere of the order of different temperatures. The maximum biosorption capacity of this green algae according to Langmuir was calculated to be 74.9 mg g^{-1} which corresponded to the steady state. Within the tested concentration range, the maximum adsorption capacity, obtained from the experiments, is about 50–60 mg g^{-1}. These values are very important considering that a cheap and easily accessible material was used. Also, these marine algae have been shown to be very stable during the regeneration process, as after ten phases of biosorption - desorption, there is a reduction of about 20% recovery of Se (IV) [22], Table 3.

Selenium and chromium biosorption and interaction with sulfur (S) of marine algae *(Chlorella vulgaris)* were investigated, which showed the highest efficiency of Se removal (95.24%), followed by S (80.01%) and Cr (59.91%). When algae were simultaneously exposed to all elements, the opposite results were obtained with the order of affinity as follows: Cr> S> Se. After exposure, 62.20% of the accumulated Se continuously evaporates into atmosphere, while 34.16% of Cr is released into water [55]. Decreased chlorophyll content and photosynthetic activity indicate the inhibitory effects of Se and Cr on algae, which were apparently worn out over time [56].

CONCLUSION

Selenium in small quantities is a nutritionally important element, but larger amounts are toxic and have side effects in humans and animals. This problem become very important for environmental protection and therefore prevention, control and removal of selenium from water are very important. Selenium occurs in water and wastewater from natural sources, but also due to the anthropogenic activities such as agriculture, mining, oil refineries and coal combustion, the typical concentrations range from a few micrograms per liter to 30 mg L^{-1}. Adsorption is a widely used procedure in water technology for removal the dissolved substances - pollutants. It can be used in drinking water treatment and wastewater treatment systems.

The following can be concluded from the given literature review:

- The adsorption effect is better for acidic and slightly acidic conditions. The typical pH value for wastewater from mining and desulphurization of flue gases is acidic, so the pH is not a worrying and limiting factor for adsorption in the treatment of these types of water. In agricultural water, the adsorp tion may not be an appropriate method or great care must be taken in a choice of adsorbent. In general, a pre-adjustment of pH value for the adsorption process is expensive and is not in line with the goal of finding an economical method for selenium removal.

- The temperature effect does not have a great influence on the adsorption process.
- The effect of competing ions, such as phosphates and sulfates, can have a major impact on the adsorption process. It has been observed that these ions have a great effect on reduction the selenium adsorption, because they often occur in water and wastewater in high concentrations. Based on this, the practical application of any adsorbent should be carefully studied. If the effect of competing ions is large, the disadvantage can be remedied by introduction the pretreatments to remove sulfates and phosphates by precipitation or a multi-stage adsorption process.
- Some adsorbents (binary metal oxides, single layer hydroxides (LDH), adsorbents based on natural materials) showed the good adsorption capacities and relatively fast adsorption kinetics.
- The natural waste and biosorbents were tested in the laboratory, where it was necessary to prepare these materials to improve the adsorption properties, study the effects of selenium concentration in solution and amount of adsorbent, assess the effect of competitive ions and metals in solution, and finally apply the process in columns with fixed layer and continuous flow.

REFERENCES

[1] Khamkhash, A., Srivastava, V., Ghosh, T., Akdogan, G., Ganguli, R., & Aggarwal, S. (2017). Mining-related selenium contamination in Alaska, and the state of current knowledge. Minerals, 7(3), 1–13. https://doi.org/10.3390/min7030046

[2] He, Y., Xiang, Y., Zhou, Y., Yang, Y., Zhang, J., Huang, H., Shang, C., Luo, L., Gao, J., & Tang, L. (2018). Selenium contamination, consequences and remediation techniques in water and soils: A review. Environmental Research, 164(February), 288–301. https://doi.org/10.1016/j.envres.2018.02.037

[3] Marković, R., Gardić, V., Jugović, B., & Stevanović, M. (2014). Dewatering of sludge obtained by neutralisation from sulfuric-acid waste solutions. Mining and Metallurgy Engineering Bor, (4), 125-136. https://irmbor.co.rs/casopis/mining-and-metallurgy-engineering-bor/

[4] Simonović, D., Pešovski, B., & Krstić, V. (2018). Electrochemical synthesis of ferrate (VI) for the wastewater treatment. Mining and Metallurgy Engineering Bor, (3-4), 49-54. https://irmbor.co.rs/casopis/mining-and-metallurgy-engineering-bor/

[5] CH2MHILL, 2010. Review of available technologies for the removal of selenium from water-final report. Prepared for North American Metals Council

[6] Santos, S., Ungureanu, G., Boaventura, R., & Botelho, C. (2015). Selenium contaminated waters: An overview of analytical methods, treatment options and recent advances in sorption methods. Science of the Total Environment, 521–522(1), 246–260. https://doi.org/10.1016/j.scitotenv.2015.03.107

[7] Gezer, N., Gülfen, M., & Aydın, A. O. (2011). Adsorption of selenite and selenate ions onto thiourea- formaldehyde resin. Journal of Applied Polymer Science, 122(2), 1134-1141.

[8] Sharrad, M. O. M., Liu, H., & Fan, M. (2012). Evaluation of FeOOH performance on selenium reduction. Separation and Purification Technology, 84, 29–34. https://doi.org/10.1016/j.seppur.2011.07.011

[9] Kongsri, S., Janpradit, K., Buapa, K., Techawongstien, S., & Chanthai, S. (2013). Nanocrystalline hydroxyapatite from fish scale waste: Preparation, characterization and application for selenium adsorption in aqueous solution. Chemical Engineering Journal, 215–216, 522–532. https://doi.org/10.1016/j.cej.2012.11.054

[10] Zhang, L., Liu, N., Yang, L., & Lin, Q. (2009). Sorption behavior of nano-TiO2 for the removal of selenium ions from aqueous solution. Journal of Hazardous Materials, 170(2–3), 1197–1203. https://doi.org/10.1016/j.jhazmat.2009.05.098

[11] Martínez, M., Giménez, J., De Pablo, J., Rovira, M., & Duro, L. (2006). Sorption of selenium(IV) and selenium(VI) onto magnetite. Applied Surface Science, 252(10), 3767–3773. https://doi.org/10.1016/j.apsusc.2005.05.067

[12] Peak, D. (2006). Adsorption mechanisms of selenium oxyanions at the aluminum oxide/water interface. Journal of Colloid and Interface Science, 303(2), 337–345. https://doi.org/10.1016/j.jcis.2006.08.014

[13] Szlachta, M., & Chubar, N. (2013). The application of Fe-Mn hydrous oxides based adsorbent for removing selenium species from water. Chemical Engineering Journal, 217, 159–168. https://doi.org/10.1016/j.cej.2012.11.100

[14] Gonzalez, C. M., Hernandez, J., Peralta-Videa, J. R., Botez, C. E., Parsons, J. G., & Gardea-Torresdey, J. L. (2012). Sorption kinetic study of selenite and selenate onto a high and low pressure aged iron oxide nanomaterial. Journal of Hazardous Materials, 211–212, 138–145. https://doi.org/10.1016/j.jhazmat.2011.08.023

[15] Gonzalez, C. M., Hernandez, J., Parsons, J. G., & Gardea-Torresdey, J. L. (2010). A study of the removal of selenite and selenate from aqueous solutions using a magnetic iron/ manganese oxide nanomaterial and ICP-MS. Microchemical Journal, 96(2), 324–329. https://doi.org/10.1016/j.microc.2010.05.005

[16] You, Y., Vance, G. F., & Zhao, H. (2001). Selenium adsorption on Mg-Al and Zn-Al layered double hydroxides. Applied Clay Science, 20(1–2), 13–25. https://doi.org/10.1016/S0169-1317(00)00043-0

[17] Das, J., Das, D., Dash, G. P., & Parida, K. M. (2002). Studies on Mg/Fe hydrotalcite-like-compound (HTlc): I. Removal of inorganic selenite (SeO_3^{2-}) from aqueous medium. Journal of Colloid and Interface Science, 251(1), 26–32. https://doi.org/10.1006/jcis.2002.8319

[18] Zhang, N., Lin, L. S., & Gang, D. (2008). Adsorptive selenite removal from water using iron-coated GAC adsorbents. Water Research, 42(14), 3809–3816. https://doi.org/10.1016/j.watres.2008.07.025

[19] Fu, Y., Wang, J., Liu, Q., & Zeng, H. (2014). Water-dispersible magnetic nanoparticle-graphene oxide composites for selenium removal. Carbon, 77, 710–721. https://doi.org/10.1016/j.carbon.2014.05.076

[20] El-Shafey, E. I. (2007a). Removal of Se(IV) from aqueous solution using sulphuric acid-treated peanut shell. Journal of Environmental Management, 84(4), 620–627. https://doi.org/10.1016/j.jenvman.2007.03.021

[21] El-Shafey, E. I. (2007b). Sorption of Cd(II) and Se(IV) from aqueous solution using modified rice husk. Journal of Hazardous Materials, 147(1–2), 546–555. https://doi.org/10.1016/j.jhazmat.2007.01.051

[22] Tuzen, M., & Sari, A. (2010). Biosorption of selenium from aqueous solution by green algae (Cladophora hutchinsiae) biomass: Equilibrium, thermodynamic and kinetic studies. Chemical Engineering Journal, 158(2), 200–206. https://doi.org/10.1016/j.cej.2009.12.041

[23] Khakpour, H., Younesi, H., & Mohammadhosseini, M. (2014). Two-stage biosorption of selenium from aqueous solution using dried biomass of the baker's yeast Saccharomyces cerevisiae. Journal of Environmental Chemical Engineering, 2(1), 532–542. https://doi.org/10.1016/j.jece.2013.10.010

[24] Nettem, K., Almusallam, A.S., 2013. Equilibrium, kinetic, and thermodynamic studies on the biosorption of selenium (IV) ions onto Ganoderma lucidum biomass. Sep. Sci. Technol. 48, 2293–2301

[25] Krstić V., Marjanović V., Pešovski B., Simonović D., Nanoadsorbensi na bazi metala/metal oksida u funkciji prečišćavanja otpadnih voda od zagađivača, Bakar, Vol. 46, 1(2021), str.13-24, https://irmbor.co.rs/casopis/casopis-bakar/

[26] Hayes, K.F., Roe, A.L., Brown, G.E., Hodgson, K.O., Leckie, J.O., Parks, G.A., 1987. In situ X-ray absorption study of surface complexes - selenium oxyanions on alpha-FeOOH. Science, 238, 783–786

[27] Jordan, N., Foerstendorf, H., Weiß, S., Heim, K., Schild, D., & Brendler, V. (2011). Sorption of selenium(VI) onto anatase: Macroscopic and microscopic characterization. Geochimica et Cosmochimica Acta, 75(6), 1519–1530. https://doi.org/10.1016/j.gca.2011.01.012

[28] Jordan, Norbert, Lomenech, C., Marmier, N., Giffaut, E., & Ehrhardt, J. J. (2009). Sorption of selenium(IV) onto magnetite in the presence of silicic acid. Journal of Colloid and Interface Science, 329(1), 17–23. https://doi.org/10.1016/j.jcis.2008.09.052

[29] Lin, T. F., & Wu, J. K. (2001). Adsorption of arsenite and arsenate within activated alumina grains: Equilibrium and kinetics. Water Research, 35(8), 2049–2057. https://doi.org/10.1016/S0043-1354(00)00467-X

[30] Su, T., Guan, X., Gu, G., & Wang, J. (2008). Adsorption characteristics of As(V), Se(IV), and V(V) onto activated alumina: Effects of pH, surface loading, and ionic strength. Journal of Colloid and Interface Science, 326(2), 347–353. https://doi.org/10.1016/j.jcis.2008.07.026

[31] Su, T., Guan, X., Tang, Y., Gu, G., & Wang, J. (2010). Predicting competitive adsorption behavior of major toxic anionic elements onto activated alumina: A speciation-based approach. Journal of Hazardous Materials, 176(1–3), 466–472. https://doi.org/10.1016/j.jhazmat.2009.11.052

[32] TAŞCI, K. (2013). 済無No Title No Title No Title. Angewandte Chemie International Edition, 6(11), 951–952., 34(2), 1–20.

[33] Jordan, Norbert, Marmier, N., Lomenech, C., Giffaut, E., & Ehrhardt, J. J. (2009). Competition between selenium (IV) and silicic acid on the hematite surface. Chemosphere, 75(1),129-134. https://doi.org/10.1016/j.chemosphere.2008.11.018

[34] Kim, S. S., Min, J. H., Lee, J. K., Baik, M. H., Choi, J. W., & Shin, H. S. (2012). Effects of pH and anions on the sorption of selenium ions onto magnetite. Journal of Environmental Radioactivity, 104(1), 1–6. https://doi.org/10.1016/j.jenvrad.2011.09.013

[35] Verbinnen, B., Block, C., Lievens, P., Van Brecht, A., & Vandecasteele, C. (2013). Simultaneous removal of molybdenum, antimony and selenium oxyanions from wastewater by adsorption on supported magnetite. Waste and Biomass Valorization, 4(3), 635–645. https://doi.org/10.1007/s12649-013-9200-8

[36] Jordan, Norbert, Müller, K., Franzen, C., & Brendler, V. (2013). Temperature impact on the sorption of selenium(VI) onto anatase. Journal of Colloid and Interface Science, 390(1), 170–175. https://doi.org/10.1016/j.jcis.2012.09.021

[37] Jordan, N., Ritter, A., Foerstendorf, H., Scheinost, A. C., Weiß, S., Heim, K., Grenzer, J., Mücklich, A., & Reuther, H. (2013). Adsorption mechanism of selenium(VI) onto maghemite. Geochimica et Cosmochimica Acta, 103, 63–75. https://doi.org/10.1016/j.gca.2012.09.048

[38] Zelmanov, G., & Semiat, R. (2013). Selenium removal from water and its recovery using iron (Fe^{3+}) oxide/ hydroxide-based nanoparticles sol (NanoFe) as an adsorbent. Separation and -Purification Technology, 103, 167–172. https://doi.org/10.1016/j.seppur.2012.10.037

[39] Shi, K., Wang, X., Guo, Z., Wang, S., & Wu, W. (2009). Se(IV) sorption on TiO_2: Sorption kinetics and surface complexation modeling. Colloids and Surfaces A: Physicochemical and Engineering Aspects, 349(1–3), 90–95. https://doi.org/10.1016/j.colsurfa.2009.07.057

[40] Chan, Y. T., Kuan, W. H., Chen, T. Y., & Wang, M. K. (2009). Adsorption mechanism of selenate and selenite on the binary oxide systems. Water Research, 43(17), 4412–4420. https://doi.org/10.1016/j.watres.2009.06.056

[41] Gu, Z., Deng, B., & Yang, J. (2007). Synthesis and evaluation of iron-containing ordered mesoporous carbon (FeOMC) for arsenic adsorption. Microporous and Mesoporous Materials, 102(1–3), 265–273. https://doi.org/10.1016/j.micromeso.2007.01.011

[42] Sigrist, M. E., Brusa, L., Beldomenico, H. R., Dosso, L., Tsendra, O. M., González, M. B., Pieck, C. L., & Vera, C. R. (2014). Influence of the iron content on the arsenic adsorption capacity of Fe/GAC adsorbents. Journal of Environmental Chemical Engineering, 2(2), 927–934. https://doi.org/10.1016/j.jece.2014.02.013

[43] Wasewar, K. L., Prasad, B., & Gulipalli, S. (2009). Removal of selenium by adsorption onto granular activated carbon (GAC) and powdered activated carbon (PAC). Clean - Soil, Air, Water, 37(11), 872–883. https://doi.org/10.1002/clen.200900188

[44] Arcibar-Orozco, J. A., Josue, D. B., Rios-Hurtado, J. C., & Rangel-Mendez, J. R. (2014). Influence of iron content, surface area and charge distribution in the arsenic removal by activated carbons. Chemical Engineering Journal, 249, 201–209. https://doi.org/10.1016/j.cej.2014.03.096

[45] Lei, Y., Chen, F., Luo, Y., & Zhang, L. (2014). Synthesis of three-dimensional graphene oxide foam for the removal of heavy metal ions. Chemical Physics Letters, 593, 122–127. https://doi.org/10.1016/j.cplett.2013.12.066

[46] Li, L., Fan, L., Sun, M., Qiu, H., Li, X., Duan, H., & Luo, C. (2013). Adsorbent for hydroquinone removal based on graphene oxide functio-nalized with magnetic cyclodextrin-chitosan. International Journal of Biological Macromolecules, 58, 169–175. https://doi.org/10.1016/j.ijbiomac.2013.03.058

[47] Yan, H., Tao, X., Yang, Z., Li, K., Yang, H., Li, A., & Cheng, R. (2014). Effects of the oxidation degree of graphene oxide on the adsorption of methylene blue. Journal of Hazardous Materials, 268, 191–198. https://doi.org/10.1016/j.jhazmat.2014.01.015

[48] Pešovski B., Krstić V., Urošević T., Gomidželović L., Trumić B., Marjanović V., Toksičnost Cu^{+2} jona i uticaj različitih adsorbenasa na njihovo izdvajanje iz otpadnih voda, Bakar, Vol. 42, 2(2017), str. 9-22, https://irmbor.co.rs/casopis/casopis-bakar/

[49] Nettem, K., & Almusallam, A. S. (2013). Equilibrium, kinetic, and thermodynamic studies on the biosorption of selenium (IV) ions onto Ganoderma lucidum biomass. Separation Science and Technology, 48(15), 2293-2301.

[50] Sabuda, M. C., Rosenfeld, C. E., DeJournett, T. D., Schroeder, K., Wuolo-Journey, K., & Santelli, C. M. (2020). Fungal Bioremediation of Selenium-Contaminated Industrial and Municipal Wastewaters. Frontiers in Microbiology, 11(September). https://doi.org/10.3389/fmicb.2020.02105

[51] Wang, J., & Chen, C. (2006). Biosorption of heavy metals by Saccharomyces cerevisiae: A review. Biotechnology Advances, 24(5), 427–451. https://doi.org/10.1016/j.biotechadv.2006.03.001

[52] Filote, C., Ungureanu, G., Boaventura, R., Santos, S., Volf, I., & Botelho, C. (2017). Green macroalgae from the Romanian coast of Black Sea: Physico-chemical characterization and future perspectives on their use as metal anions biosorbents. Process Safety and Environmental Protection, 108, 34–43. https://doi.org/10.1016/j.psep.2016.06.002

[53] Gan, X., Huang, J. C., Zhou, C., He, S., & Zhou, W. (2019). Relationship between selenium removal efficiency and production of lipid and hydrogen by Chlorella vulgaris. Chemosphere, 217, 825–832. https://doi.org/10.1016/j.chemosphere.2018.11.075

[54] He, J., & Chen, J. P. (2014). A comprehensive review on biosorption of heavy metals by algal biomass: Materials, performances, chemistry, and modeling simulation tools. Bioresource Technology, 160, 67–78. https://doi.org/10.1016/j.biortech.2014.01.068

[55] Wang, Y., Wang, Z.-J., Huang, J.-C., Zhou, C., Zou, H., He, S., & Chen, V. Y.-C. (2021). Feasibility of using Chlorella vulgaris for the removal of selenium and chromium in water: Competitive interactions with sulfur, physiological effects on algal cells and its resilience after treatment. Journal of Cleaner Production, 313(February), 127939. https://doi.org/10.1016/j.jclepro.2021.127939

[56] Santos, S., Ungureanu, G., Boaventura, R., & Botelho, C. (2015). Selenium contaminated waters: An overview of analytical methods, treatment options and recent advances in sorption methods. Science of the Total Environment, 521–522(1), 246–260. https://doi.org/10.1016/j.scitotenv.2015.03.107

INSTRUCTIONS FOR THE AUTHORS

Journal **MINING AND METALLURGY ENGINEERING BOR** is published four times per a year and publishes the scientific, technical and review paper works. Only original works, not previously published and not simultaneously submitted for publication elsewhere, are accepted for publication in the journal. The papers should be submitted in both, Serbian and English language. The papers are anonymously reviewed by the reviewers after that the editors decided to publish. The submitted work for publication should be prepared according to the instructions below as to be included in the procedure of reviewing. Inadequate prepared manuscripts will be returned to the author for finishing.

Volume and Font size. The work needs to be written on A4 paper (210x297 mm), margins (left, right, upper and bottom) with each 25 mm, in the Microsoft Word later version, font Times New Roman, size 12, with 1.5 line spacing, justified to the left and right margins. It is recommended that the entire manuscript cannot be less than 5 pages and not exceed 10 pages.

Title of Work should be written in capital letters, bold, in Serbian and English. Under the title, the names of authors and institutions where they work are written under the title. The author of work, responsible for correspondence with the editorial staff, must provide his/her e-mail address for contact in a footnote.

Abstract is at the beginning of work and should be up to 200 words, include the aim of the work, the applied methods, the main results and conclusions. The font size is 10, italic.

Key words are listed below abstract. They should be minimum 3 and maximum of 6. The font size is 10, italic.

Basic text. The papers should be written concisely, in understandable style and logical order that, as a rule, including the introductory section with a definition of the aim or problem, a description of the methodology, presentation of the results as well as a discussion of the results with conclusions and implications.

Main titles should be done with the font size 12, bold, all capital letters and aligned with the left margin.

Subtitles are written with the font size 12, bold, aligned to the left margin, large and small letters.

Figure and Tables. Each figure and table must be understandable without reading the text, i.e., must have a serial number, title and legend (explanation of marks, codes, abbreviations, etc.). The text is stated below the figure and above the table. Serial numbers of figures and tables are given in Arabic numbers.

References in the text are referred to in angle brackets, exp. [1, 3]. References are enclosed at the end in the following way:

[1] Willis B. A., Mineral Procesing Technology, Oxford, Pergamon Press, 1979, pg. 35. (for the chapter in a book)

[2] Ernst H., Research Policy, 30 (2001) 143–157. (for the article in a journal)

[3] www: http://www.vanguard.edu/psychology/apa.pdf (for web document)

Specifying the unpublished works is not desirable and, if it is necessary, as much as possible data on the source should be listed.

Acknowledgement is given where appropriate, at the end of the work and should include the name of institution that funded the given results in the work, with the name and number of project, or if the work is derived from the master theses or doctoral dissertation, it should give the name of thesis / dissertation, place, year and faculty where it was defended. Font size is 10, italic.

The paper works are primarily sent by e-mail or in other electronic form.

Editorial address : Journal MINING AND METALLURGY ENGINEERING BOR
Mining and Metallurgy Institute
35 Zeleni bulevar, 19210 Bor
E-mail: nti@irmbor.co.rs; milenko.ljubojev@irmbor.co.rs
Telephone: +381 (0) 30/435-164; +381 (0) 30/454-110

We are thankful for all authors on cooperation

CIP - Каталогизација у публикацији
Народна библиотека Србије, Београд

622

MINING and Metallurgy Engineering Bor / editor-in-chief Milenko Ljubojev. - 2013, no. 2- . - Bor : Mining and Metallurgy Institute Bor, 2013- (Bor : Grafomedtrade). - 24 cm

Tromesečno. - Je nastavak: Rudarski radovi = ISSN 1451-0162
ISSN 2334-8836 = Mining and Metallurgy Engineering Bor
COBISS.SR-ID 201387788